THE EFFECTS OF SLOPE ASPECT ON THE FORMATION OF SURFACE HOAR AND DIURNALLY RECRYSTALLIZED NEAR-SURFACE FACETED CRYSTALS

by

Michael Stephen Cooperstein

A thesis submitted in partial fulfillment
of the requirements for the degree

of

Master of Science

in

Earth Sciences

MONTANA STATE UNIVERSITY
Bozeman, Montana

May, 2008

APPROVAL

of a thesis submitted by

Michael Stephen Cooperstein

This thesis has been read by each member of the thesis committee and has been found to be satisfactory reguarding content, English usage, format, citations, bibliographic style, and consistency, and is ready for submission to the Division of Graduate Education.

Dr. Kathy J. Hansen

Dr. Karl W. Birkeland

Approved for the Department of Earth Science

Dr. Stephan Custer

Approved for the Division of Graduate Education

Dr. Carl A. Fox

STATEMENT OF PERMISSION TO USE

In presenting this thesis in partial fulfillment of the requirements for a master's degree at Montana State University, I agree that the Library shall make it available to borrowers under rules of the Library.

If I have indicated my intention to copyright this thesis by including a copyright notice page, copying is allowable for scholarly purposes, consistent with "fair use" as prescribed in the U.S. Copyright Law. Requests for permission for extended quotation from reproduction of this thesis in whole or in part may be granted only by the copyright holder.

Michael Stephen Cooperstein

May, 2008

TABLE OF CONTENTS

TABLE OF CONTENTS - CONTINUED

LIST OF TABLES

LIST OF TABLES - CONTINUED

LIST OF TABLES - CONTINUED

Table Page

LIST OF FIGURES

LIST OF FIGURES – CONTINUED

LIST OF FIGURES – CONTINUED

LIST OF FIGURES – CONTINUED

Figure Page

LIST OF FIGURES – CONTINUED

Figure Page

LIST OF FIGURES – CONTINUED

LIST OF FIGURES - CONTINUED

Figure Page

LIST OF FIGURES - CONTINUED

LIST OF FIGURES – CONTINUED

LIST OF FIGURE – CONTINUED

Figure Page

ABSTRACT

This research was conducted to determine if slope aspect played a role in the formation, size and shape of surface hoar and near-surface faceted crystals and on the meteorological variables that are known to result in the formation of these two weak layers. No studies have specifically studied the effects of slope aspect on the size and shape of these crystals nor the effects of slope aspect on the meteorological variables which are known to result in differences in temperature and vapor pressure gradients and ultimately result in the formation of these two weak layers.

Experimental stations were placed on north-, south-, and east-facing aspects of Pioneer Mountain, Montana, to measure meteorological variables such as wind speed and direction and incoming and diffuse shortwave radiation. Snowpack and air temperatures were also measured. Each time a surface hoar or near-surface faceted crystal layer formed, the snowpack and meteorological variables were recorded and snow crystals were collected, measured, characterized and photographed so that crystal size and structure could be compared between aspects. Temperature gradients, vapor pressure gradients, incoming shortwave radiation, and snow surface temperatures were also compared and graphed on each aspect.

Results showed a significant difference in the size and amount of development of surface hoar and near-surface faceted crystals based on slope aspect. During the events studied here surface hoar crystals grew larger and persisted longer on north-facing aspects followed by east- and south-facing aspects, respectively, and near-surface faceted crystals were better developed, with striations and cupping, on south- and east-facing aspects, than on north-facing aspects. These differences in crystal structure appear to be caused by the unequal distribution of incoming shortwave radiation on different slope aspects resulting in significant differences in both temperature and vapor pressure gradients based on slope aspect.

These aspect-dependent differences may have far reaching implications for avalanche forecasting, avalanche hazard rating, and avalanche hazard mitigation. This study demonstrates the importance of understanding the formation of different weak layers on different aspects for reliable prediction of patterns of avalanche activity.

CHAPTER 1

INTRODUCTION

Avalanches cause a significant number of deaths and sizable financial losses every year. Twenty-seven people were killed in avalanches in North America during the 2006-2007 winter (Avalanche.org 2007). Over the past 22 years, almost 3,000 people have been killed in avalanches in reporting countries, worldwide, nearly 500 have died in the United States, and 63 fatalities have occurred in Montana, where this study was conducted (Avalanche.org 2007). In fact, Voight et al. (1990) found that avalanches cause more fatalities than earthquakes and other landslide hazards in the United States, with economic losses due to avalanches exceeding a million dollars a year. Jamieson and Johnston (1992) estimated much higher financial costs in Canada of about 40 million dollars per year. To understand these costly and deadly hazards and more accurately predict their occurrence requires an intimate knowledge of the snowpack properties that most often result in avalanche release.

Each year the snowpack is laid down in layers. Each storm deposits snow in varying amounts and with differing densities. Once the snow is deposited, many processes affect its distribution and characteristics. The snow may be redistributed by the wind and/or begin to metamorphose. During metamorphosis, the snow can begin to round (bond and strengthen) or facet (become angulated, lose cohesion, and weaken). Rounding and faceting occur under different temperature gradient regimes which are caused by different meteorological

conditions. As the snowpack increases in depth through the season, it takes on a layered composition. In some cases the entire snowpack may be made up of rounded and well bonded crystals, but more commonly it is interspersed with strong and weak layers. These weak layers in the stratified snowpack typically create the failure plane for avalanches (McClung and Schaerer 1993).

Though weak layers or interfaces can be comprised of virtually any kind of snow crystals, typical persistent weak layers are often made up of three types of faceted grains: depth hoar, surface hoar, and near-surface faceted crystals. Depth hoar, which creates a weak basal layer, has been studied relatively extensively (Giddings and LaChapelle 1961; Bradley 1970; Akitaya 1974; Bradley et al. 1977; Perla 1978; and Colbeck 1982). While depth hoar undeniably creates a dangerous weak layer, researchers and avalanche forecasters are now beginning to realize that faceted layers forming at or just beneath the snow surface, such as surface hoar and near-surface faceted crystals, create more common weak layers for human-triggered avalanches in many snow climates (Birkeland 1998; Jamieson and Johnston1999; and McCammon and Schweizer 2002).

The meteorological processes contributing to the formation of surface hoar (Lang et al. 1984; Colbeck 1988; Hachikubo and Akitaya 1997a and b; Höller 1998; Hachikubo 2001) and its mechanical properties (Jamieson and Johnston 1999; Jamieson and Schweizer 2000) have been the subject of a sizable body of research. Likewise, the meteorological processes that contribute to the formation

of near-surface faceted crystals (Fukuzawa and Akitaya 1993; Birkeland 1998; Birkeland et al. 1998; McElwaine et al. 2000; Hardy et al. 2001: Bakersman 2006; Bakersman and Jamieson 2006) are becomingly increasingly better understood. Although many noteworthy studies have been conducted on the meteorological conditions necessary for the formation of surface hoar and near-surface faceted crystals and on the strength and strength changes over time of these persistent weak layers (Jamieson and Johnston 1999; Jamieson and Schweizer 2000), thus far little to no research has focused on slope aspect as a deterministic factor for surface hoar and near-surface faceted crystal formation. This lack of knowledge has led to the research presented here. Such work is important since understanding the development of these layers in regard to slope aspect will help to improve regional avalanche forecasting.

This study attempts to improve knowledge of the formation and distribution of two important weak layers in the alpine snowpack, surface hoar and near-surface faceted crystals by testing the following hypotheses.

- There are significant differences in the crystal size and/or crystal shape, of surface hoar and near-surface faceted crystals formed on north-, south-, and east-facing aspects.

- On days when surface hoar and/or near-surface faceted crystals form, there are statistically significant differences in temperature gradients and their resultant vapor pressure gradients based on slope aspect.

- On days when surface hoar and/or near-surface faceted crystals form, differences in crystal size and/or shape can be attributed to differences in the temperature gradients and the resultant vapor pressure gradients on north-, south-, and east-facing aspects.

- On days when surface hoar and/or near-surface faceted crystals form, differences in the temperature gradients and vapor pressure gradients can be attributed to differences in incoming shortwave and outgoing longwave radiation on north-, south-, and east-facing aspects.

By better understanding how slope aspect affects the formation of surface hoar and near-surface faceted crystals, we can better forecast, model, and evaluate the occurrence of slab avalanches. This will help save lives, reduce costs due to avalanches, and further our knowledge about faceted grains and avalanche release.

CHAPTER 2

LITERATURE REVIEW

Introduction

Stratified Snowpack

The formation of snow crystals in the atmosphere begins when ice crystals form in supersaturated clouds from interactions of liquid water, water vapor, and freezing nuclei. Because the triple point of water is so close to 0° C, water can exist in all three of its phases (ice crystals, water vapor, and water droplets) in the clouds at the same time. Since the vapor pressure around ice crystals is lower than the vapor pressure around water droplets, water vapor diffuses across the pressure gradient and subsequently sublimates onto the colder ice crystals and freezing nuclei. Eventually the ice crystals gain enough mass that they begin to fall. As they fall, they collide with super-cooled water droplets in the clouds, grow in size, and take on the characteristics of the atmosphere within which they formed. Factors such as the temperature and super-saturation of the air exert a strong influence on the shape of the falling snowflakes (McClung and Schaerer 1993) as well as on the density, size, degree of riming, and other characteristics. After the snow crystals are deposited on the ground or on an old snow surface, they are often redistributed by the wind and deposited on lee slopes and in gullies. Storm after storm deposits more snow, with their own atmospheric characteristics, which is subsequently redistributed by the wind and

further differentiated by metamorphism, rounding or faceting, and a complex set of layers forms throughout the season. This complex layered snowpack results in snow avalanche formation and release.

Types of Avalanches

A snow avalanche is a mass of snow sliding downhill under the force of gravity. Two different types of avalanches commonly occur: 1) loose snow avalanches, also called point release avalanches, and 2) slab avalanches. These two types are further classified as wet (free liquid water in the snowpack) and dry (no free water) snow avalanches.

Natural, loose snow avalanches occur because of a loss of cohesion in new snow layers, often due to solar heating, rain, or metamorphism of snow crystals in the upper layers of the snowpack, on slopes that exceed the angle of repose. Loose snow avalanches fan out in a triangle and typically involve only surface snow layers (McClung and Schaerer 1993). They occur most often after recent snow, on warm days, or during rain events, and their timing is fairly well understood. Loose snow avalanches, both wet and dry, are usually not very deadly or destructive because they are usually slow moving, involve only the top layers of the snow, and, if triggered by a skier, fail below or just at the feet of the skier and seldom sweep the skier away.

Slab avalanches are more dangerous than loose snow avalanches because they are larger, their failure occurs deeper in the snowpack, and their timing and extent are more difficult to predict. Slab avalanches, both wet and

dry, are the most deadly and destructive types of avalanches; however, dry slab avalanches are more frequently responsible for fatalities (McClung and Schaerer 1993). In Canada, 84% out of 339 recreational avalanche accidents resulted from a dry slab release (Canadian Avalanche Association 2005). For a dry snow slab avalanche to occur, it is necessary to have a slab (a cohesive mass of snow), a weak layer (less cohesive snow), a bed surface (something for the snow to slide on), a slope that is steep enough to slide (between 30° and 45° but most often 35° to 38°), and a trigger (weight added to the snow surface by a skier, by an explosive, or by the addition of new or wind transported snow).

Snow Metamorphism

Rounding

Slabs are simply cohesive masses of snow. They can be comprised of any type of snow crystals, but many slabs contain well-bonded, rounded snow grains formed by equilibrium metamorphic processes. Equilibrium metamorphism occurs when very small, microscale temperature gradients exist around the snow crystals and there is no significant interlayer temperature gradient in a snowpack (gradients generally less than 10° C m^{-1}). Areas of the snow structure with convex curvature (e.g., the arms of stellar crystals) have a slightly higher vapor pressure than concave areas. The difference in vapor pressure between convex (higher pressure) and concave (lower pressure) parts of the snow crystal causes a net loss of water vapor from angular and convex features and a net gain of

water vapor in concave areas. If this process continues under an equilibrium regime, snow crystals quickly lose their sharp edges and arms, grow increasingly rounded features, and metamorphose into stable forms (small rounded grains). In addition, snow crystal inter-granular bonding is increased. Water vapor molecules sublimate from the convex surfaces and deposit on the concave neck between grains (Colbeck 1980). These equilibrium processes produce rounded and sintered, tightly bonded, ice grains which form a cohesive mass or a slab.

Faceting

There are many different types of weak layers commonly found in a mountain snowpack: low density new snow, graupel, old/new snow interfaces, and faceted crystals (Tremper 2001). However, faceted crystals are the most prevalent weak layers found in the snowpack, with over 80% of all weak layers found in the snowpack consisting of faceted crystals (Föhn 1992).

Faceting, also termed kinetic growth or temperature gradient metamorphism, occurs due to temperature differences, which cause vapor pressure differences and the subsequent movement of water vapor from warmer, higher vapor pressure areas, to colder, lower vapor pressure areas (Armstrong 1985). As water vapor diffuses down gradient, it comes into contact with colder snow crystals and is deposited forming square-shaped facets, feather-shaped, cup-shaped, or needle-shaped surface hoar crystals, or cup-shaped depth hoar crystals. The minimum temperature gradient considered to be the threshold for

facet formation is 10° C m^{-1} (Akitaya 1974; Marbouty 1980; Colbeck 1982; Armstrong 1985).

Although the magnitude of the temperature gradient is typically used to describe the extent of faceting, the magnitude of the vapor pressure gradient really controls the amount of faceting. For beginning facets to form at temperatures close to 0° C, a vapor pressure gradient of 5 mb m^{-1} is necessary (Armstrong 1985). However, the extent of facet formation also depends on snow grain size, snow density, and snow hardness.

Three types of faceted crystals are commonly discussed in the literature: depth hoar, surface hoar, and near-surface faceted crystals. Of the three types, depth hoar has received the most attention in the literature and is the best understood crystal type.

Depth Hoar Depth hoar forms early in the season at the ground/snow interface due to large temperature gradients between the warmer ground and the colder snow or air above. This large temperature gradient causes a migration of water vapor from the warmer crystals close to the ground to the colder crystals above where it is deposited, forming intricate facets. Colbeck, et al. (1990) classify these crystals as 5a (cup-shaped, striated crystals, usually hollow) and 5b (depth hoar, large, cup-shaped, striated, hollow crystals arranged in columns) and note that they are extremely weak because they lack inter-crystalline bonds.

The formation of depth hoar and its mechanical strength are explained extensively in recent avalanche books (McClung and Schaerer 1993; Tremper

2001) and are reasonably well understood. Also, many studies have been conducted on the formation of depth hoar (Giddings and LaChapelle 1961; Bradley 1970; Akitaya 1974; Bradley, et al. 1977; Perla and Martinelli 1978; Colbeck 1982; Sturm and Benson 1997). Of these studies, the most comprehensive study to date on the growth and mechanical strength characteristics of depth hoar was carried out by Akitaya (1974). Through observation and experimentation, he developed a depth hoar crystal classification, looked extensively at crystal strength changes, and studied depth hoar crystal formation under varying vapor pressure gradients and with different sized air spaces. Akitaya (1974) concluded that it is possible for depth hoar to form from fine-grained rounded snow, typical of many mid-latitude snowpacks, if that snow is exposed to a significantly large temperature gradient for an extended period of time. He then concluded that the magnitude of the temperature gradient is directly related to the extent of faceting. Consequently, a larger temperature gradient causes more advanced faceting. He also concluded that large air/pore spaces in large-grained snow allow greater formation of advanced depth hoar crystals.

Recently, attempts have been made to predict variations in deep snow temperature gradients based on terrain (slope aspect and elevation) to more accurately predict the occurrence of depth hoar. These results suggest that, while terrain is an important consideration for the magnitude of deep snow temperature gradients, "topography alone cannot account for the spatial variation

found in deep snow temperature gradients" and slope aspect is an inconsistent predictor of deep snow temperature gradients (Deems 2002).

Researchers previously believed that layers made up of depth hoar crystals were the most problematic faceted layer in the snowpack. However, recent studies show otherwise. Birkeland (1998), working in southwest Montana, found that out of 51 avalanches from 1991-1996, most (46) failed on a layer formed at or near the snow surface. Of those 46 avalanches, 30 (65%) were attributed to near-surface faceted crystals and 16 (35%) to buried layers of surface hoar. Jamieson and Johnston (1992), studying surface hoar in the Columbia Mountains of western Canada, found that surface hoar was implicated in 34% of fatal slab avalanches. Further, Jamieson and Johnston (1992) documented that 50% of the fatal avalanche accidents involving avalanche professionals occurred on buried surface hoar layers, emphasizing the difficulty in predicting the behavior of these layers. Finally, McCammon and Schweizer (2002), studied 145 human-triggered avalanches and determined that weak layers that are < 1 m from the snow surface, that are ≤0.10 m thick, that have a hand hardness (Greene et al. 2004) difference of ≥1 step, that are composed of persistent grain types (near-surface facets, surface hoar, and depth hoar), and that have a grain size difference of ≥1 mm from their adjacent layers are the factors that most accurately predict human-triggered avalanche release. Layers of surface hoar and near-surface faceted crystals, more often than depth hoar and other weak layers, possess all of the qualities listed by McCammon and

Schweizer (2002). Since layers of surface hoar and diurnally recrystallized near-surface faceted crystals are noted more often than depth hoar in fatal avalanches, it is important to learn as much as possible about these two deadly weak layers.

Surface Hoar Surface hoar develops due to micro-meteorological conditions that cause large temperature gradients at the snow/air interface. On cold, clear nights longwave radiation losses from the snow surface cool the snow to well below the temperature of the adjacent air, creating large temperature gradients at the snow/air interface. Water vapor moves across the vapor pressure gradient from the warmer, higher pressure air to the cooler, lower pressure snow surface where it deposits, forming feather-like facets (type 7a) (Colbeck et al. 1990).

The meteorological processes contributing to the formation of surface hoar and its mechanical properties have been the subject of a sizable body of research. Lang et al. (1984) conducted a comprehensive study of surface hoar to better understand the formation, physical properties, and subsequent metamorphism of this weak layer. They made numerous measurements during the winters 1982-1983 and 1983-1984 on a flat study site in Big Sky, Montana. Lang et al. (1984) measured snow/air temperatures, measured near-surface air movement with a set of mesh flags, conducted night-time growth observations, conducted numerous mechanical strength measurements using a modified shear frame, and made some *in situ* photographs of a buried layer of surface hoar.

They measured temperature gradients in excess of 300° C m^{-1} at the snow/air interface, however, they did not calculate the resultant vapor pressure gradient. They concluded that buried surface hoar layers may persist for weeks and warned field workers to keep track of buried surface hoar layers regardless of the degree of surface hoar development. In their conclusion they indicated that the snow surface is remarkably dynamic and that heat and mass transfer processes at the snow surface are not easily explainable and demand further research.

Hachikubo and Akitaya (1997a) also conducted a comprehensive study of surface hoar formation, expanding on the work of Lang et al. (1984). They conducted numerous field observations of surface hoar layers and measured the water vapor deposition rate, the snow surface and air temperatures, relative humidity, wind speed, and net radiation on nights when surface hoar crystals formed. They found that it is possible to estimate the deposition rate of surface hoar using meteorological variables. In general, they concluded that surface hoar grows when the snow surface temperature is ≥ 5° C below that of the air temperature, the relative humidity is higher than 90%, and there is a slight wind (approximately 2-3 m s^{-1}).

Many studies have been conducted on the effects of wind on the formation of surface hoar. Originally Lang et al. (1984) concluded that any perceptible wind would preclude the formation of surface hoar, but later this theory was dispelled by Colbeck (1988) who theorized that surface hoar could not grow at the observed rates if molecular diffusion is the only mechanism for vapor transfer to

the snow surface. He concluded that some wind is necessary for turbulent transfer of water vapor from the air to the snow surface for surface hoar formation to take place. Hachikubo and Akitaya (1997 a and b) found that surface hoar deposition rates were highest when the wind speed was 2-3 m s^{-1} at a height of 1m above the snow surface and showed that condensation rate was dependent on wind speed and relative humidity. They showed that the deposition rate increased with wind speed (to a level of about 3 m s^{-1}) if the relative humidity was high.

The spatial distribution of surface hoar layers has also been the topic of recent research. Höller (1998) conducted field studies on the distribution of surface hoar in forested environments. He measured air temperatures, wind speed, relative humidity, and net radiation 1 m above the snow surface in open fields, sparsely forested areas, and densely forested stands and determined that surface hoar formation is possible in sparsely forested stands if the relative humidity is above 75%. Feick et al. (2007) concluded that variations in surface hoar formation can be explained by variations in local wind regimes. Schweizer and Kronholm (2004) concluded that the prevailing wind direction and solar warming/melting after surface hoar deposition controls the spatial variability of surface hoar. They found that the surface hoar layer studied was least frequently found on southerly and northwesterly slopes and felt that the pattern was caused by the destruction of surface hoar crystals by the sun on southerly-facing slopes and by the wind on northwesterly-facing slopes after the layer was deposited.

They did not study the crystal size and shape when the layer was deposited based on slope aspect.

The strength of surface hoar layers and strength changes over time have been the focus of a great deal of research, predominantly in the Columbia Mountains of western Canada. Jamieson and Johnston (1999) measured over 300 changes in shear strength of buried surface hoar layers in the Columbia Mountains from 1994-1998. Jamieson and Schweizer (2000) related changes in the texture of surface hoar to changes in the layer strength and monitored formation and burial of surface hoar layers in the Columbia Mountains using *in-situ* microphotography and shear tests. They pointed out that, as the buried layers aged, the surface hoar crystals became embedded in the layers above and below, slowly increasing the layer's strength and decreasing the layer's thickness. They found that layers of large-grained surface hoar gain strength more slowly than layers made up of smaller crystals. They also pointed out that large-grained surface hoar layers are more dangerous because they can persist in the snowpack for periods of up to 100 days since it takes longer for the larger grains to be completely embedded in the layer above. Similar results are discussed by Davis et al. (1996). Recently, while conducting slope scale spatial variability research in Montana, Birkeland et al. (2004), Logan (2005), and Logan et al. (2007) tested the strength changes of layers of buried surface hoar at a very fine scale and noted an increase in strength over time.

Near-surface Faceted Crystals Near-surface faceted crystals are another crystal type often implicated in fatal slab avalanches. Stratton (1977) discussed what he termed "upper level temperature gradient snow" and later Birkeland (1998) noted three mechanisms for the formation of what he termed "near-surface faceted crystals": radiation recrystallization, melt layer recrystallization, and diurnal recrystallization. Radiation recrystallization (Lachapelle 1970; LaChapelle and Armstrong 1970; Armstrong 1985) occurs on south-facing aspects at low latitudes and high altitudes, like Colorado's San Juan mountains, where the absorption of solar radiation just below the snow surface increases the temperature in the sub-surface layers. Longwave radiation losses from the snow surface cool the snow surface relative to the warmer layer below and a strong temperature gradient is set up causing water vapor to move from the warmer, lower layer and deposit on the colder, upper layer. Morstad (2004) and Morstad et al. (2007) conducted a number of laboratory experiments on radiation recrystallization. They showed that shortwave solar inputs, a portion of which are absorbed into the snowpack and may reach depths of 0.3 m, and longwave losses, which occur only at a plane on the snow surface, create a temperature gradient which is large enough to cause radiation recrystallized, near-surface faceted crystals. He also determined that densities greater than those of new snow preclude the formation of facets by this mechanism.

Melt layer recrystallization occurs when water is added to the snow surface, either by rain or by snowmelt. It has also been called wet layer

metamorphism by Jamieson and van Herwijnen (2002). If cold, new snow is deposited on top of a wet surface layer, a strong temperature gradient is formed and faceting occurs as water vapor migrates toward the surface and deposits onto the colder crystals (Birkeland 1998). Fukuzawa and Akitaya (1993) observed temperature gradients greater than 174° C m^{-1} near the snow surface after new snow had fallen on an old, wet snow layer. They were also able to create similar temperature gradients in the cold lab by sieving snow over a wet snow layer. Jamieson and Johnston (1997) studied a faceted layer that formed on a rain crust in November, 1996. They noted a difference in the degree of faceting in various areas, due to variations in the amount of snow deposited. Areas that received less snow on top of the rain crust were subject to larger temperature gradients. They also noted that thicker wet layers had more stored energy than thin wet layers so that lower elevation areas where it rained more during the storm had thicker wet layers and larger facets.

Diurnal recrystallization, the only type of near-surface faceted crystal studied in this research, occurs due to diurnal fluctuations in the temperature in the upper 0.3 m of the snowpack. LaChapelle and Armstrong (1977) and Armstrong (1985) recognized that there are diurnal fluctuations in temperature in the upper 0.3 m of the snowpack and that the temperature at and below 0.3 m remains relatively constant. Because of this, a temperature gradient is formed, which in turn creates a vapor pressure gradient, and there is subsequent movement of water vapor. On sunny days, the snow surface is heated by inputs

of shortwave radiation and relatively warmer air advection over the snow surface, but the temperature of the layer about 0.3 m below the surface stays relatively constant, so a temperature gradient forms between the warmer snow surface and the relatively colder snow below. Water vapor moves down gradient from the uppermost levels of the snowpack and deposits on the tops of the colder crystals, forming facets.

If the weather is dominated by high pressure and clear skies prevail nighttime longwave radiation losses quickly cool the snow surface to below the temperature of the snow 0.3 m below the snow surface. Large temperature gradients now form in the opposite direction, and water vapor migrates from the relatively warmer snow 0.3 m below the snow surface towards the colder snow surface where it deposits on the bottom of the snow crystals forming facets. Unlike any other faceted form, because the temperature gradient is multi-directional, faceting occurs both on the top and bottom of the crystals (Birkeland 1998; Birkeland et al. 1998). The crystals formed are classified by Colbeck et al. (1990) as type 4b, small faceted crystals, but Birkeland (1998) pointed out that these crystals can be well developed even showing cupping and striations and can grow larger than the 0.5mm, the maximum size previously reported.

Colbeck (1989) showed that it is possible for near-surface faceted crystals to form because of swings in the temperature in the upper snowpack and pointed out that growth rates in the sub-surface snow could, under certain conditions, be as high as growth rates that are observed in the basal layers of the snow during

depth hoar formation. Birkeland et al. (1998) measured near-surface temperatures, calculated vapor pressure gradients, and studied a diurnally recrystallized near-surface faceted layer and its resultant avalanche activity for 9 days after its formation. They measured near-surface temperature gradients greater than -200° C m^{-1} and a directional switch to 100° C m^{-1}. They calculated bi-directional vapor pressure gradients greater than 25 mb m^{-1} and observed 1 mm facets form within 36 hours. Recently, McElwaine et al. (2000) observed and attempted to model a layer of diurnally recrystallized near-surface faceted crystals which formed the weak layer of the Niseko Haru no Taki avalanche in Japan. Hardy et al. (2001) recognized the importance of high inputs of shortwave radiation and day-time absorption of solar radiation in the formation of a layer of diurnally recrystallized near-surface faceted crystals in the Bolivian Andes, and Hood et al. (2005) conducted experiments and had similar findings to Birkeland et al. (1998). Bakermans (2006) and Bakermans and Jamieson (2006) studied near-surface temperature changes over terrain. They placed experimental stations on different aspects of a knoll and measured snow temperatures and calculated net radiation fluxes with in the near-surface snow. They concluded that small changes in aspect can result in substantial differences in near-surface warming. They attributed the differences in near-surface temperature to differences in incoming solar radiation, and found that near-surface temperature fluctuations were larger on south-facing aspects on sunny

days. They also found that on overcast days the difference in near-surface temperatures based on aspect was not as large.

Although much research has been conducted on the meteorological conditions necessary for the formation of surface hoar and diurnally recrystallized near-surface faceted crystals, as well as changes in strength of buried faceted layers over time, the effects of slope aspect on the formation of these deadly and persistent weak layers has not been extensively studied. Birkeland et al. (1998) in their summary statement suggested that more quantification of near-surface faceting is necessary. Specifically, they called for studies on changes in bonding, faceting, and strength with time and space to help determine future avalanche conditions. This has led, in part, to the research presented here.

CHAPTER 3

RESEARCH METHODS

Geographic Location

This study was conducted at The Yellowstone Mountain Club on Pioneer Mountain in the Madison Range of southwest Montana UTM NAD 1983 coordinates Zone 12, 464,638 meters E and 5,008,690 meters N (Cooperstein et al. 2004) (Figure 3.1). Montana is about 1000 km long (east/west) and 450 km wide (north/south). Bordered by Canada on the north, by Idaho and Wyoming on the south, by North and South Dakota on the east, and by Idaho on the west, Montana covers 380,847 km^2, making it the 4th largest state in the US. The elevation ranges from Granite Peak at 3901 m above sea level to the Kootenai River at 549 m above sea level. The eastern portion of Montana is covered by the Great Plains and the western portion by mountainous terrain often classified as the Rocky Mountain Region.

The Madison Range of southwest Montana is fairly small, encompassing only about 1500 km^2. The range is approximately 52 km long, extending from just south of Pioneer Mountain north to the Gallatin Valley and is approximately 25 km wide at its widest east/west extent reaching from the Gallatin River to the Madison River. It is predominantly a north/south trending fault-block mountain range that contains sedimentary, metamorphic, and igneous rock, mostly

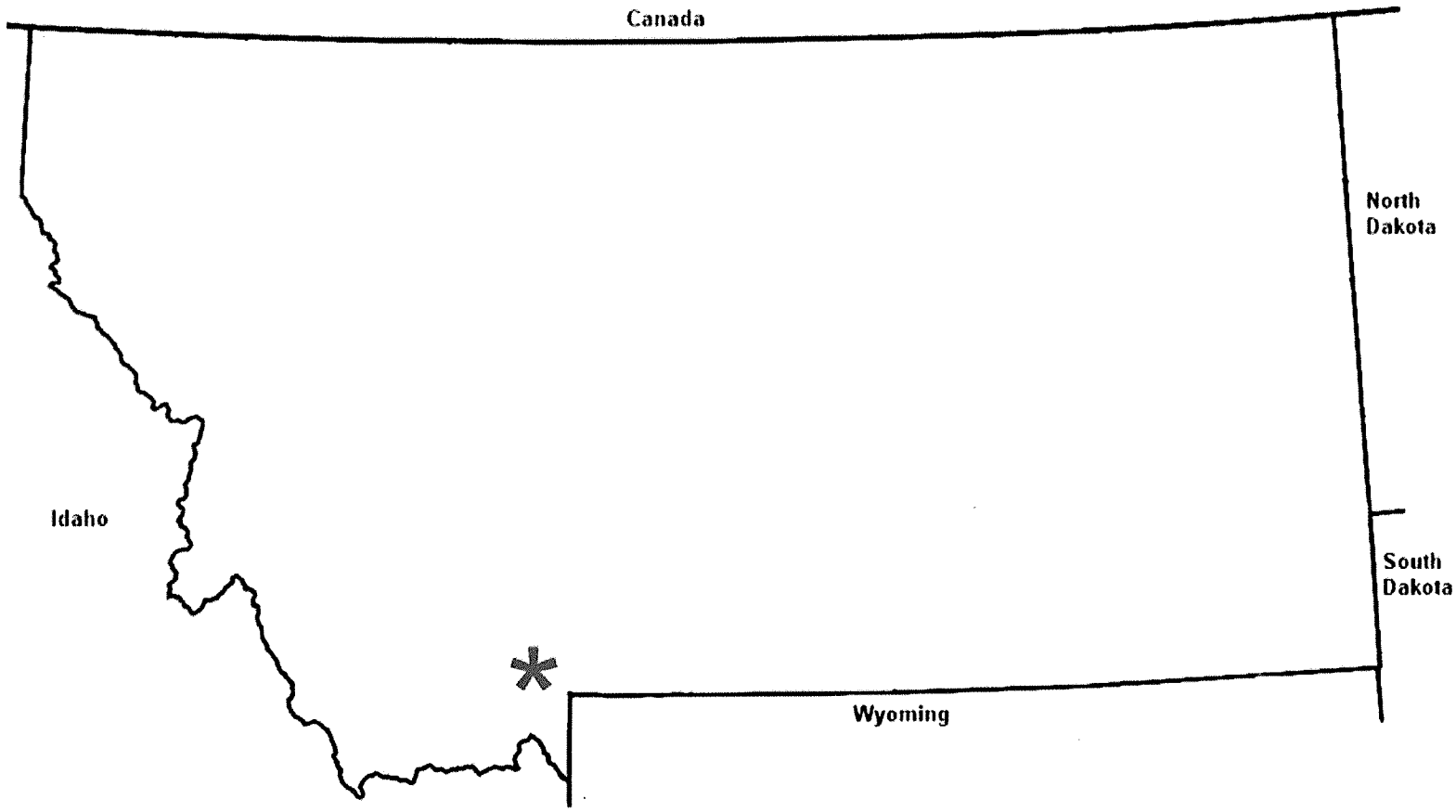

Figure 3.1: The location of the study area and Pioneer Mountain in red UTM NAD 1983 coordinates Zone 12, 464,638 meters E and 5,008,690 meters N.

granites and gneiss, which are exposed across large areas (Radbruch-Hall et al. 1982).

The Yellowstone Mountain Club is located in the southern Madison Range at 464,638 E and 5,008,690 N on the Universal Transverse Mercator, NAD 1983 Zone 12. The Yellowstone Mountain Club encompasses approximately 23 km^2 of skiable terrain, and Pioneer Mountain, with a north/south trending ridgeline, is about 2.25 km long. The Yellowstone Mountain Club's ski lifts provided easy, frequent access to study locations.

Weather and Climate of Study Site

The average winter temperature (measured for 7 years) from December 1 to April 30 at the Yellowstone Mountain Club is -8°C, however, due to its high elevation continental location winter temperatures can range from -29° C to 10° C. The Yellowstone Mountain Club receives an average of 5.5 m of snowfall a year and is favored by storms on a westerly flow that are strong enough to persist across the larger ranges to the west. Storms also come from the Snake River Plain to the south, but these storms tend to favor the Teton Range in Wyoming and Yellowstone National Park. Storms that originate in the north Pacific also affect the Madison range, but these storms often tend to favor more northerly mountains such as the Bridger Range.

The neighboring Big Sky Resort was classified as an intermountain snow climate 3 out of 5 years by Mock and Birkeland (2000) but seems to have

exhibited a continental snow climate more often than an intermountain snow climate in the past 10 years. When the snow climate for Pioneer Mountain was calculated using the methods outlined by Mock and Birkeland (2000) for the winters of 2000-2001 to 2004-2005, each year is best classified as a continental snow climate, which is characterized by large December temperature gradients, cold winter temperatures, and low snowfall (Table 3.1).

Table 3.1: An overview of the snow climate of the Yellowstone Club from the winter of 2000-2001 through the winter of 2004-2005 as discussed by Mock and Birkeland (2000).

	2000-2001	**2001-2002**	**2002-2003**	**2003-2004**	**2004-2005**
Average Dec. Temp. Gradient	7.9°C m^{-1}	8.9°C m^{-1}	17.8°C m^{-1}	9.0°C m^{-1}	9.7°C m^{-1}
Average Temperature	-7.9°C	-9.5°C	-7.2°C	-7.3°C	-9.7°C
Average Snow Base	127cm	139cm	113cm	143cm	120cm
Total Snow	496cm	530cm	567cm	629cm	509cm
Total SWE	13cm	16cm	33cm	28cm	22cm
	Continental	**Continental**	**Continental**	**Continental**	**Continental**

Description and Instrumentation of Study Sites

To investigate the role that slope aspect plays in the formation of surface hoar and near-surface faceted crystals meteorological data were gathered from the north-, south-, and east-facing aspects of Pioneer Mountain (Figure 3.2). Lack of funding prevented the installation of a site on a west-facing aspect. To limit confounding variables, the sites were situated so that they had large unobstructed sky views and were located in areas which had similar substrate and which were protected from the wind as much as possible.

North Study Site

The north site was located just outside the ski area boundary on a scree slope with a 14° true compass bearing at 2538 m above sea level on a 30° slope in an area known as TG Woods (464,230 meters E and 5,010,592 meters N, Zone 12 UTM NAD 1983). The clearing had an area of approximately 2900 m^2 (Figure 3.3) and was approximately 2.25 km due north of the south study site and approximately 2.2 km east-northeast of the east study site.

The north site was outfitted with a Met One 034A anemometer (Figure 3.4 and 3.5) which was fixed to a movable arm. The anemometer measured wind speed and direction at 1 meter above the snow surface.

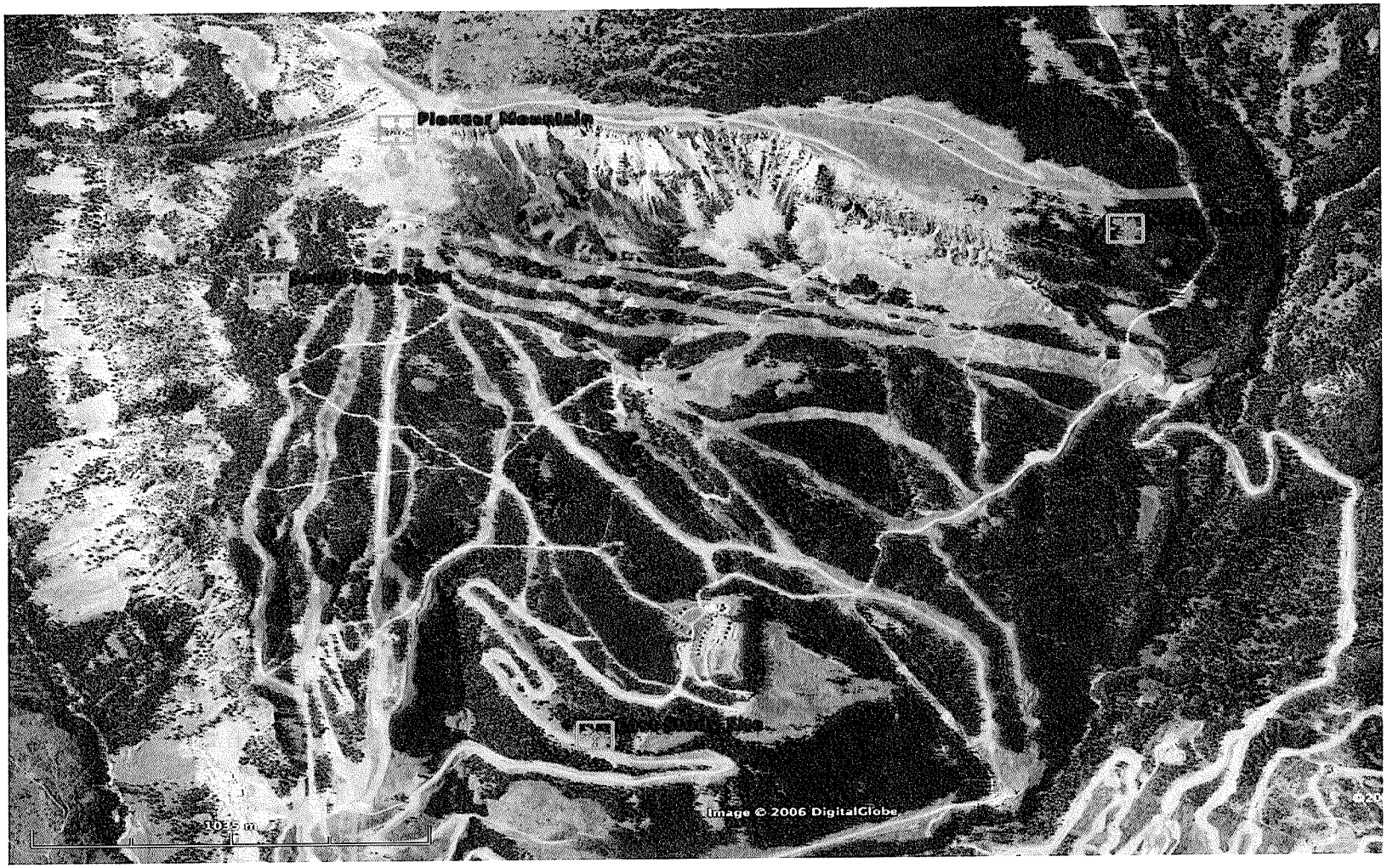

Figure 3.2: A broad overview of the Yellowstone Mountain Club (Pioneer Mountain) with the north, south, and east study sites marked on the map.

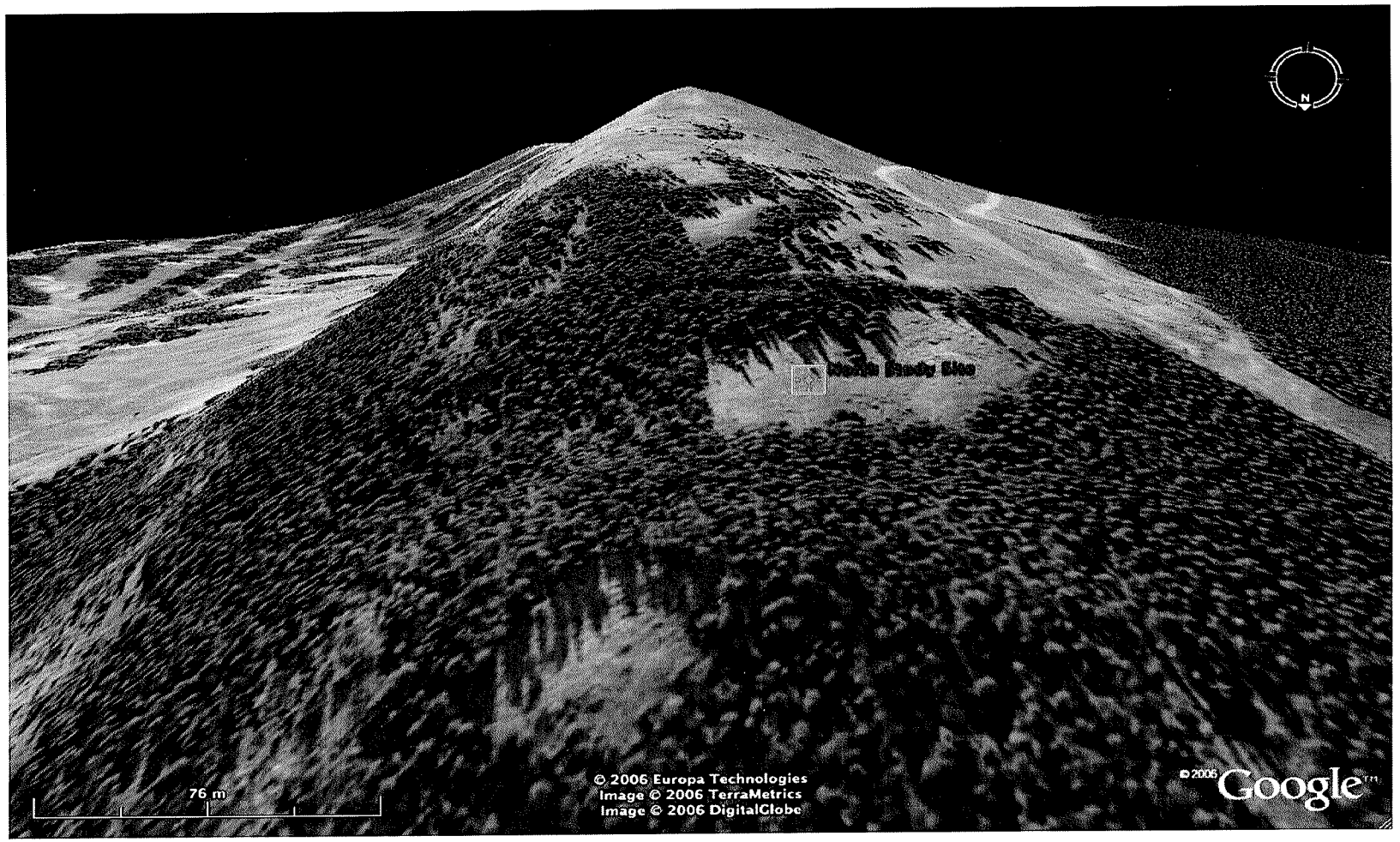

Figure 3.3: The location of the north study site in 3D. The north study site faces due north (14° true compass angle) and has a slope angle of 30°. It is located at 464,230 meters E and 5,010,592 meters N Zone 12, on the UTM NAD 1983.

Figure 3.4: The north study site in the summer time. It clearly shows the scree slope, the movable anemometer, and the pyranometers mounted on the arm at the top of the photograph.

Figure 3.5: The north study site in the winter, showing the anemometer with its movable arm and the pyranometers. Also in view are the datalogger and the thermocouple array (center of photograph).

Air and snow temperatures were measured with a thermocouple array (Figure 3.6), consisting of a stack of type-T copper-constantine thermocouple wires (± 0.2° C) mounted in graphite tubes of diameter 0.3 mm and placed through a wooden dowel rod. Temperatures were measured every 0.05 m from 0.10 m above the snow-surface to 0.35 m below the snow surface. The array was carefully inserted into the snow, as close to slope perpendicular as possible, and the entire apparatus was rotated ¼ turn to get the wire ends in contact with undisturbed snow. The array was checked daily and was reset after each snow or when it visually appeared askew. The array seemed to settle with the snowpack and was carefully monitored in an attempt to gather the most precise data possible.

Incoming and outgoing shortwave radiation were measured with LI-COR pyranometers (Figure 3.7). The pyranometers were placed slope parallel and back-to-back, one measuring incoming shortwave radiation and one measuring diffuse shortwave radiation (Figure 3.7).

Snow surface temperatures were also measured using an Everest Interscience 4000.4ZL infrared surface thermometer. The infrared thermometer was mounted at slope parallel on the arm next to the pyranometers (Figure 3.7).

The instrumentation on the north study site was connected to a Campbell Scientific AM 16/32 multiplexer which was connected to a Campbell CR 10 X datalogger. Wind speed, wind direction, snow and air temperatures, incoming and diffuse shortwave radiation, and infrared snow surface temperature

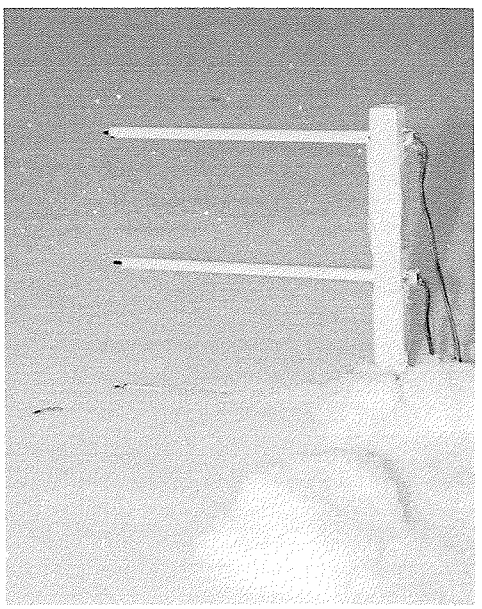

Figure 3.6: The thermocouple array placed at slope parallel in the snow with the 0.10 m and 0.05 m above the snow surface thermocouples visible and the snow surface thermocouple at the snow air interface border.

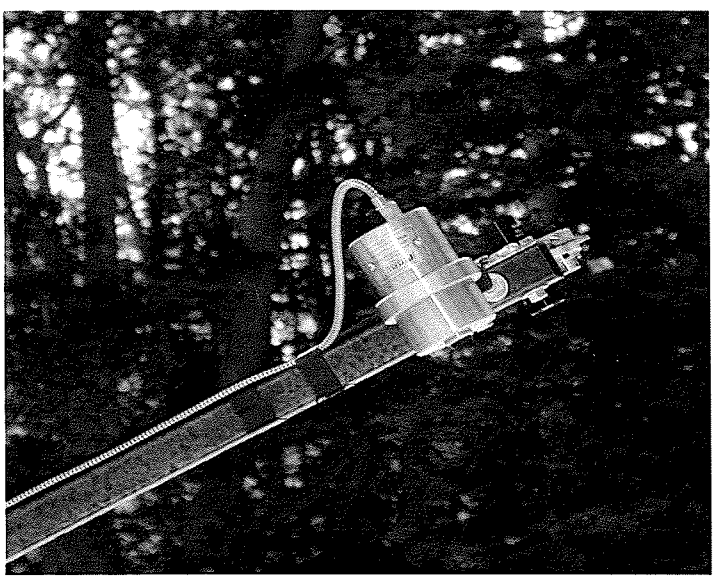

Figure 3.7: The two pyranometers, in the background of the photograph, mounted back-to-back at slope parallel, and the infrared snow-surface thermometer, silver cylinder in the foreground also mounted at slope parallel.

were measured every 3 seconds and then averaged for each hour. Maximum hourly wind gust, time of that gust, and direction of the gust were reported each hour. The maximum and minimum snow and air temperature, infrared snow surface temperature, incoming and diffuse shortwave radiation, and average wind speed and direction were also reported for each 24-hour period running from 0900 hours to 0900 hours.

South Study Site

The south site was located just outside of the ski area boundary on a scree slope with a 201° true compass bearing at 2723 m asl on a 30° slope in an area called Teva's Meadow (465,268 meters E and 5,008,583 meters N, Zone 12 UTM NAD 1983). This site was situated in a clearing with an area of about 3700 m^2 about 1.75 km southwest of the east study site (Figures 3.8, 3.9, and 3.10). This site was instrumented identically to and measurements were collected exactly the same way as on the north study site.

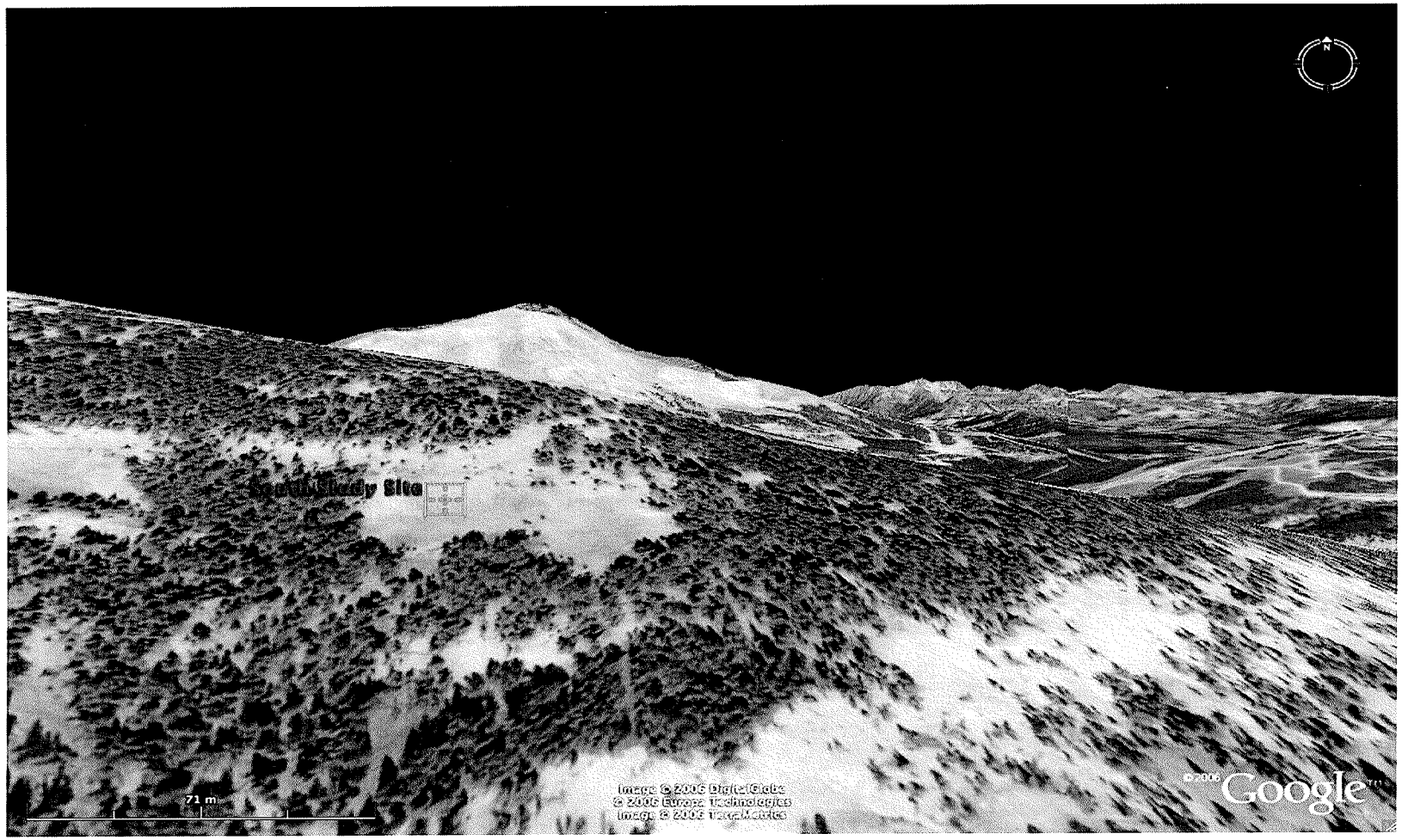

Figure 3.8: The location of the south study site in 3D. The south study site faces 201° true compass bearing and has a slope angle of 30°. It is located at 465,268 meters E and 5,008,583 meters N, Zone 12 on the UTM NAD 1983.

Figure 3.9: The south study site in the summer time. It clearly shows the scree slope and the movable anemometer arm in the foreground as well and gives an idea of the sky view on the south slope.

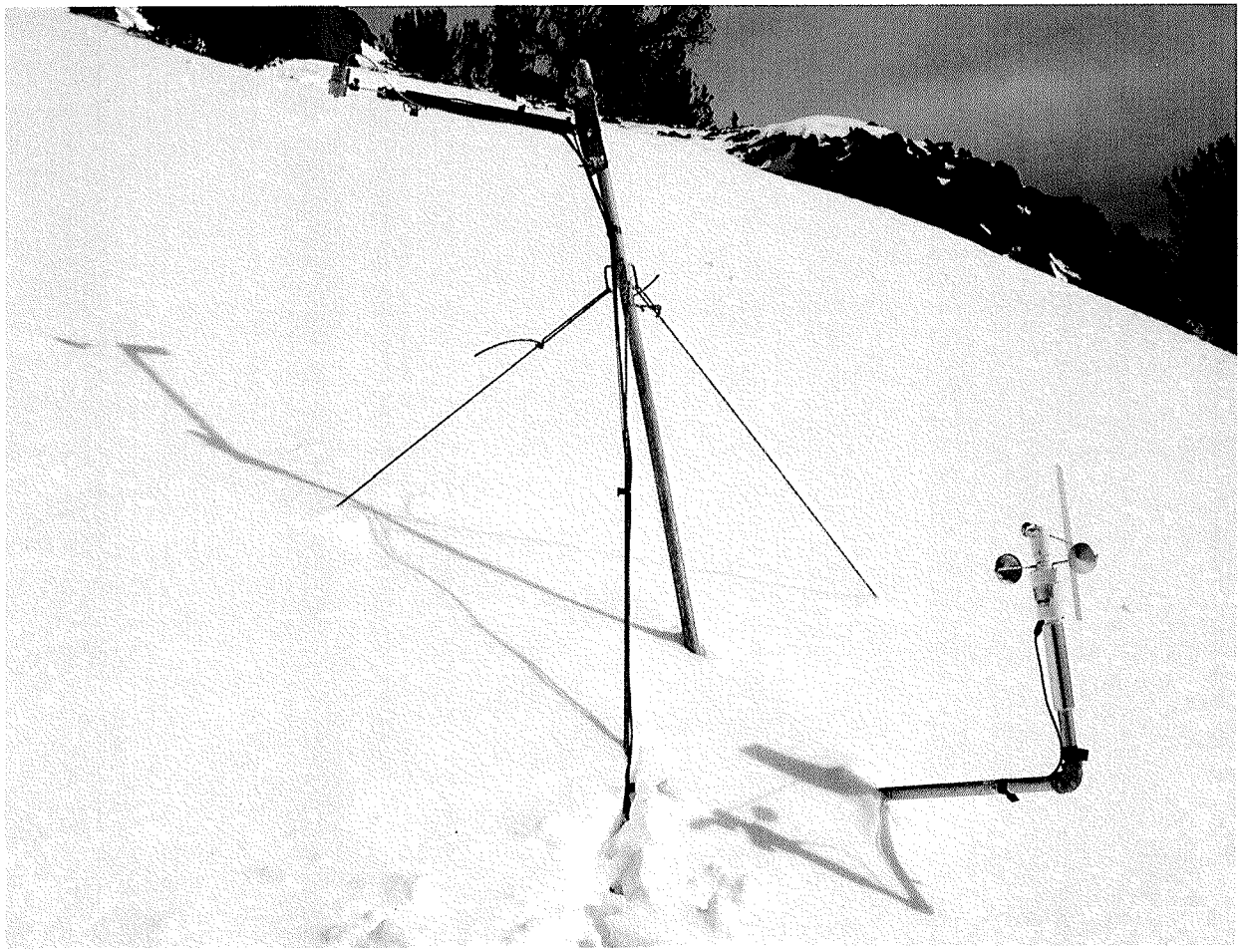

Figure 3.10: The south study site in the winter, showing the anemometer with its movable arm, the pyranometers, and the infrared snow surface thermometer.

East Study Site

The east site, Cabins Road Meadow (Figure 3.11 and 3.12), was located above a road cut in a permanently closed area with grassy substrate 106° true compass bearing at 2513 m asl on 24° slope (466,332 meters E and 5,009,989 meters N, Zone 12 UTM NAD 1983). This site was situated in a grassy meadow with an area of about 2500 m^2. Due to lack of funding, this site contained less instrumentation.

Wind speed and direction were measured exactly the same as on the north- and south-facing aspects. Air and snow temperatures were again measured with a thermocouple array but, due to lack of funding, were only measured from 0.10 m above the snow surface to 0.25 m below the snow surface.

The instrumentation of the east study site was connected directly to a Campbell CR 21X micrologger. The micrologger collected measurements of wind speed and direction and snow and air temperatures every 3 seconds and averaged them for the hour. Maximum wind gust, direction, and time of maximum gust were also collected for each hour. The maximum and minimum snow and air temperature and the average wind speed and direction were also reported for each 24-hour period which ran from 0900 hours to 0900 hours. Incoming and diffuse radiation and infrared snow surface temperature were not measured on the east study site.

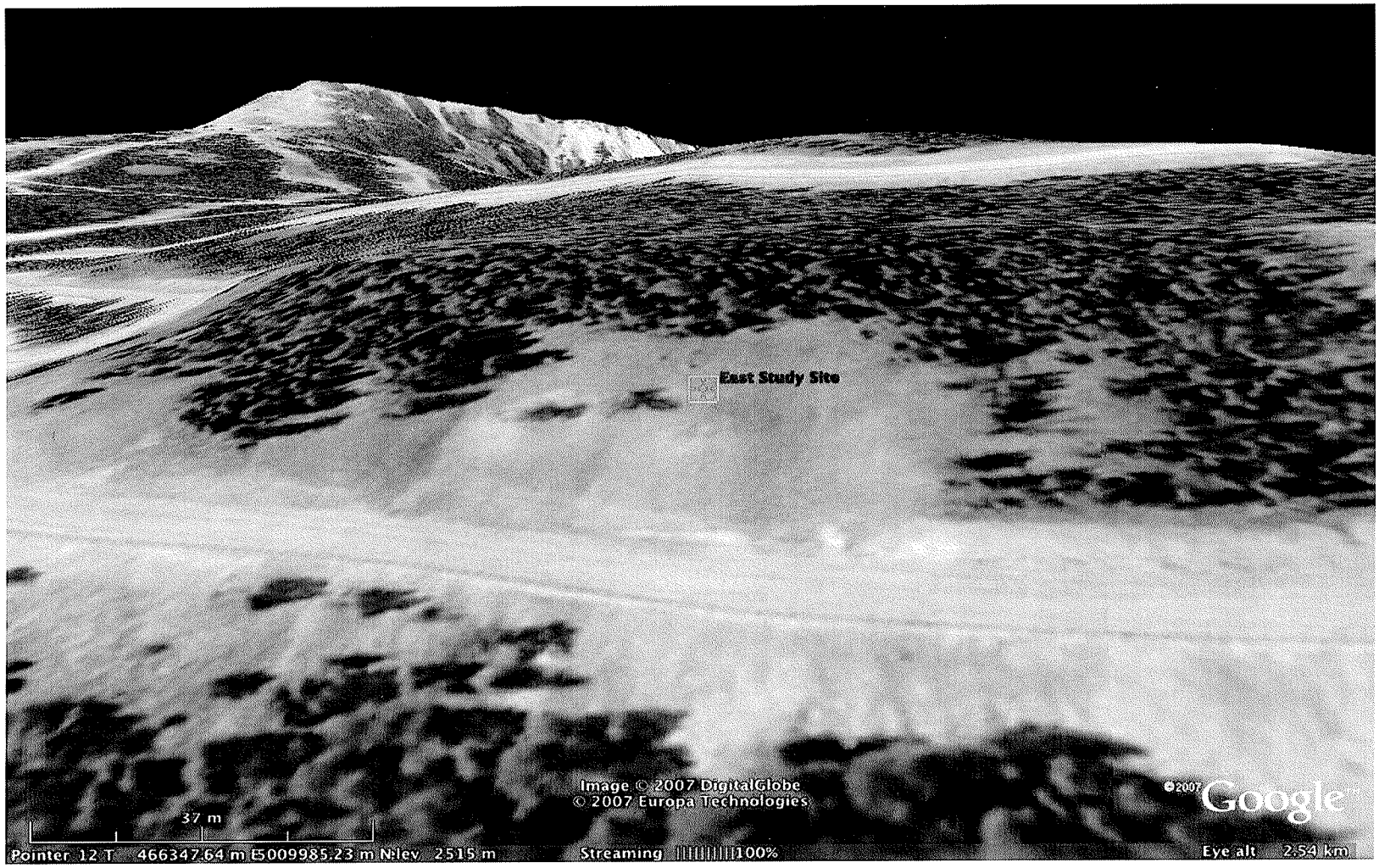

Figure 3.11: The location of the east study site in 3D. The east study site faces 106° true compass bearing and has a slope angle of 24°. It is located at 466,332 meters E and 5,009,989 meters N, Zone 12 UTM NAD 1983.

Figure 3.12: The east study site in the summer time. It clearly shows the grassy slope and gives an idea of the sky view on the east slope.

Yellowstone Club Timberline Study Site

Meteorological data has been recorded by the Yellowstone Mountain Club Snow Safety Department since the winter 2000-2001 at the Timberline snow study site, located at 2858 m asl in a flat meadow approximately 147 m below the ridge line. At this station data on air temperature, relative humidity, total snow depth, storm snow depth, snow water equivalent, and wind speed and direction at 2650 m and also at the ridge top at 2909 m are collected. The data are collected by a Campbell Scientific CR 10 X datalogger every 5 seconds and averaged for the hour. Twenty-four hour maximum and minimum air temperature, maximum wind gust, time of maximum wind gust, and direction of maximum gust are measured at 2650 m and also at 2909 m; maximum 24-hour snow, and total snow are measured, average relative humidity, and total snow water equivalent are also reported from 0900 hours to 0900 hours.

Analytical Methods

The meteorological data from north-, south-, and east-facing stations were downloaded weekly to a Palm Pilot and compiled as a running text file. Due to some battery malfunctions, data from the north and south stations are not complete for the season. The east data, however, are complete for the entire season. Faulty data, due to equipment limitations such as temperatures above 0° C recorded below the snow surface, positive incoming solar radiation values at night, or negative net shortwave radiation values, accounted for about 1% of the

total yearly data and were manually removed from all aspects. Otherwise, no changes were made to the data.

The stations were visited daily, the pyranometers were cleaned of snow, the thermocouples were re-set to the snow surface, and the anemometer height was measured and re-set if necessary. A 20x hand lens was used to study the snow crystals on the snow surface and at -0.05 m.

Each time signs of faceting were noted, detailed field notes were made and measurements were taken. *In situ* digital photographs were taken whenever possible, and crystals were collected to compare the extent of faceting between aspects.

On every day that faceting was observed, the temperature gradients and vapor pressure gradients were graphed by hour, and statistical analyses were carried out on the north-, south-, and east-facing aspects for the 24-hours leading up to the faceting event to see if there was a statistically significant difference in these gradients based on slope aspect. Incoming shortwave radiation, diffuse shortwave radiation, and snow surface temperature were also studied on the north- and south-facing aspects for the 24 hours leading up to the faceting event to see if any of these meteorological variables corresponded to similarities or differences in the temperature and vapor pressure gradients. Additionally, if surface hoar was noted, the wind speed and direction on the north-, south-, and east-facing aspects were compared to see what, if any, effect they had on

surface hoar formation. Relative humidity at the Timberline Snow Study site was also analysed to see how it affected surface hoar formation.

Measurements of Faceted Crystals

If a surface hoar or near-surface faceted layer formed, snow crystals were collected at the snow surface and from -0.05 m, below, the snow surface and were placed in a solution of Iso-Octane, labeled, and placed in a freezer. Each week the crystals were taken to the Montana State University's Cold Lab where they were photographed under a microscope at varying magnifications, measured, and classified. The crystals were all measured across their longest axis. An attempt was made to randomly sample 15 crystals from each collection, however, many of the largest, most fragile, crystals may have been broken during transport.

Temperature Gradients

When surface hoar or near-surface faceted crystals formed, hourly calculations of temperature gradient between 0.05 m and the snow surface and between -0.05 and -0.10 m on the north-, south-, and east-facing aspects were made using the equation:

$$TG = (T_1 - T_2) / d$$

where TG ($^\circ$ C m $^{-1}$) is the temperature gradient between T_1 (temperature in $^\circ$ C at height 1 always the upper thermocouple) and T_2 (temperature in $^\circ$ C at height 2 always the lower thermocouple) and d (distance in meters between T_1 and T_2).

The hourly temperature gradients for each aspect were tested for normality using the Kolmogorov-Smirnov Test (Bain and Engelhardt, 1992) with a 95% confidence level. Results suggest that some temperature gradient data were normally distributed while other data were not. As such, on days when surface hoar crystals were noted the nonparametric Mann-Whitney U test (Bain and Engelhardt, 1992) was used to statistically compare the nighttime temperature gradients on each aspect to decide if these gradients were sampled from different populations thus showing aspect dependant differences in surface hoar formation. The Mann-Whitney U test z statistic is reported in this paper along with the two-tailed significance level. A significance level of 0.05 is used for all statistical comparisons. Birkeland et al. 1998 and Birkeland 1998 suggest that the diurnal change in temperature gradients cause the formation of diurnally recrystallized near-surface faceted crystals. Due to the change in direction of the gradients between day and night statistical analysis on the central tendency of the entire data set were not useful. Since the maximum positive and negative deviation from the center is what drives near-surface facet formation, the Levene's test for homogeneity of variance (Bain and Engelhardt, 1992) was used to test the hypothesis that the temperature gradients were from similar populations and consequently had equal variances. The Levene's f statistic is reported along with the significance level.

Temperature gradients were graphed against hour for each aspect (north, south, and east) between 0.05 m and the snow surface and between -0.05 and -

0.10 m on days when surface hoar or near-surface faceted crystals were noted. This allowed visual inspection of the difference in temperature gradient for each aspect during faceting events.

Vapor Pressure

When surface hoar or near-surface faceted crystals formed, vapor pressure was also calculated between 0.05 m and the snow surface and between -0.05 and -0.10 m on the north-, south-, and east-facing aspects using the Goff-Gratch Formulation for the saturation vapor pressure over a surface of pure water and pure ice is given by:

$$VP_x = \log_{10} e_i = -9.09718(T_o/T-1)-3.56654 \log_{10}(T_o/T)+0.876793(1-T/T_o)+\log_{10} e_{io}$$

VP_x= Vapor Pressure at height x
e_{io} = saturation vapor pressure over a plane surface of pure ordinary liquid water at ice point which is 6.1071mb
e_i = saturation vapor pressure over a plane surface of pure ordinary water ice (mb)
T = absolute (thermodynamic) temperature (° K)
T_o = ice point temperature (273.16° K)

The Goff-Gratch formulation is an integration of the Clausius-Claperon equation considering the deviations from a perfect gas (List 1949). These methods were used by Armstrong (1985) and by Birkeland et al. (1998).

Vapor Pressure Gradients

When surface hoar or near-surface faceted crystals formed, hourly calculations of vapor pressure gradients were made between 0.05 m and the

snow surface and between -0.05 and -0.10 m on the north-, south-, and east-facing aspects using the equation:

$$VPG = (VP_1 - VP_2) / d$$

where VPG (mb m^{-1}) is the vapor Pressure gradient between VP_1 (vapor pressure in mb at height 1 always the upper VP) and VP_2 (vapor pressure in mb at height 2 always the lower VP) and d (distance in meters between VP_1 and VP_2. These data were compiled in SPSS for each hour.

The hourly vapor pressure gradients between 0.05 m and the snow surface and between -0.05 and -0.10 m on each aspect were tested for normality using the Kolmogorov-Smirnov test with a 95% confidence level. Not all of the data passed the Kolmogorov-Smirnov test so nonparametric statistics were utilized. On days when surface hoar crystals were noted, the Mann-Whitney U test was used to statistically compare nighttime vapor pressure gradients on each aspect. As with comparisons of temperature gradients for near-surface facets, the Levene's test for homogeneity of variance was used to test the hypothesis that the vapor pressure gradients had equal variances.

Vapor pressure gradients were graphed against hour for each aspect (north, south, and east) between 0.05 m and the snow surface and between -0.05 and -0.10 m on days when surface hoar or near-surface faceted crystals were noted. This allowed visual inspection of the difference in vapor pressure gradientfor each aspect. Box plots were also constructed to draw conclusions about the distribution of the data.

The methods outlined above were carried out on each day that surface hoar or near-surface faceted crystals were noted and are shown in the Results and Discussion chapter which follows. A randomly picked day for each, surface hoar and near-surface faceted crystals, when faceting did not occur "non-event day" was chosen in SPSS from all days when data was available from all three aspects and when no faceting was noted. The temperature and vapor pressure gradients and the meteorological variables outlined above are also analyzed on the non-event day.

CHAPTER 4

RESULTS and DISCUSSION

Surface Hoar

Surface Hoar 10 January 2004

On 9 January, The Yellowstone Mountain Club's Snow Safety Department's morning, 0700 hour, meteorological observations reported broken skies, ridge top wind speeds averaging 6 m s^{-1} from the southwest, an air temperature of -2.6° C, and a relative humidity of 91%. By the afternoon, 1600 hours, on 9 January the skies were overcast, ridge top winds were averaging 6.3 m s^{-1} from the southwest, the temperature had risen to 0.3° C, and the relative humidity was 82%. By 0700 hours on 10 January, the skies were scattered to clear and ridge top winds remained around 6 m s^{-1} (Appendix A). By 0800 hours on 10 January, it was apparent that a layer of surface hoar had formed over night. The study sites were visited quickly, crystals were collected, and the study began.

Crystal Characteristics Surface hoar was observed on the north-facing and south-facing aspects, but not on the east-facing aspect on the morning of 10 January. Surface hoar collected from the south- and north-facing study sites at about 0815 and 0900 hours, respectively, on the morning of 10 January was clearly identifiable as type 7a, feather-shaped (Colbeck et al. 1990). The crystals collected from the north-facing aspect (Figure 4.1 and 4.2) were larger and better

developed than those collected from the south-facing aspect (Figure 4.3). Laboratory measurements confirmed that the crystals that formed on the north-facing aspect averaged 6mm and were better developed and more striated than those collected on the south-facing aspect which averaged only 3mm (Figure 4.4).

At about 0930 hours, crystals were collected from the east study site. There was no sign of surface hoar on the east-facing aspect on this day. The crystals collected from the east site (Figure 4.5) appeared to be new-snow stellar and broken stellar crystals, type 2a and 2b (Colbeck et al. 1990) and averaged 1.5 mm.

Since there was a disparity in the size and characteristics of the crystals that formed on 9-10 January among aspects, the temperature and vapor pressure gradients on all three aspects were compared to determine if the temperature and vapor pressure gradients differed by slope aspect.

Temperature Gradient The median, minimum, and maximum nighttime temperature gradients (from 1600 hours on 9 January to 0700 hours on 10 January on the north-facing slope far exceeded those on the south-facing slope (Table 4.1). The median and minimum temperature gradients on the east-facing aspect differed greatly from the north- and south-facing aspects because they were negative, precluding surface hoar formation.

Figure 4.1: A 6mm surface hoar crystal harvested from the north-facing site on 10 January 2004. This crystal is classified by Colbeck et al. (1990) as type 7a.

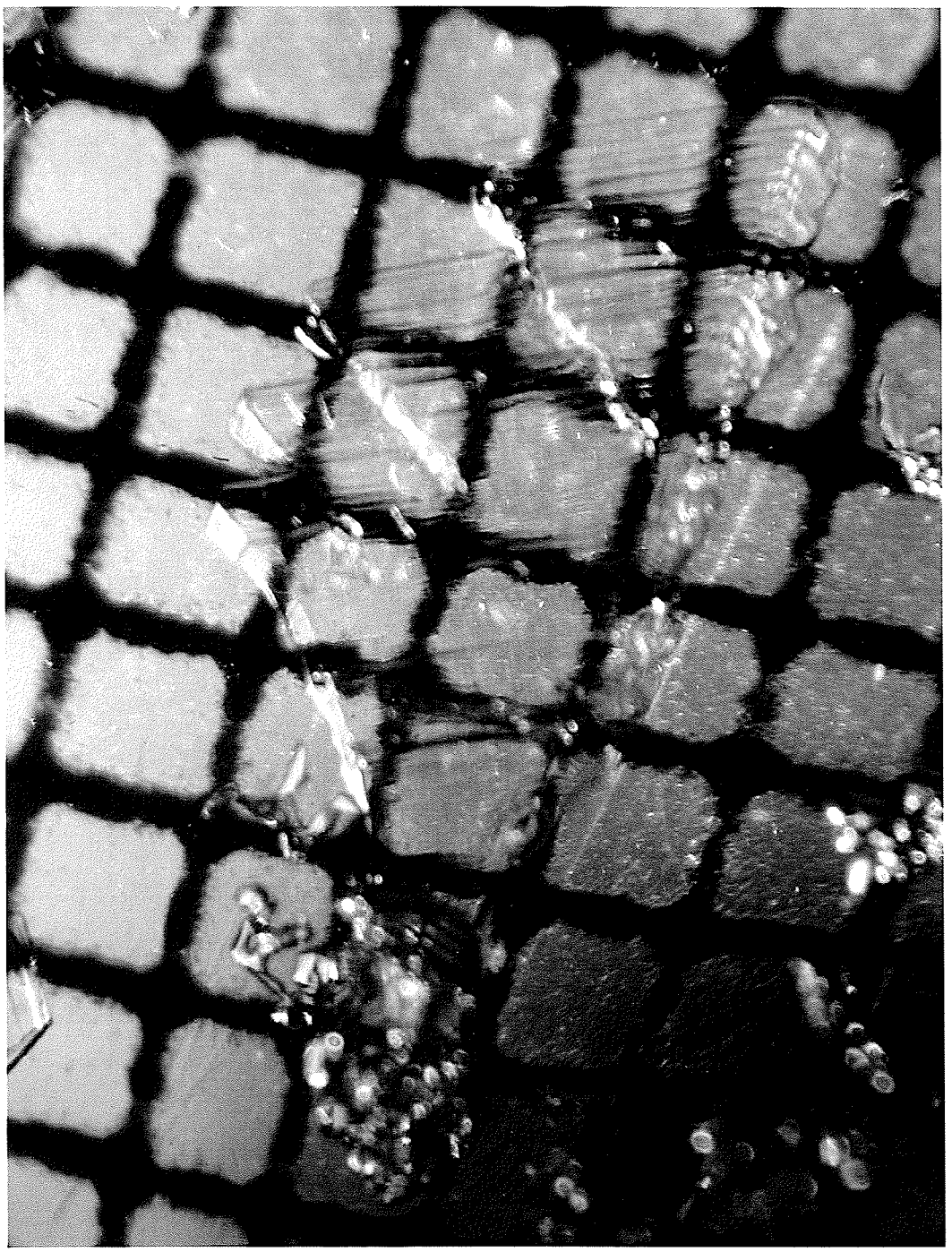

Figure 4.2: A 7mm surface hoar crystal harvested from the north-facing study site on 10 January 2004. This crystal is classified by Colbeck et al. (1990) as type 7a.

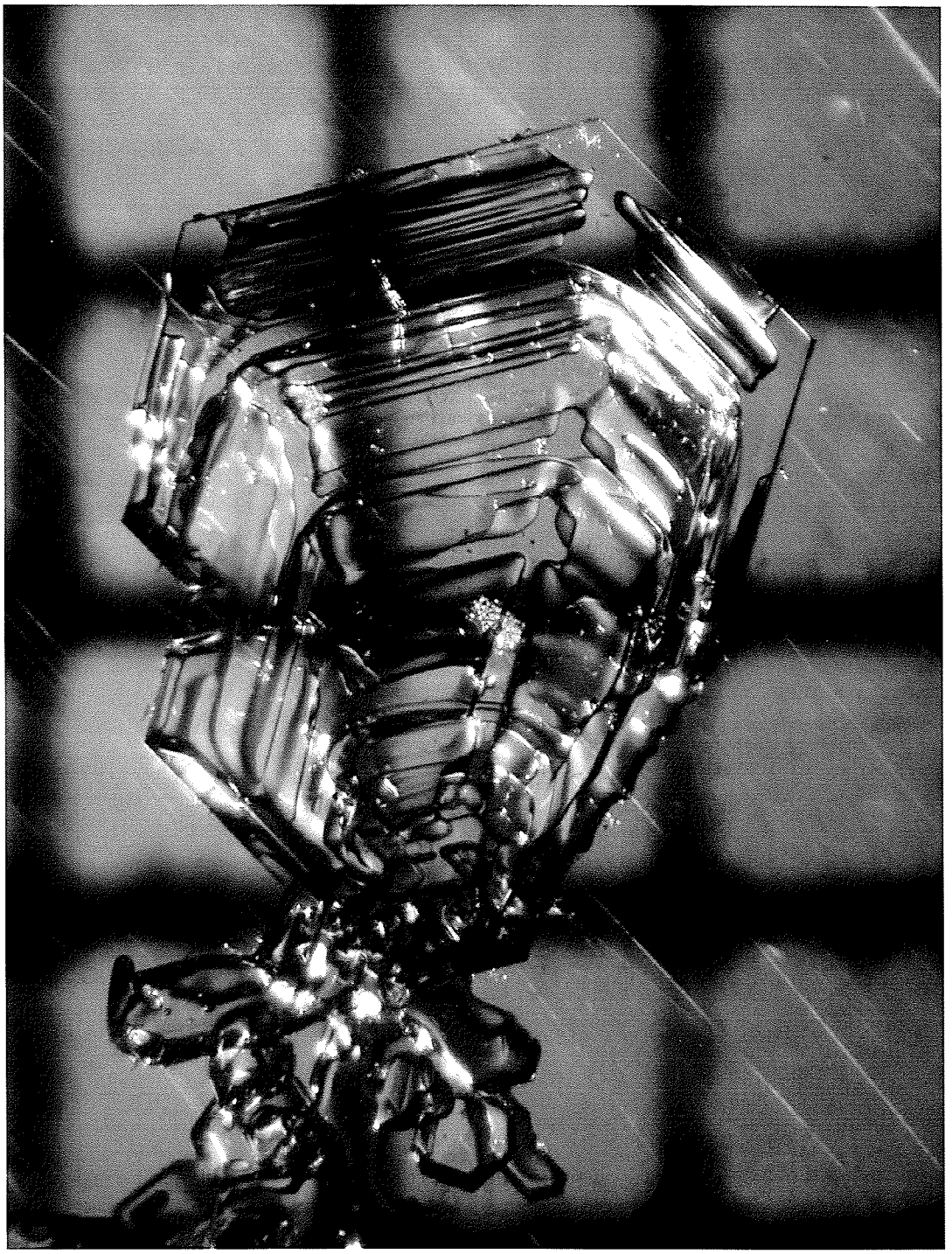

Figure 4.3: A 3mm surface hoar crystal harvested from the south-facing study site on 10 January 2004. This crystal is classified by Colbeck et al. (1990) as type 7a.

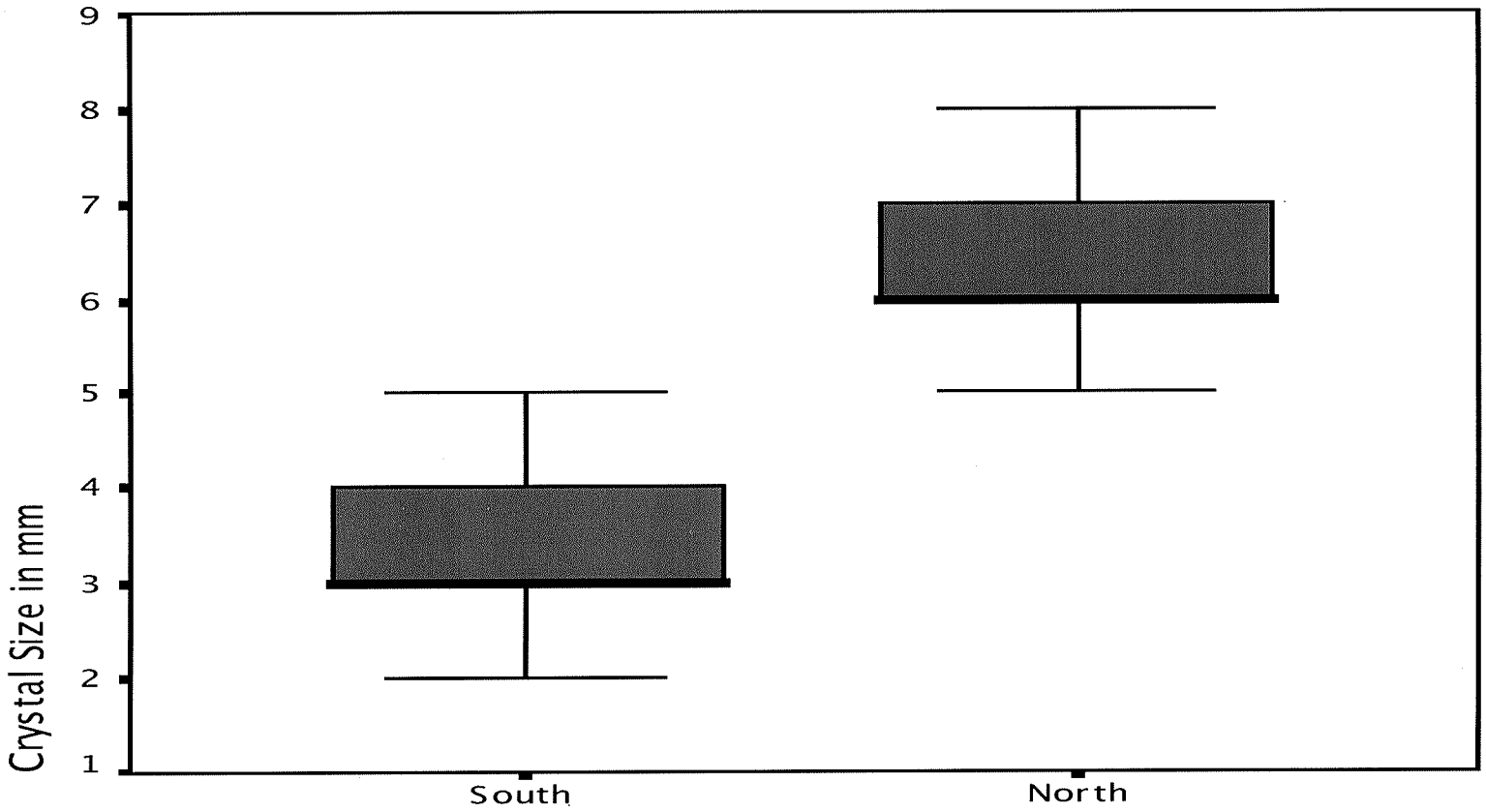

Figure 4.4: Box plot of crystal size in mm on 10 January 2004 versus slope aspect for the north- and south-facing aspects. The surface hoar crystals on the north aspect grew 2 times larger than those on the south. The Box plots show the median (darker black line), interquartile range (top and bottom of the box), and the minimum and maximum crystal size (the whiskers). N = 15 crystals on both the North and South aspects.

Figure 4.5: A 2 mm broken precipitation particle harvested from the surface of the south-facing study site on 10 January 2004. This crystal is classified by Colbeck et al. (1990) as type 2a/b.

Table 4.1: The median, minimum, and maximum nighttime temperature gradients (° C m^{-1}) from 1600 hours on 9 January 2004 to 0700 hours on 10 January 2004.

Aspect	N	Median	Minimum	Maximum
East	15	-21.8° C m^{-1}	-22.6° C m^{-1}	4.1° C m^{-1}
South	15	19.8° C m^{-1}	6.6° C m^{-1}	28.3° C m^{-1}
North	15	66.4° C m^{-1}	57.2° C m^{-1}	92.0° C m^{-1}

The mean hourly temperature gradient at the snow/air interface from 1200 hours on 9 January to 1100 hours on 10 January are shown in Figure 4.6 for the north-facing, south-facing, and east-facing aspects for the 24-hour period surrounding the surface hoar-forming event. The maximum temperature gradient on the north-facing aspect, 92° C m^{-1} reached at 1800 hours, was more than 3 times that on the south-facing aspect. The north-facing aspect also never dropped out of the positive surface hoar forming realm.

The temperature gradient on the south-facing aspect, on the other hand, was not as large as on the north-facing aspect, reaching a maximum temperature gradient of only 28° C m^{-1} at 2200 hours. The south-facing aspect also dropped into the negative realm for one hour. These data indicate that a sufficient gradient was in place for surface hoar formation on the south-facing aspect; however, the gradient was not as large as on the north-facing aspect. Consequently, the surface hoar on the south-facing aspect did not grow as large as the surface hoar on the north-facing aspect.

Figure 4.6: The mean temperature gradient by hour from 1200 hours on 9 January 2004 to 1100 hours on 10 January 2004 on the north- facing, south-facing, and east-facing aspects at the snow/air interface.

The temperature gradient on the east-facing aspect on 9-10 January appears to be anomalous since the temperature gradients were in the negative realm during the nighttime hours (Figure 4.6). However, after further investigation, these are probably not anomalous values and are more likely due to cold air drainage or another local topographically induced meteorological process, which occurred during the evening of January 9 into the morning of 10 January (Figure 4.7), causing cold air to be trapped on the east-facing aspect.

The air temperatures at the Timberline Snow Study Site (2858 m), on the north-facing (2538 m), south-facing (2723 m), and east-facing aspects (2513 m), and at the Base Area Snow Study Site (2195 m) for the 24 hours surrounding the surface hoar event were analyzed (Figure 4.7). The air temperature on the east-facing site remained lower than the air temperature on the other aspects and the temperature at lower elevations. Due to the cold air trapped at the east-facing site, the outgoing longwave radiation losses from the snow surface on the east aspect could not cool the snow surface to a temperature below that of the adjacent air. Consequently, a positive temperature gradient was precluded, and surface hoar did not form.

To test the hypothesis that the slopes have equal temperature gradients and thus would be from the same or similar populations, a Mann-Whitney U Test was conducted. The hypothesis of equality was rejected in all cases (Table 4.2).

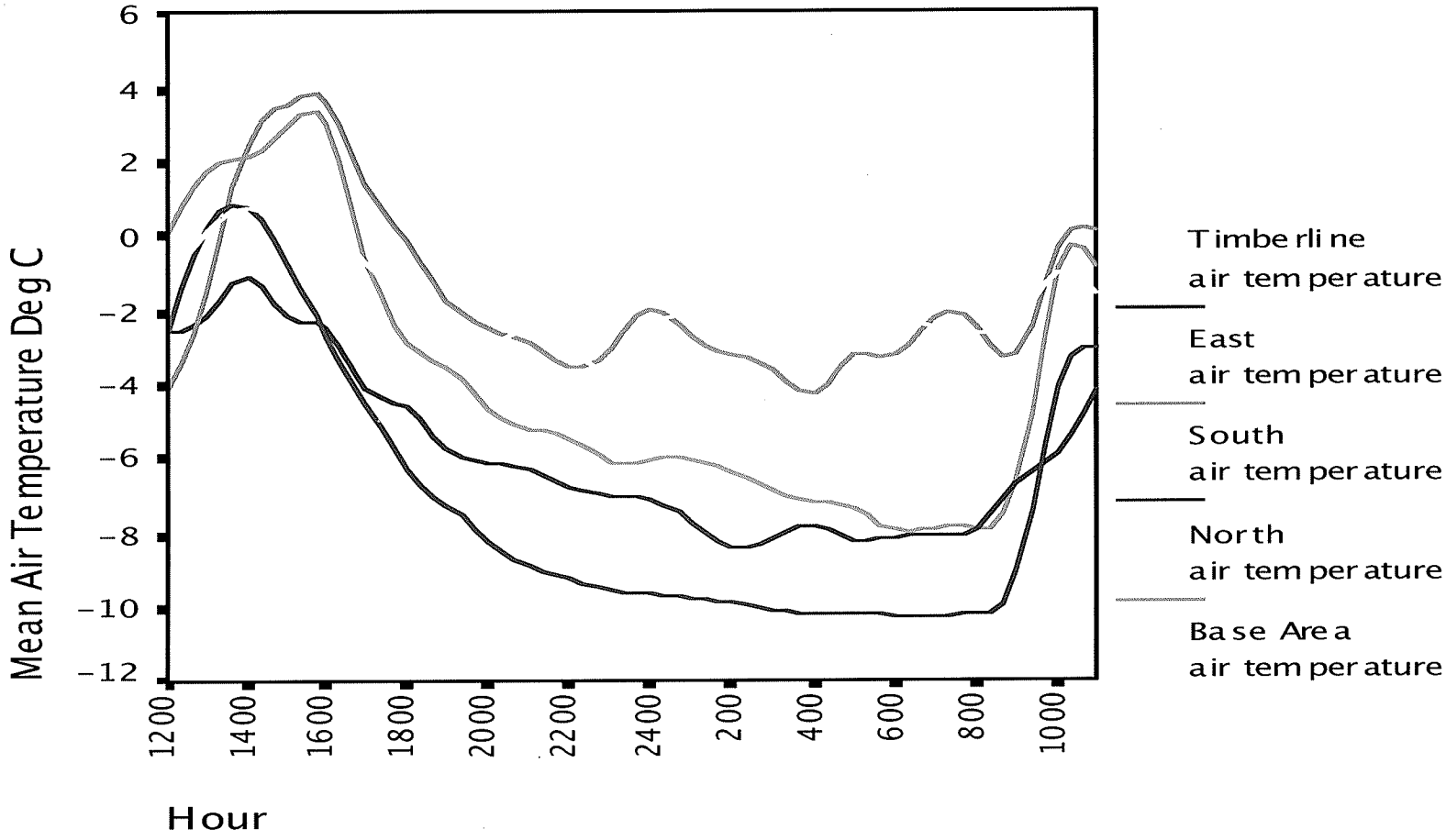

Figure 4.7: The air temperature (° C) at the Timberline snow study site (2858 meters), the east-facing site (2513 meters), the south-facing site (2723 meters), the north-facing site (2538 meters), and the Base Area snow study site (2195 meters) for 24 hours surrounding the surface hoar event on 9 January and 10 January 2004.

Table 4.2: The Man-Whitney U test z-statistic, the two tailed significance level, and the statistical decision between all aspects for the temperature gradients (Table 4.1) at the snow/air interface for 9-10 January 2004.

Aspect	Z-statistic	p-value	Hypothesis
East/South	3.939	0.00	Reject
East/North	-5.444	0.00	Reject
North/South	-4.310	0.00	Reject

Vapor Pressure Gradient The vapor pressure gradients at the snow/air interface on the north-, south-, and east-facing aspects were also studied. Figure 4.8 shows the mean vapor pressure gradient from 1200 hours on 9 January to 1100 hours on 10 January and Table 4.3 shows the median, minimum, and maximum vapor pressure gradients from 1600 hours on 9 January to 0700 hours on 10 January. The results are similar to the temperature gradient section above.

The north-facing aspect had the highest vapor pressure gradient of the three aspects and was never negative. Therefore, it should have had the ability to produce larger, more advanced surface hoar than the south-facing and east-facing aspects on which the vapor pressure gradients were much lower. The median (15.3 mb m^{-1}) vapor pressure gradient on the north-facing aspect was more than 2 times the south-facing aspect (7.3 mb m^{-1}), and the maximum vapor pressure gradient (25.2 mb m^{-1}) on the north-facing aspect was more than 2 times the maximum on the south-facing aspect (10.8 mb m^{-1}). The median vapor pressure gradient on the east-facing aspect (-5.8 mb m^{-1}) did not reach

Figure 4.8: The mean vapor pressure gradient by hour from 1200 hours on 9 January 2004 to 1100 hours on 10 January 2004 on the east- facing, south-facing, and north-facing aspects at the snow/air interface.

into the positive, surface hoar-forming realm, precluding surface hoar formation on the east-facing aspect.

The larger crystals observed on the north-facing aspect can be explained by larger temperature and vapor pressure gradients on the north-facing aspect. To determine why there was such a large difference in temperature and vapor pressure gradients on different slope aspects, meteorological variables that are known to affect surface hoar formation were investigated, including incoming shortwave radiation, wind speed, and relative humidity.

Meteorological Variables The south-facing site reached a maximum amount of incoming shortwave radiation of more than 500 W m^{-2} at about 1300 hours at the same time the north-facing site reached its maximum of about 150 W m^{-2} (Figure 4.9). So the south-facing aspect received more than 3 times the amount of incoming shortwave radiation as the north- facing aspect. The amount of incoming shortwave radiation incident on the north-facing slope also

Table 4.3: The median, minimum, and maximum nighttime vapor pressure gradient (mb m^{-1}) from 1600 hours on 9 January 2004 to 0700 hours on 10 January 2004.

Aspect	N	Median	Minimum	Maximum
East	15	-5.8 mb m^{-1}	-6.2 mb m^{-1}	1.54 mb m^{-1}
South	15	7.3 mb m^{-1}	3.5 mb m^{-1}	10.8 mb m^{-1}
North	15	15.3 mb m^{-1}	12.4 mb m^{-1}	25.2 mb m^{-1}

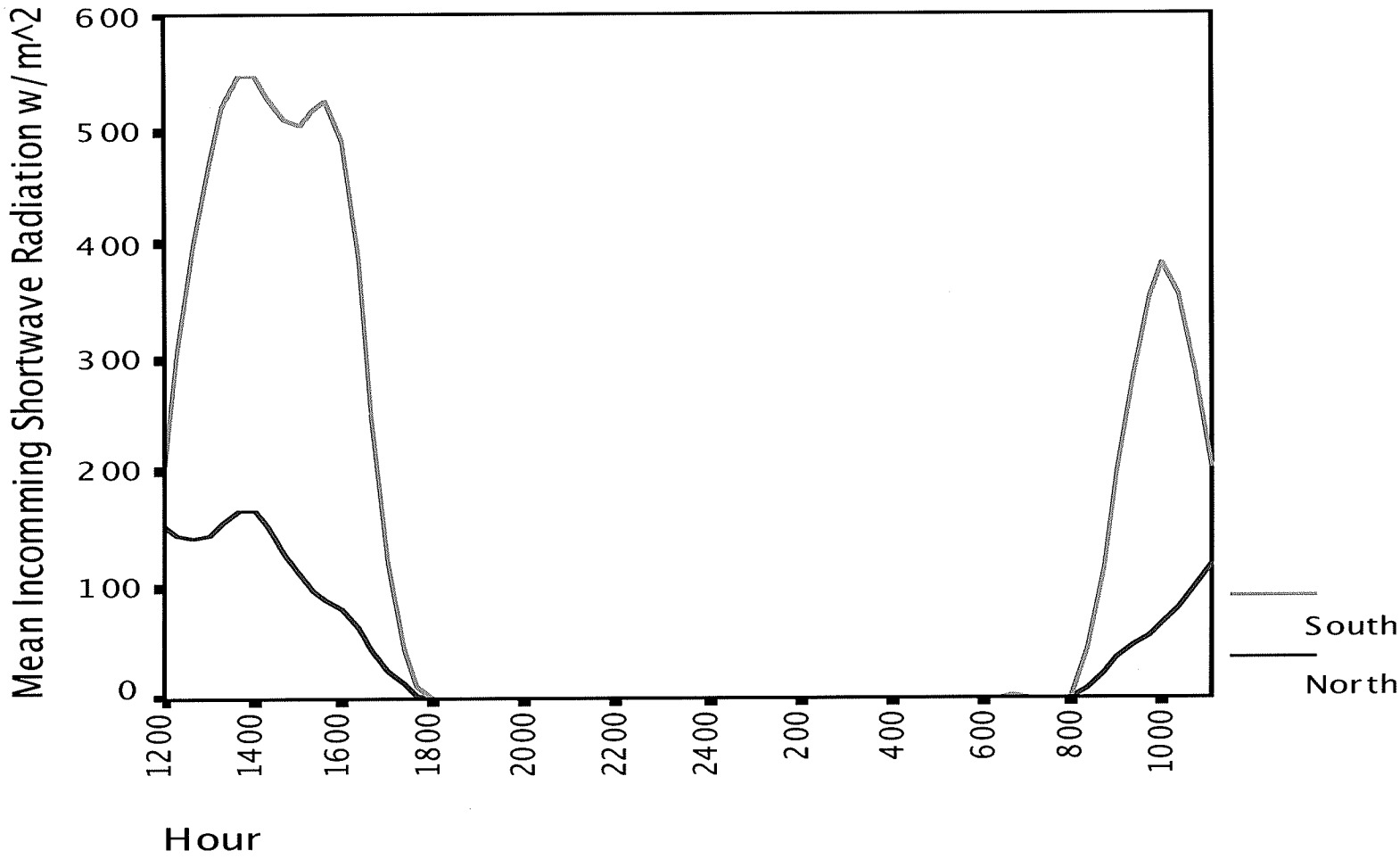

Figure 4.9: The mean incoming shortwave radiation (W m^{-2}) by hour from, 1200 hours on 9 January 2004 to 1100 hours on 10 January 2004 measured at the north-facing and south-facing study sites.

began to fall at about 1400 hours dropping below 100 W m^{-2} by 1500 hours. It is not until 2 hours later that the incoming shortwave radiation on the south-facing aspect dropped below 100 W m^{-2}. The large input of shortwave radiation on the south-facing aspect resulted in a warmer snow surface temperature on the south-facing aspect than on the north-facing aspect (Figure 4.10) by 2-4° C, resulting in smaller temperature and vapor pressure gradients on the south-facing aspect and, consequently, smaller surface hoar crystals. Bakermans (2006) and Bakermans and Jamieson (2006) report similar results.

The wind speed on all three aspects was close to the range of 2-3 m s^{-1} reported by Colbeck (1988) and Hachikubo and Akitaya (1997 a, b) for optimal surface hoar formation (Figure 4.11). However, the average speed on the south-facing site was about 1-2 m s^{-1} higher than the north-facing and east-facing sites and may have helped to limit the growth of the surface hoar crystals on the south-facing aspect.

The maximum relative humidity occurred during the day on 9 January and by 1900 hours began to fall drastically (Figure 4.12). When the relative humidity was at its peak, temperature and vapor pressure gradients on the north-facing slope were higher than on the south-facing aspect. It may have been possible for surface hoar formation to begin earlier on the north-facing aspect than on the south-facing aspect. The relative humidity was never over 90%, which Hachikubo and Akitaya (1997a) reported as necessary for surface hoar formation. In fact, the relative humidity was below 60% for approximately

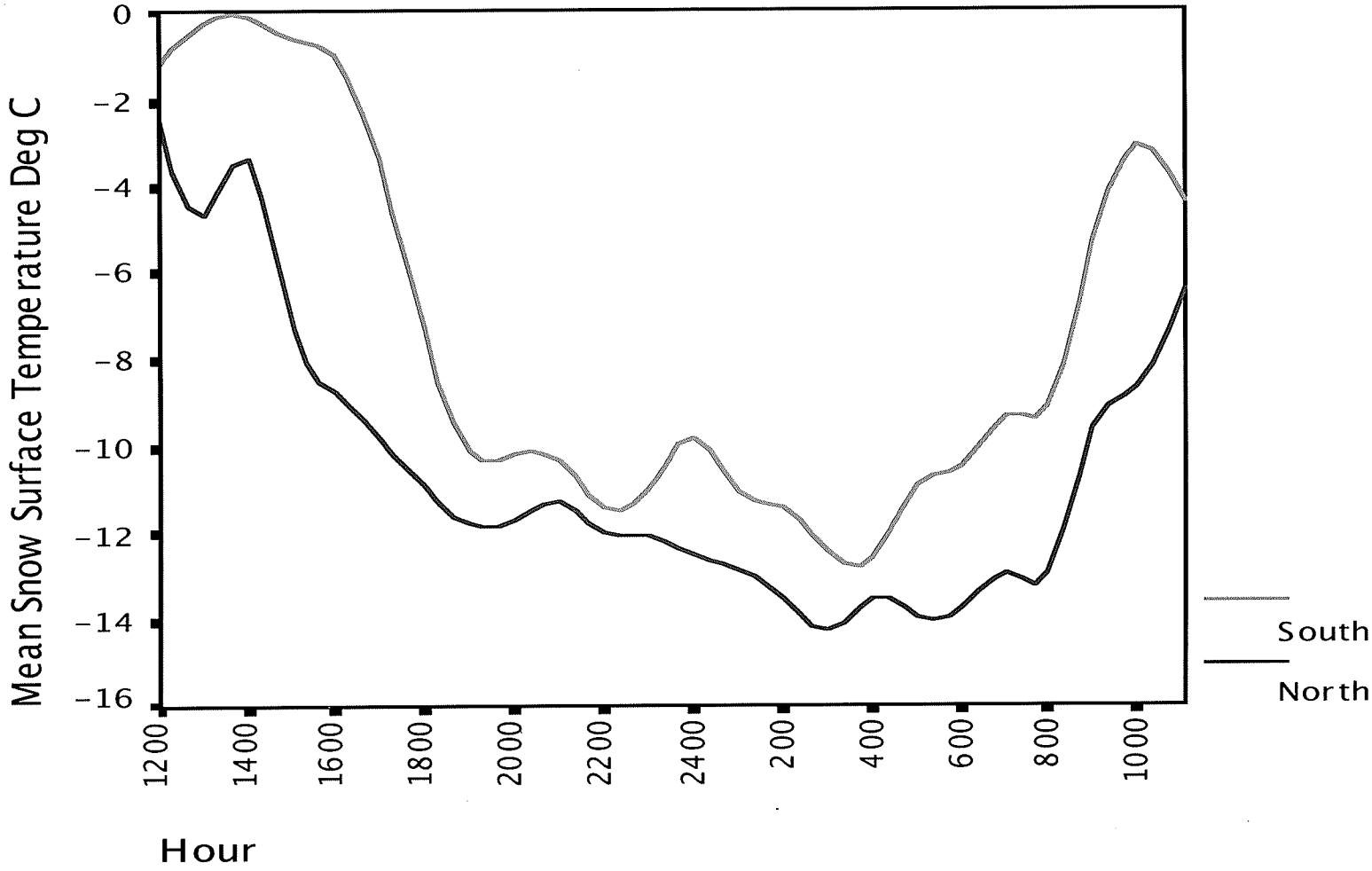

Figure 4.10: The mean snow surface temperature (° C) by hour from 1200 hours on 9 January 2004 to 1100 hours on10 January 2004 on north-facing and south-facing aspect.

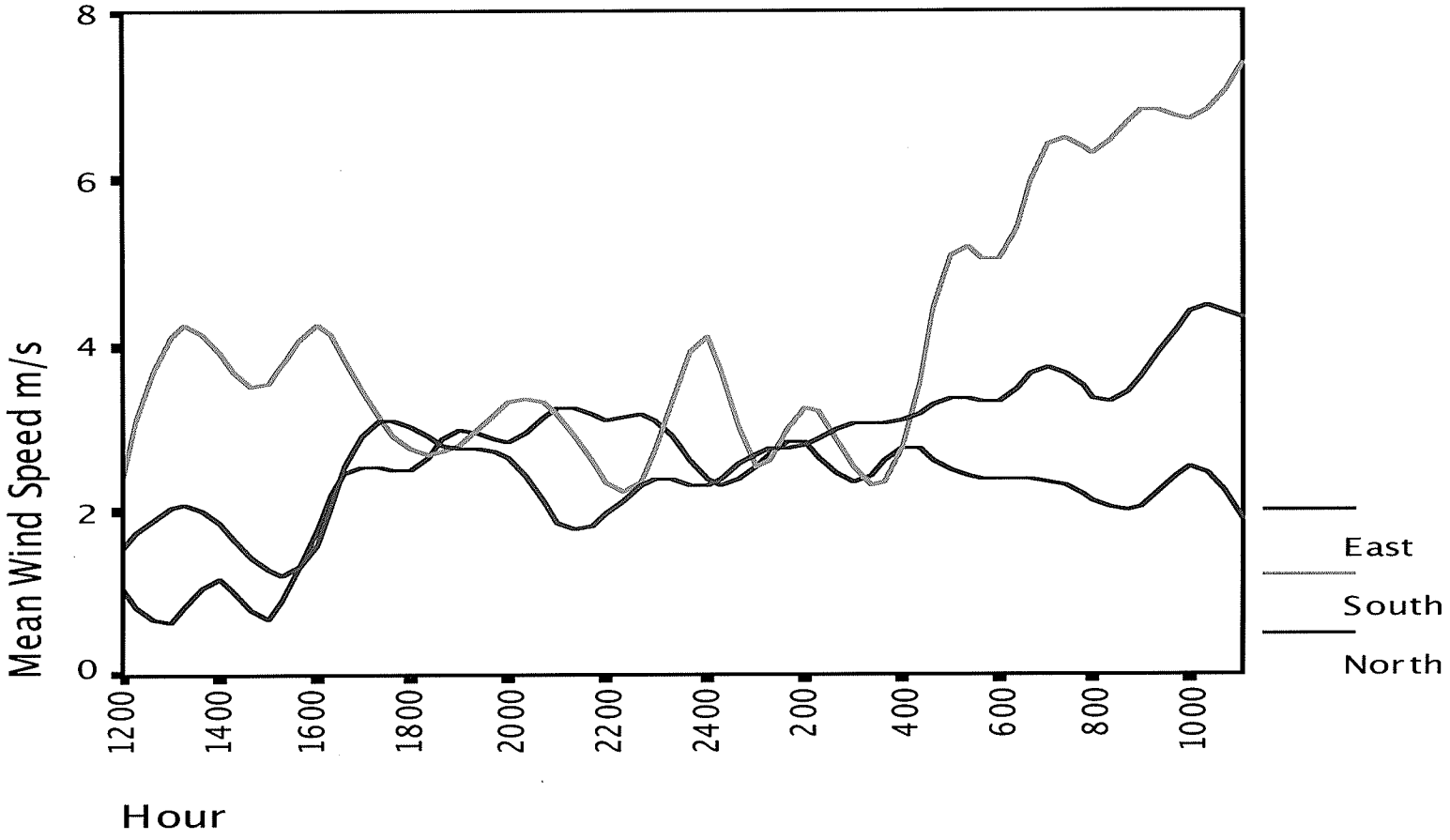

Figure 4.11: The mean wind speed (m s^{-1}) by hour from, 1200 hours on 9 January 2004 to 1100 hours on 10 January 2004 on north-facing, south-facing, and east-facing aspects.

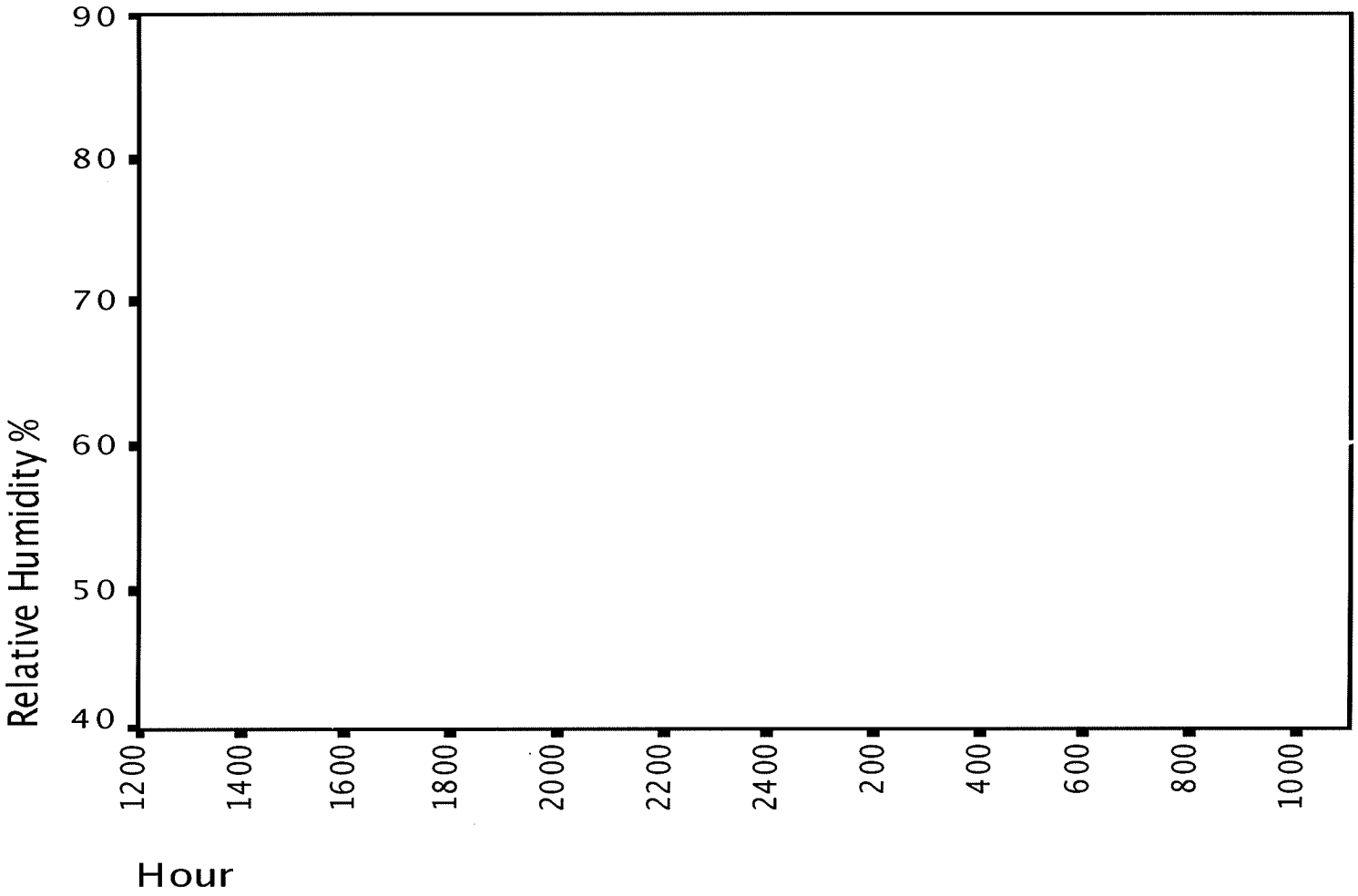

Figure 4.12: The mean relative humidity (%) by hour from, 1200 hours on 9 January 2004 to 1100 hours on 10 January 2004 measured at the Timberline Snow Study Site.

11 hours during the 24-hour period surrounding the surface hoar event. This may show that relative humidity numbers previously reported may be much higher than necessary for surface hoar formation to occur.

The large difference in temperature and vapor pressure gradients between the north-facing and south-facing aspects appears to be caused by greater inputs of shortwave solar radiation on the south-facing aspect than on the north-facing aspect during the day (Figure 4.9). This leads to an overall warmer snow surface temperature on the south-facing aspect (Figure 4.10). The nighttime longwave radiation losses on the south-facing aspect must first overcome the daytime shortwave radiation gains before the snow surface can be cooled enough to form substantial temperature and vapor pressure gradients. The north-facing site, which did not receive as much shortwave radiation during the day, does not have to overcome large shortwave gains in order for the snow surface to be cooled. Therefore, a stronger temperature gradient forms more quickly on the north-facing aspect than on the south facing aspect and the surface hoar crystals grow larger on the north-facing aspect than on the south-facing aspect. The east-facing aspect, on the other hand, did not form any surface hoar crystals during this period. The lack of surface hoar formation on the east-facing aspect appears to have been caused by a localized topographically induced meteorological process which trapped cold air over the east-facing aspect.

Surface Hoar Layer 13 January 2004

The surface hoar layer that formed on 9-10 January was not buried by a subsequent snowstorm and there was no sign of surface hoar crystals on the north- or south-facing aspects by the morning of 11 January. The Yellowstone Mountain Club's morning (0700 hour) meteorological observations for 12 January reported clear skies and ridge top winds averaging 6 m s^{-1} from the southwest. The temperature was 6° C. The afternoon (1600 hour) observations reported clear skies, which remained throughout the rest of the night and into the morning of 13 January (Appendix A). By 0800 hours on 13 January, it was apparent that another layer of surface hoar had formed over night. The study sites were visited quickly, crystals were collected, and the second day of the study began.

Crystal Characteristics Surface hoar was again noted on the north-facing and south-facing aspects, and this time also on the east-facing aspect, on the morning of 13 January. Snow crystals collected from the snow surface on the south-, north-, and east-facing study sites, at 0835, 0900, and 0945 hours respectively on the morning of 13 January were clearly identifiable as type 7a, feather-shaped, surface hoar as classified by Colbeck et al. (1990). The crystals collected from the north-facing aspect (Figure 4.13) were significantly larger ($p= 0.031$) and better developed, with more striations, than those collected on the south-facing aspect (Figure 4.14). The crystals collected from the east-facing aspect were more similar to those on the north-facing aspect ($p= 0.22$), but the size distribution was larger (Figure 4.15). The crystals, especially on the north-

facing and east-facing slopes, seemed to be more fragile than the crystals that formed on 10 January resulting in many broken crystals during transport to the cold lab. Laboratory measurements confirmed that the crystals that formed on the north-facing aspect had a median size of 8.5 mm and were larger than the crystals that formed on the east-facing and south-facing aspects which had a median size of 8 mm and 5 mm respectively (Figure 4.16).

Again there was a disparity in crystal size and the characteristics of the crystals that formed on 12-13 January among aspects. Therefore, the temperature and vapor pressure gradients on all three aspects were compared to determine if the gradients differed by slope aspect and if, consequently, the disparity in crystal size could be attributed to differences in these gradients alone.

Temperature Gradient The median, minimum, and maximum nighttime temperature gradients from 1600 hours on 12 January to 0700 hours on 13 January on the north-facing aspect far exceeded the south-facing and east-facing aspects, and the temperature gradients on the east-facing aspect also exceeded the temperature gradients on the south-facing aspect (Table 4.4). In fact, the minimum nighttime temperature gradient (86.0° C m^{-1}) on the north-facing slope was more than 3 times the maximum gradient on the south-facing aspect (27.5° C m^{-1}), and the minimum temperature gradient on the east-facing aspect (38.4° C m^{-1}) also exceeded the maximum temperature gradient on the south-facing aspect.

Figure 4.13: A 11mm surface hoar crystal harvested from the north-facing study site on 13 January 2004. This crystal is classified by Colbeck et al. (1990) as type 7a.

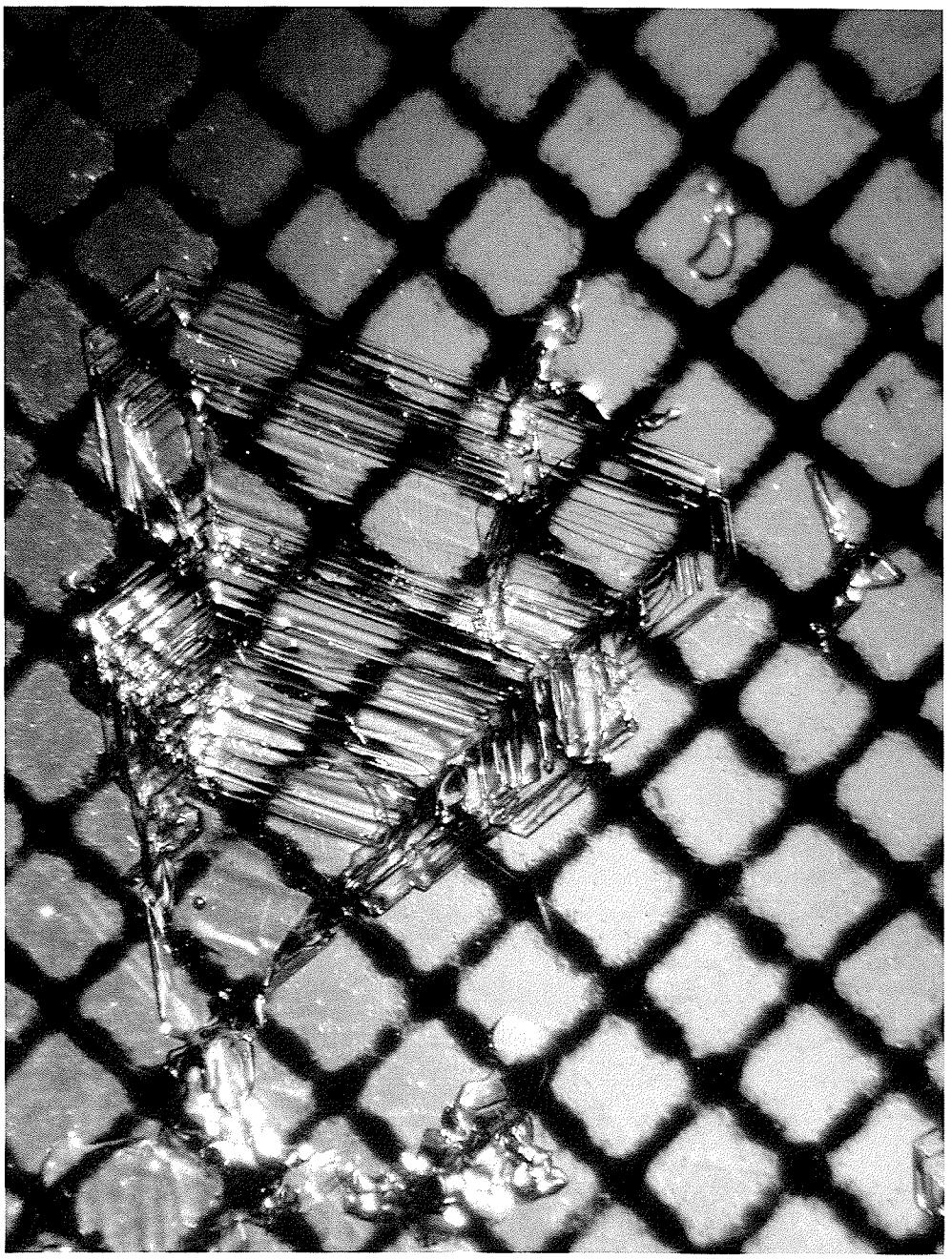

Figure 4.14: A 7.5 mm surface hoar crystal harvested from the east-facing study site on 13 January 2004. This crystal is classified by Colbeck et al. (1990) as type 7a.

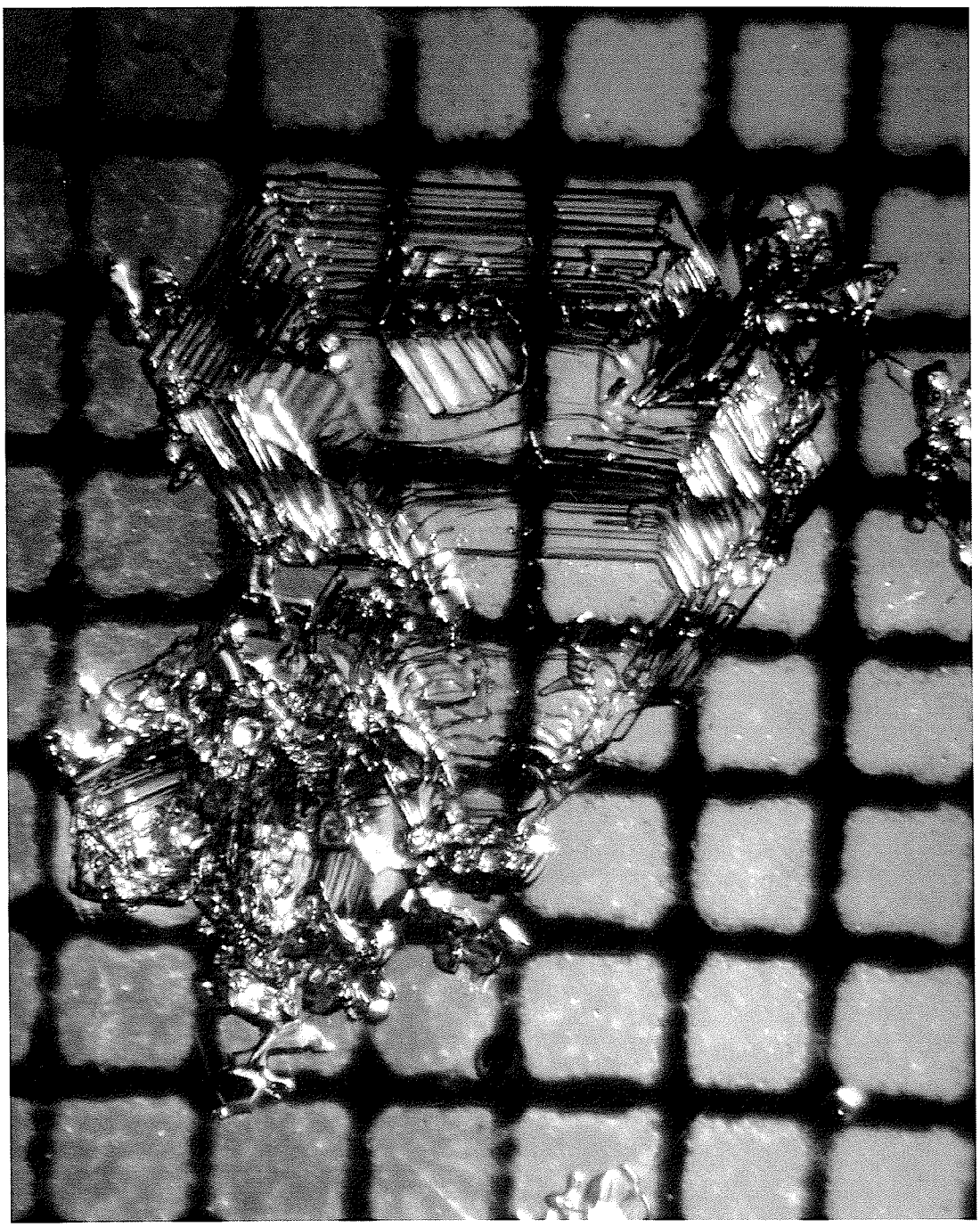

Figure 4.15: A 5.5 mm surface hoar crystal harvested from the south-facing study site on 13 January 2004. This crystal is classified by Colbeck et al. (1990) as type 7a.

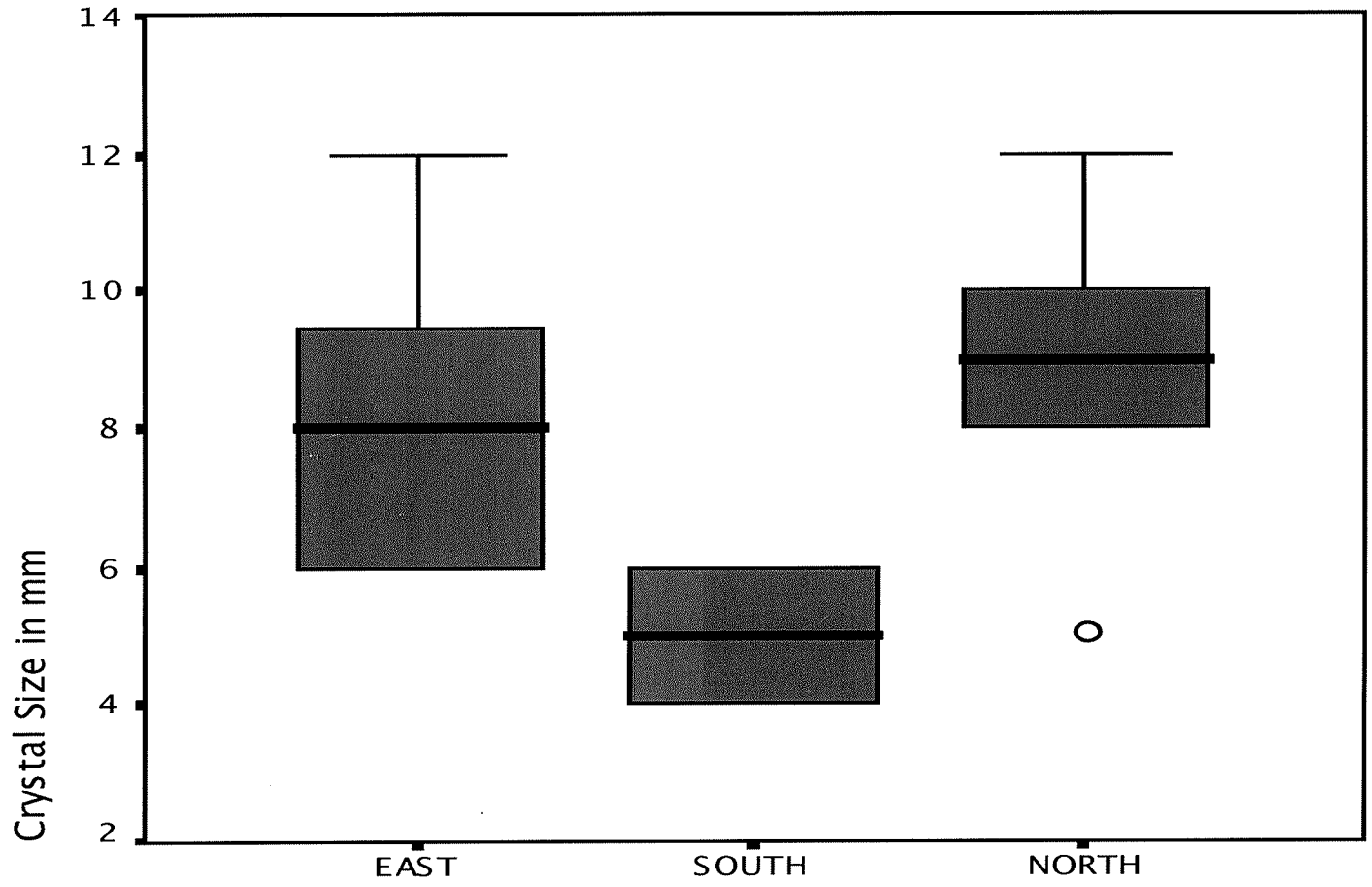

Figure 4.16: Box plot of crystal size in mm on 13 January 2004 versus slope aspect. The surface hoar crystals on the north aspect grew large than those on the south, but about the same size as those on the east. The Box plots show the median (darker black line), interquartile range (top and bottom of the box), and the minimum and maximum crystal size (the whiskers). N = 15 crystals on the North, South, and East aspects.

Table 4.4: The median, minimum, and maximum nighttime temperature gradient (° C m^{-1}) from 1600 hours on 12 January 2004 to 0700 hours on 13 January 2004.

Aspect	N	Median	Minimum	Maximum
East	16	59.1° C m^{-1}	38.4° C m^{-1}	76.6° C m^{-1}
South	16	18.0° C m^{-1}	4.0° C m^{-1}	27.5° C m^{-1}
North	16	92.4° C m^{-1}	86.0° C m^{-1}	105.0° C m^{-1}

The maximum temperature gradient reached on the north-facing aspect (105.0° C m^{-1}) was more than 3 times that reached on the south-facing aspect (27.5° C m^{-1}) (Table 4.4). The maximum temperature gradient reached on the east-facing aspect (76.6° C m^{-1}) was almost 3 times that reached on the south-facing aspect and seemed to fall nicely between the temperature gradients on north-facing and south-facing aspects. The hypothesis of equality was rejected in all cases (Table 4.5).

Table 4.5: The Man-Whitney U test z-statistic, the two tailed significance level, and the statistical decision between all aspects for the temperature gradients (Table 4.4) at the snow/air interface for 12-13 January 2004.

Aspect	Z-statistic	p-value	Hypothesis
East/South	-4.825	0.00	Reject
East/North	-4.825	0.00	Reject
North/South	-4.820	0.00	Reject

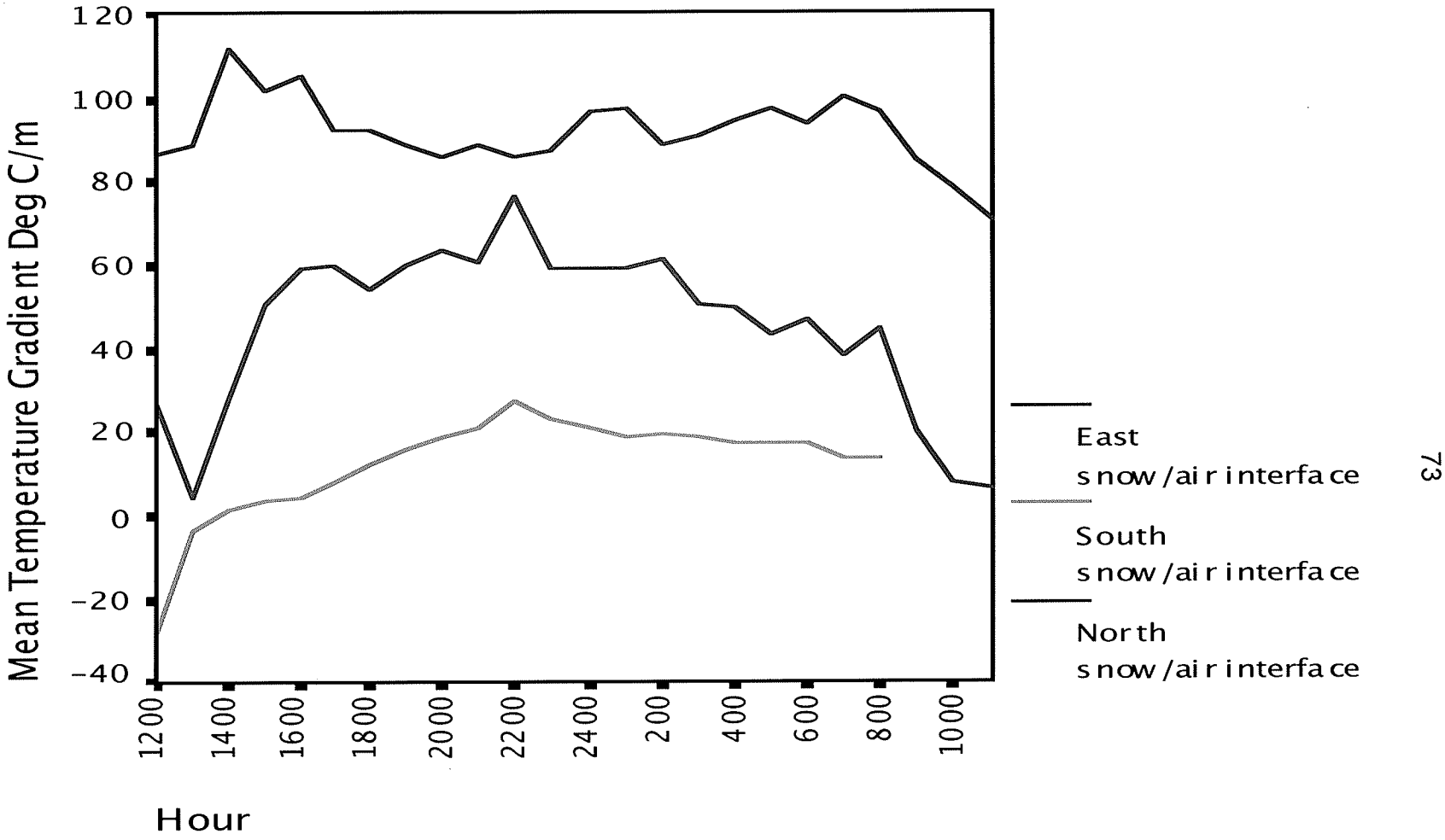

Figure 4.17: The mean temperature gradient by hour from 1200 hours on 12 January 2004 to 1100 hours on 13 January 2004 on the north-facing, south-facing, and east-facing aspects at the snow/air interface.

Vapor Pressure Gradients The results are similar to those for the temperature gradient section. The north-facing aspect had the highest vapor pressure gradient. The maximum vapor pressure gradient on the north-facing aspect occurred at 1400 hours, while the maximum vapor pressure gradient on the south-facing and east-facing aspects did not occur until 2200 hours. In addition the north-facing and east-facing aspects did not go into the negative realm while the south-facing aspect did. The north-facing and east-facing aspects both had a significantly larger vapor pressure gradient than the south-facing aspect ($z = <0.000$) (Figure 4.18).

The north aspect had larger positive temperature and vapor pressure gradients and, subsequently, the surface hoar crystals that formed on the north-facing aspect grew to an average size of 8.5 mm, 3 mm larger than the crystals on the south-facing slope, but about the same size as the crystals on the east-facing slope which averaged about 8 mm. Because there was a statistically significant difference in the temperature and vapor pressure gradients on the north-, south-, and east-facing aspects which caused the surface hoar crystals to grow to different sizes, the meteorological variables that are known to affect the temperature and vapor pressure gradients and, consequently, to cause facet formation were again investigated.

Meteorological Variables The south-facing site received a maximum amount of incoming shortwave radiation of more than 800 W m^{-2} at about 1200 hours at the same time the north-facing site reached its maximum of about

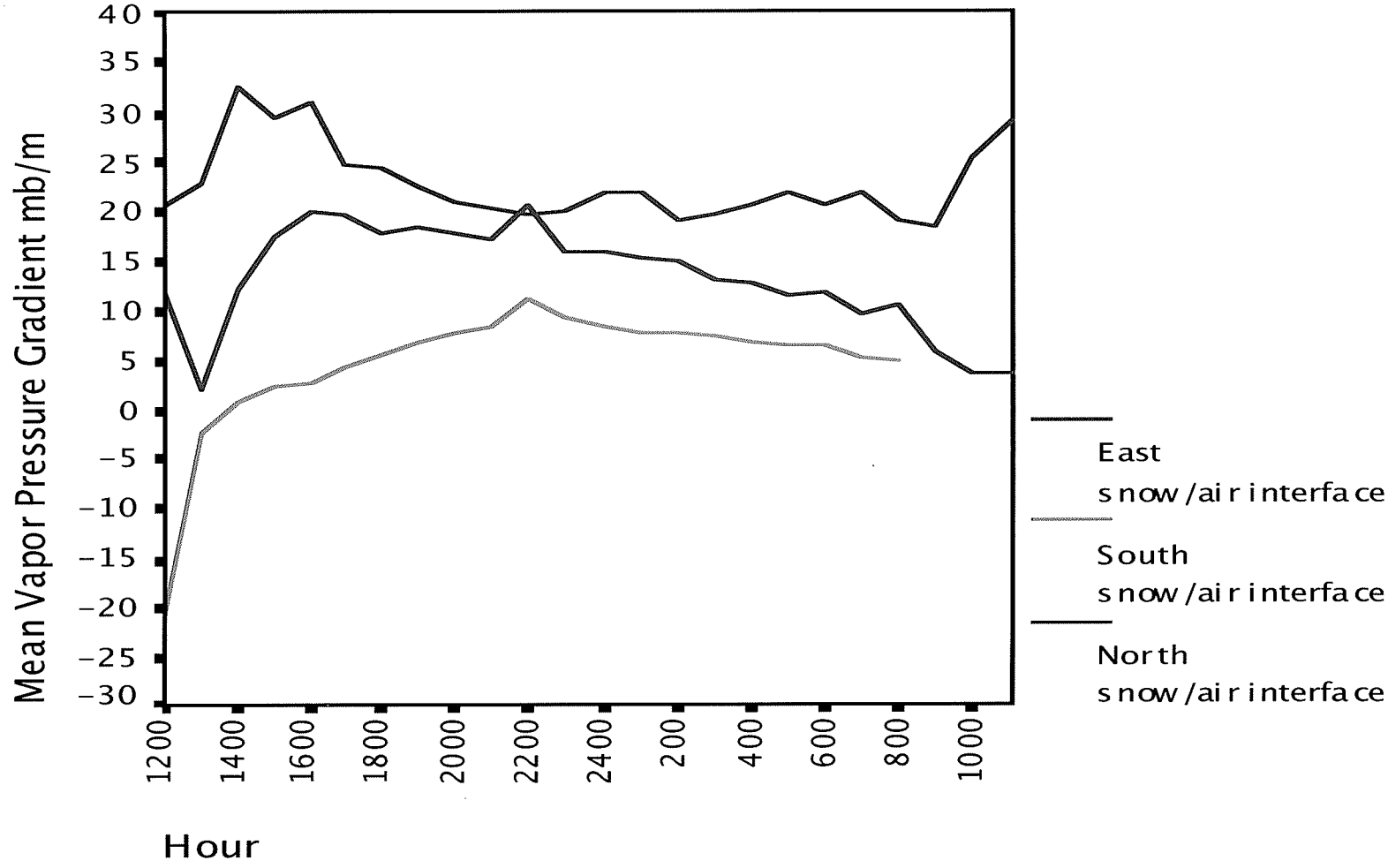

Figure 4.18: The mean vapor pressure gradient by hour from 1200 hours on 12 January 2004 to 1100 hours on 13 January 2004 on the north-facing, south-facing, and east-facing aspects at the snow/air interface.

125 W m^{-2} (Figure 4.19). Thus, the south-facing received more than 6 times the amount of incoming shortwave radiation as the north-facing aspect. The amount of incoming shortwave radiation incident on the north-facing slope also began to fall at about 1400 hours, dropping quickly below 100 W m^{-2}. It was not until 2 hours later that the south-facing slope dropped below 100 W m^{-2}. The larger input of shortwave radiation on the south-facing aspect resulted in a warmer snow surface temperature on the south-facing aspect than on the north-facing aspect (Figure 4.20). The snow surface temperature on the north-facing aspect was always colder than the snow surface temperature on the south-facing aspect. Neither the incoming shortwave radiation nor the snow surface temperature were measured on the east-facing aspect, so unfortunately, comparisons could not be made.

Figure 4.21 shows mean wind speeds (m s^{-1}) at 1 meter above the snow surface on the north-facing, south-facing, and east-facing aspects for the 24-hour period surrounding the surface hoar event. The wind speeds on all three aspects were close to the range reported by Colbeck (1988) and Hachikubo and Akitaya (1997 a, b) for optimal surface hoar formation (2-3 m s^{-1} at 1 meter above the snow surface). The average speed on the south-facing site was about 1-2 m s^{-1} higher than on the north-facing and east-facing sites during the daylight hours, so it probably did not preclude maximum surface hoar growth on that aspect.

Figure 4.22 shows the mean relative humidity (%) at the Timberline Snow Study Site for the 24-hour period surrounding the surface hoar event. As seen in

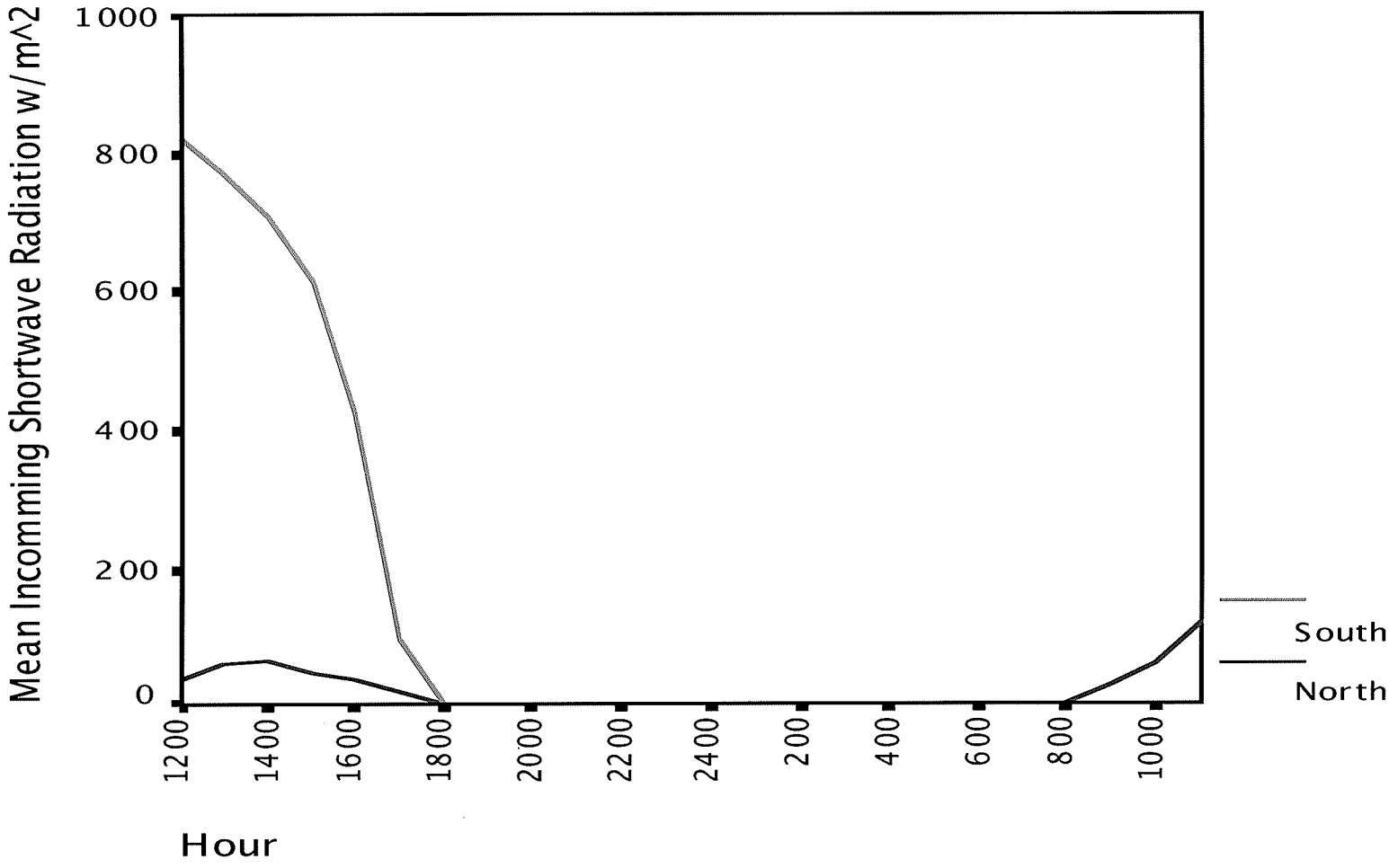

Figure 4.19: The mean incoming shortwave radiation (W m^{-2}) by hour from, 1200 hours on 12 January 2004 to 1100 hours on 13 January 2004 measured at the north-facing and south-facing study sites.

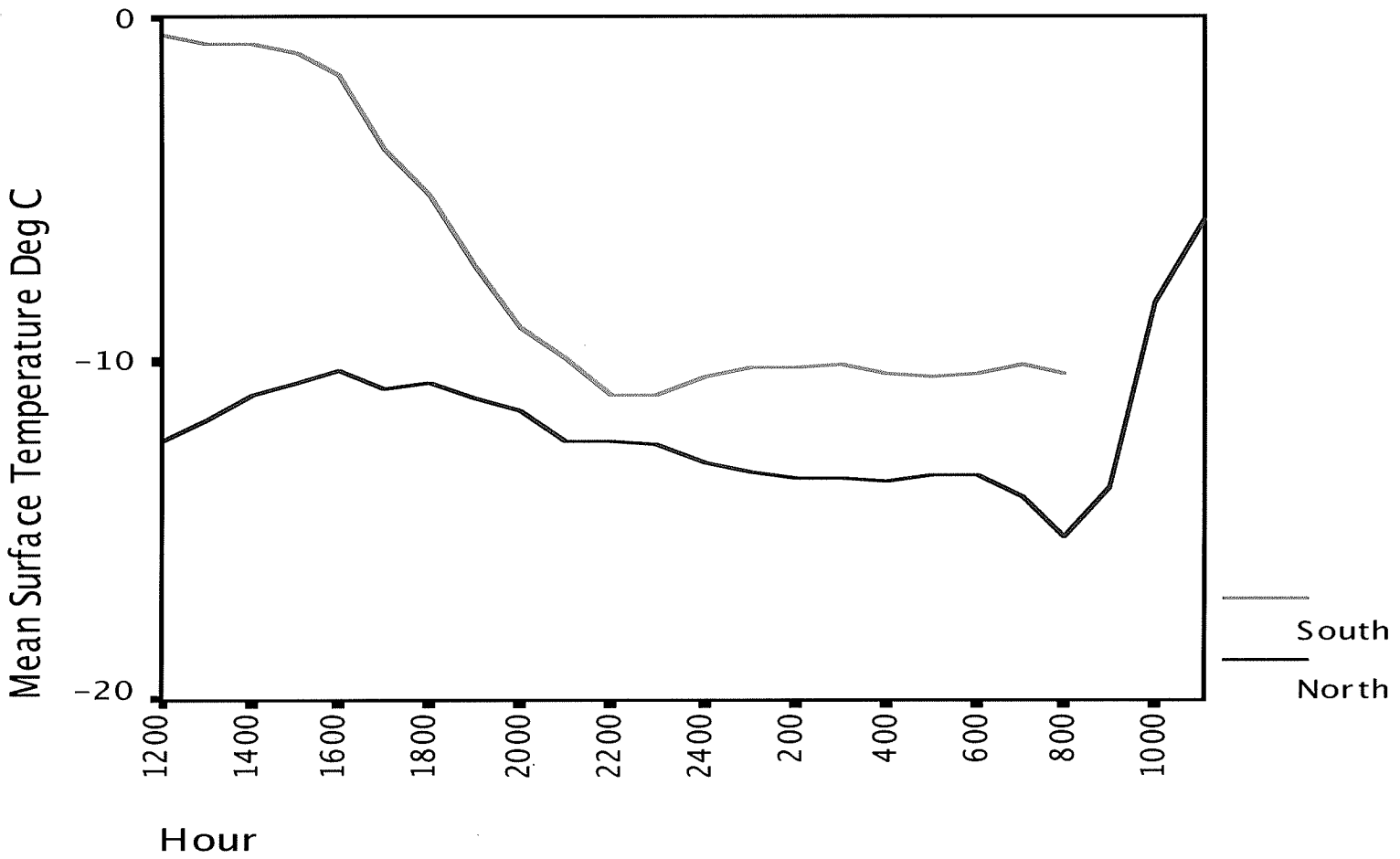

Figure 4.20: The mean snow surface temperature (° C) by hour from 1200 hours on 12 January 2004 to 1100 hours on 13 January 2004 on north-facing and south-facing aspect.

Figure 4.22, the maximum relative humidity (65%) occurred at about 0200 hours on the morning of 13 January. The relative humidity was much lower than the 90% that Hachikubo and Akitaya (1997a) reported as necessary for surface hoar formation. In fact, the relative humidity was below 60% for approximately 23 hours during the 24-hour period surrounding the surface hoar event, but clearly the relative humidity was high enough for surface hoar growth. The maximum relative humidity occurred while all aspects were above the critical temperature and vapor pressure gradient thresholds, indicating that the value of the temperature and vapor pressure gradients may be more important for surface hoar formation than the value of the relative humidity.

Again the large difference in temperature and vapor pressure gradients between the north- and south-facing aspects appears to be caused by greater inputs of shortwave solar radiation on south-facing aspects than on north-facing aspects (Figure 4.19) during the day. This leads to an overall warmer snow surface temperature on south-facing aspects (Figure 4.20). The nighttime longwave radiation losses on the south-facing aspect have to first overcome the daytime shortwave radiation gains before the snow surface can be cooled enough to form a temperature and vapor pressure gradient sufficient for facet formation. The north-facing aspect, which does not receive as much shortwave radiation during the day, does not have to overcome big shortwave gains in order for the snow surface to be cooled; therefore, a stronger temperature gradient forms more quickly on the north-facing aspect than on the south-facing aspect

Figure 4.21: The mean wind speed (m s^{-1}) by hour from, 1200 hours on 12 January 2004 to 1100 hours on 13 January 2004 on north-facing, south-facing, and east-facing aspects.

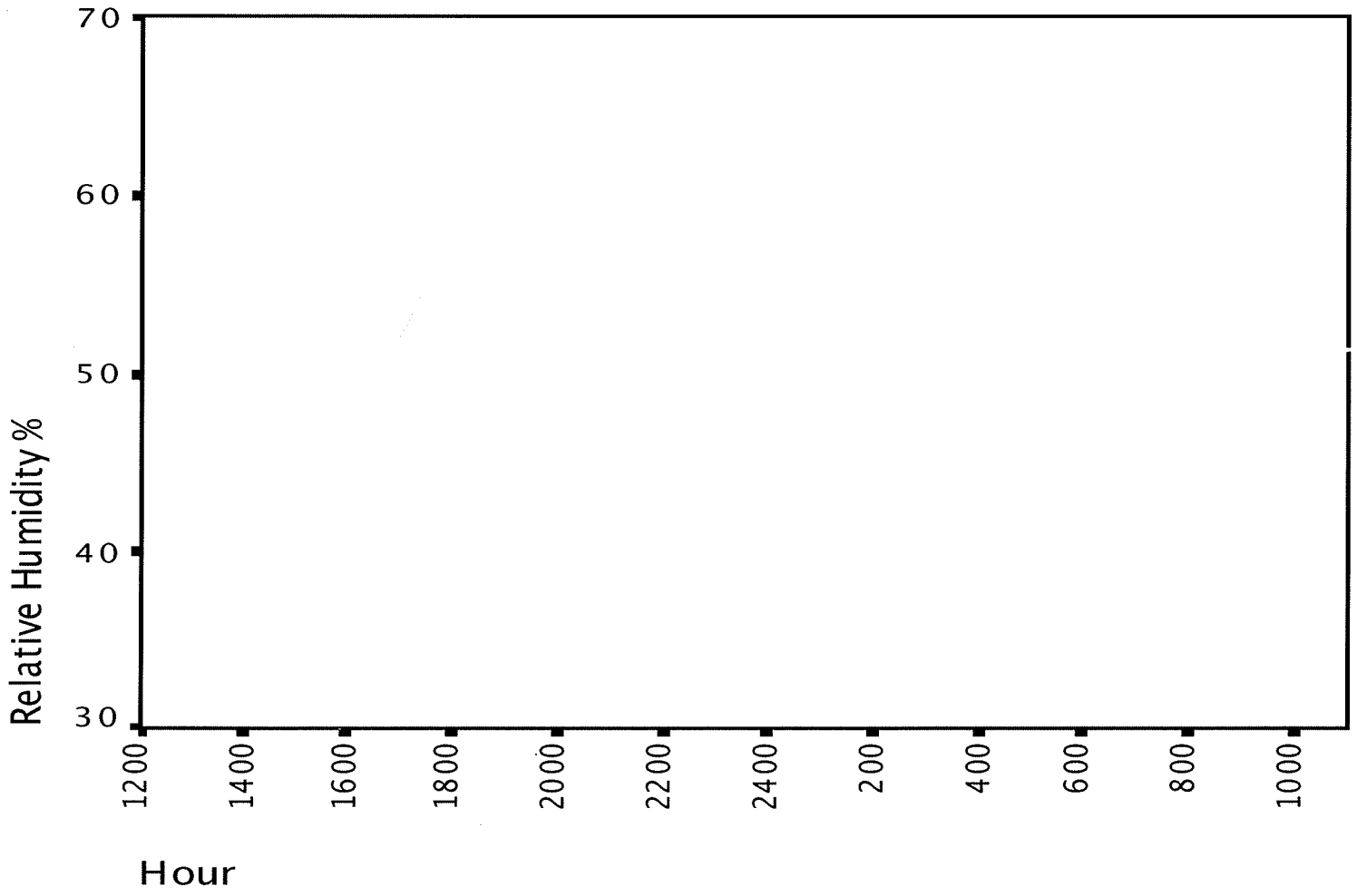

Figure 4.22: The mean relative humidity (%) by hour from, 1200 hours on 12 January 2004 to 1100 hours on 13 January 2004 measured at the Timberline Snow Study Site.

and the surface hoar crystals grow larger on the north-facing aspect than on the south-facing aspect. The east-facing aspect, on the other hand, is probably intermediate between the north- and south-facing aspects. In the morning the east-facing slope is in direct sun and probably receives a maximum amount of incoming shortwave radiation but by the afternoon this site is in the shade and cools off faster than the southerly aspects.

Aspect Comparison During Overcast Conditions 24 January 2004

To see if there were differences based on slope aspect on days when surface hoar did not form, a comparison was made of the temperature and vapor pressure gradients and the meteorological variables necessary for surface hoar formation on 23-24 January, a date randomly selected from available overcast days. The 0700 hour morning observations on 23 January reported overcast skies, due to a low-pressure system that was centered just south of Montana. The skies remained overcast for the next 9 days. Five centimeters of new snow fell during the evening and night of 23-24 January (Appendix A). On the morning of 24 January the study sites were visited and the snow surface was viewed through a 20x hand lens. No surface hoar was found.

Crystal Characteristics Field notes, recorded at 0830 hours on the north-facing slope, 0915 hours on the south-facing slope, and 1030 hours on the east-facing slope, indicated 2 mm stellar precipitation particles, type 1d, (Colbeck et al. 1990) were present on the north-facing, south-facing, and east-facing aspects.

Since no surface hoar was observed, no crystals were collected, and photographs were not taken.

To see if the temperature and vapor pressure gradients also differed by slope aspect on days when surface hoar did not form, temperature and vapor pressure gradients were graphed by hour from 1200 hours on 23 January to 1100 hours on 24 January on the north-facing, south-facing, and east-facing aspects at the snow/air interface.

Temperature Gradient The nighttime temperature gradients from 1600 hours on 23 January to 0700 hours on 24 January on the north-facing, south-facing, and east-facing aspects at the snow/air interface were mostly negative and were all very small, except for the east aspect on the morning of 24 January. In fact, none of the nightly temperature gradients exceeded 2° C m^{-1} (Table 4.6 and Figure 4.23). The crystals maintained their original form, precipitation particles, and faceting did not occur.

Table 4.6: The median, minimum, and maximum nighttime temperature gradient (° C m^{-1}) from 1600 hours on 23 January 2004 to 0700 hours on 24 January 2004.

Aspect	N	Median	Minimum	Maximum
East	16	-1.4° C m^{-1}	-5.4° C m^{-1}	1.8° C m^{-1}
South	16	-0.0° C m^{-1}	-0.8° C m^{-1}	1.5° C m^{-1}
North	16	-1.2° C m^{-1}	-1.8° C m^{-1}	-0.2° C m^{-1}

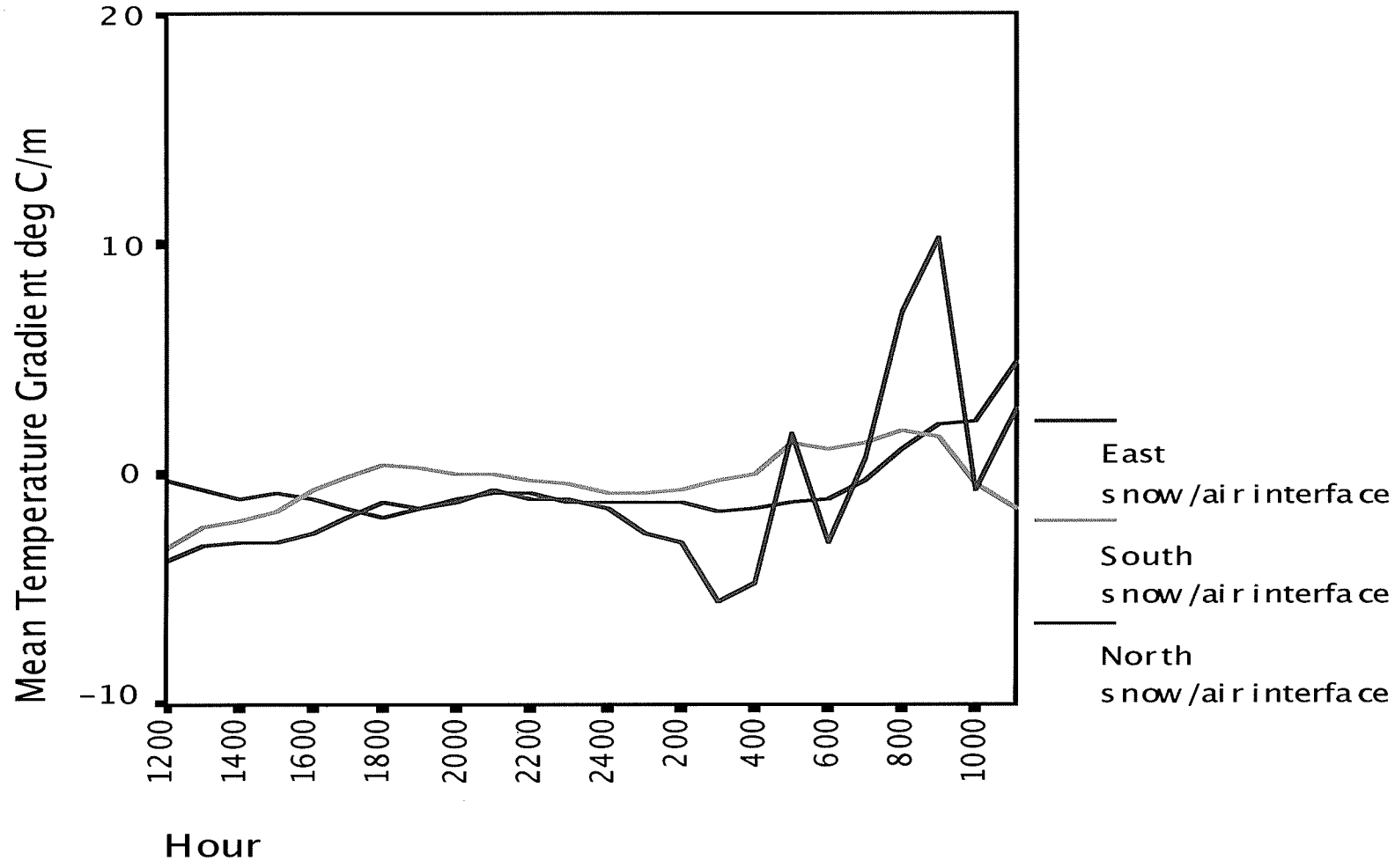

Figure 4.23: The mean temperature gradient by hour from 1200 hours on 23 January 2004 to 1100 hours on 24 January 2004 on the east facing, south facing, and north facing aspects at the snow/air interface.

To test the hypothesis that the slopes have equal nighttime temperature gradients and thus would be from the same or similar populations, a Mann-Whitney U Test was conducted (Table 4.7). The east- and north-facing aspects were statistically similar while the north- and south-facing aspects and the south- and east-facing aspects are statistically different.

Vapor Pressure Gradient The mean and median vapor pressure gradients on all aspects were close to 0 mb m^{-1}, and most of the vapor pressure gradients were negative. In fact, the maximum vapor pressure gradient did not exceed 1 mb m^{-1}, which is not a sufficient gradient for surface hoar formation. The results are similar to those for the temperature gradients (Figure 4.24 and Table 4.8).

Meteorological Variables Neither the north-facing nor the south-facing aspects received more than 250 W m^{-2} of incoming shortwave radiation, and, unlike 9-10 and 12-13 January, the south- facing aspect barely exceeded the north-facing aspect. So the snow surface temperatures on the north-facing and south-facing aspects were always within one to two degrees of each other (Figure 4.25).

Table 4.7: The Man-Whitney U test z-statistic, the two tailed significance level, and the statistical decision between all aspects for the temperature gradients (Table 4.6) at the snow/air interface for 23-24 January 2004.

Aspect	Z-statistic	p-value	Hypothesis
East/South	-3.602	0.00	Reject
East/North	-1.350	0.177	Fail to Reject
North/South	-4.559	0.00	Reject

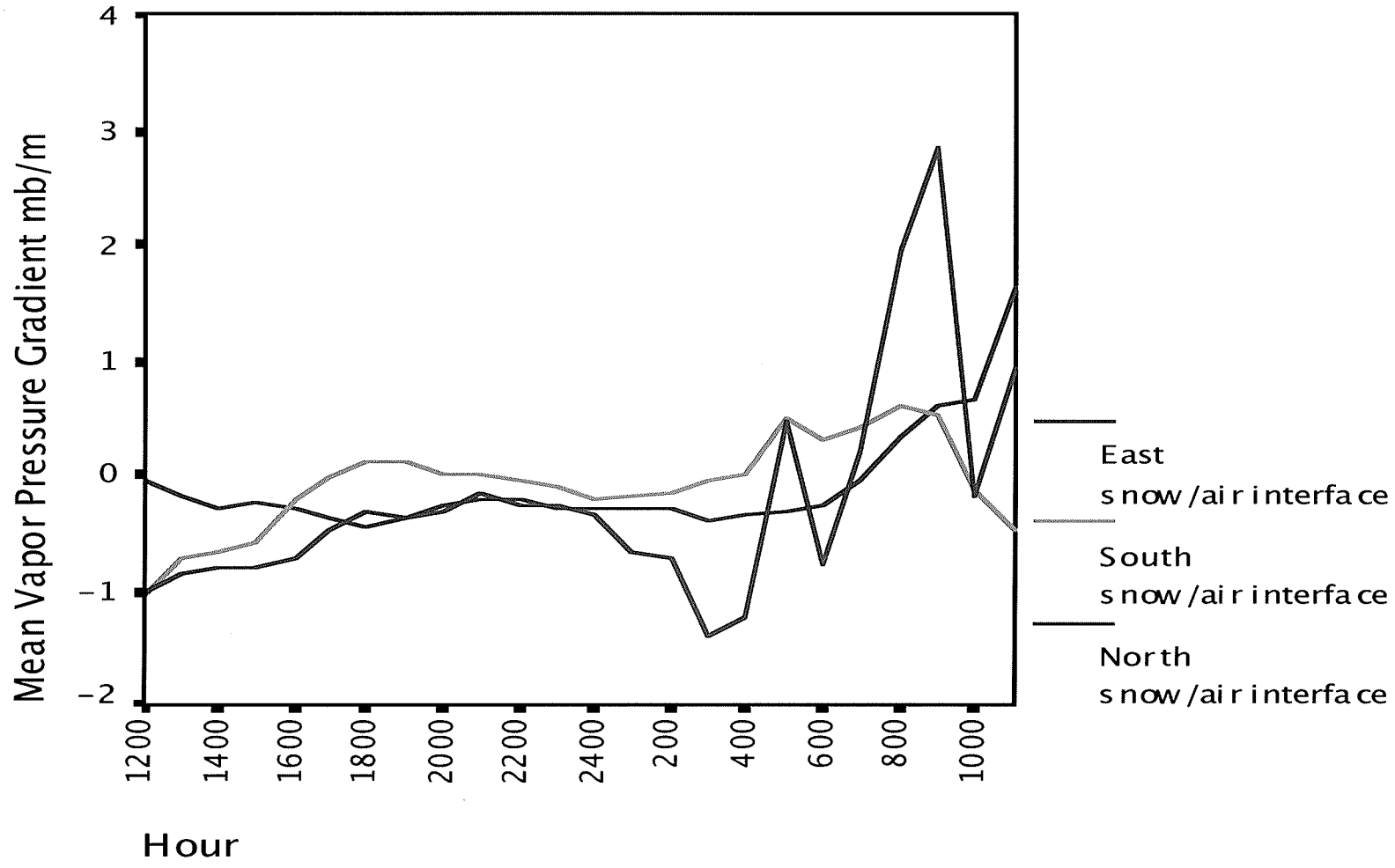

Figure 4.24: The mean vapor pressure gradient by hour from 1200 hours on 23 January 2004 to 1100 hours on 24 January 2004 on the east- facing, south-facing, and north-facing aspects at the snow/air interface.

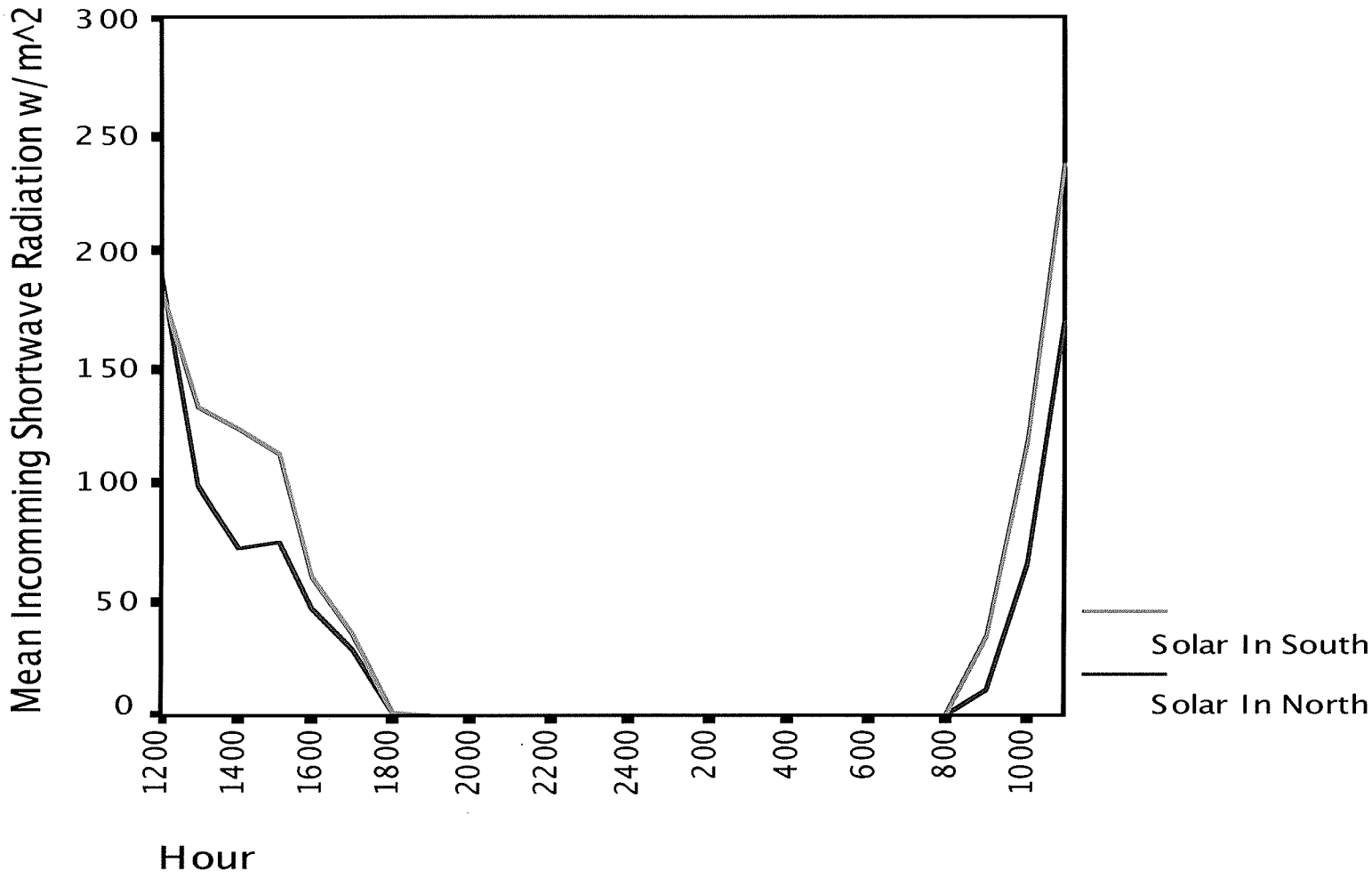

Figure 4.25: The mean incoming shortwave radiation (W m $^{-2}$) by hour from, 1200 hours on 23 January 2004 to 1100 hours on 24 January 2004 measured at the north-facing and south-facing study sites.

Table 4.8: The median, minimum, and maximum nighttime vapor pressure gradient (mb m^{-1}) from 1600 hours on 23 January 2004 to 0700 hours on 24 January 2004.

Aspect	N	Median	Minimum	Maximum
East	16	-.3 mb m^{-1}	-1.3 mb m^{-1}	0.4 mb m^{-1}
South	16	-0.0 mb m^{-1}	-0.2 mb m^{-1}	0.5 mb m^{-1}
North	16	-0.2 mb m^{-1}	-0.4 mb m^{-1}	-0.0 mb m^{-1}

The wind speed on all three aspects was close to the range reported by Colbeck (1988) (Figure 4.26).

The maximum relative humidity (Figure 4.27) was above (90%) until 0400 hours on 24 January, which was high enough for surface hoar formation (Hachikubo and Akitaya 1997a).

During overcast periods, although the temperature and vapor pressure gradients on the north- and south-facing and the south- and east-facing aspects were statistically different, there are smaller differences in temperature and vapor pressure gradients on north-, south-, and east-facing aspects and the gradients are unable to reach large enough levels for surface hoar formation. When the skies are overcast less shortwave solar radiation reaches the snow surface due to reflection and refraction by the clouds, and longwave radiation losses occurring at the snow surface are re-radiated by the clouds keeping the snow surface relatively warm on all aspects. Consequently, strong gradients between the snow and air are minimized and surface hoar formation is precluded on all aspects, the crystals appear to maintain their original shapes, and slope-aspect dependent differences are minimized.

Figure 4.26: The mean wind speed (m s^{-1}) by hour from, 1200 hours on 23 January 2004 to 1100 hours on 24 January 2004 on north-facing, south-facing, and east-facing aspects.

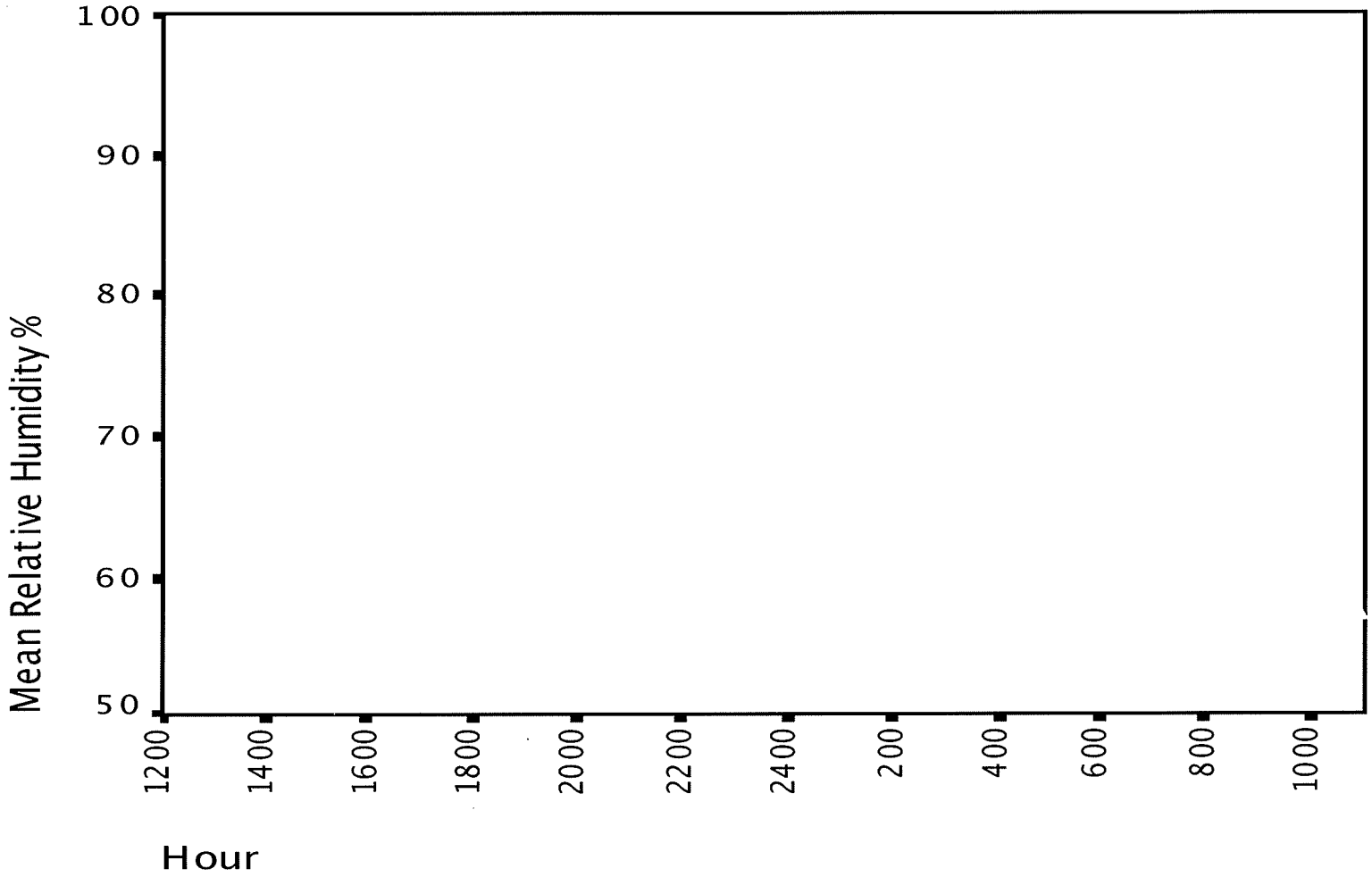

Figure 4.27: The mean relative humidity (%) by hour from, 1200 hours on 23 January 2004 to 1100 hours on 24 January 2004 measured at the Timberline Snow Study Site.

Diurnally Recrystallized Near-Surface Faceted Crystals

Near-Surface Faceted Layer 13 January 2004

Crystal Characteristics Near-surface facets were noted on the south-facing and east-facing aspects on the morning of 13 January. Crystals were collected from -0.05 m on the south-facing study site at about 0935 hours on the morning of 13 January. The crystals were clearly identifiable as type 5a, cup-shaped crystals (Colbeck et al. 1990) and were better developed, with striations and even visible cupping, than those collected from the other aspects (Figure 4.28). At about 1000 hours the same procedure was used to sample the north-facing site. The crystals collected on the north-facing aspect were smaller than those on the east- and south-facing aspects; however, the difference was not easily measurable (Figure 4.29). At about 1025 hours crystals were collected from the east study site and were identified as type 4a, solid faceted particles, (Colbeck et al. 1990). The crystals collected from the east-facing aspect were obviously faceted but were not striated or cupped as they were on the south-facing aspect, but were better developed than those collected from the north-facing aspect (Figure 4.30). Since there was a disparity in the characteristics of the crystals that formed on 12-13 January based on slope aspect, the temperature gradients and vapor pressure gradients between -0.05 m and -0.10 m from 0800 hours on 12 January to 0800 hours on 13 January were compared to determine if the

Figure 4.28: A 1.5 mm near-surface faceted crystal harvested from the south-facing study site on 13 January 2004. This crystal is classified by Colbeck et al. (1990) as type 5a, cup shaped crystal.

Figure 4.29: A 0.5mm near-surface faceted crystal harvested from the north-facing study site on 13 January 2004. This crystal is classified by Colbeck et al. (1990) as type 4b, small faceted particles.

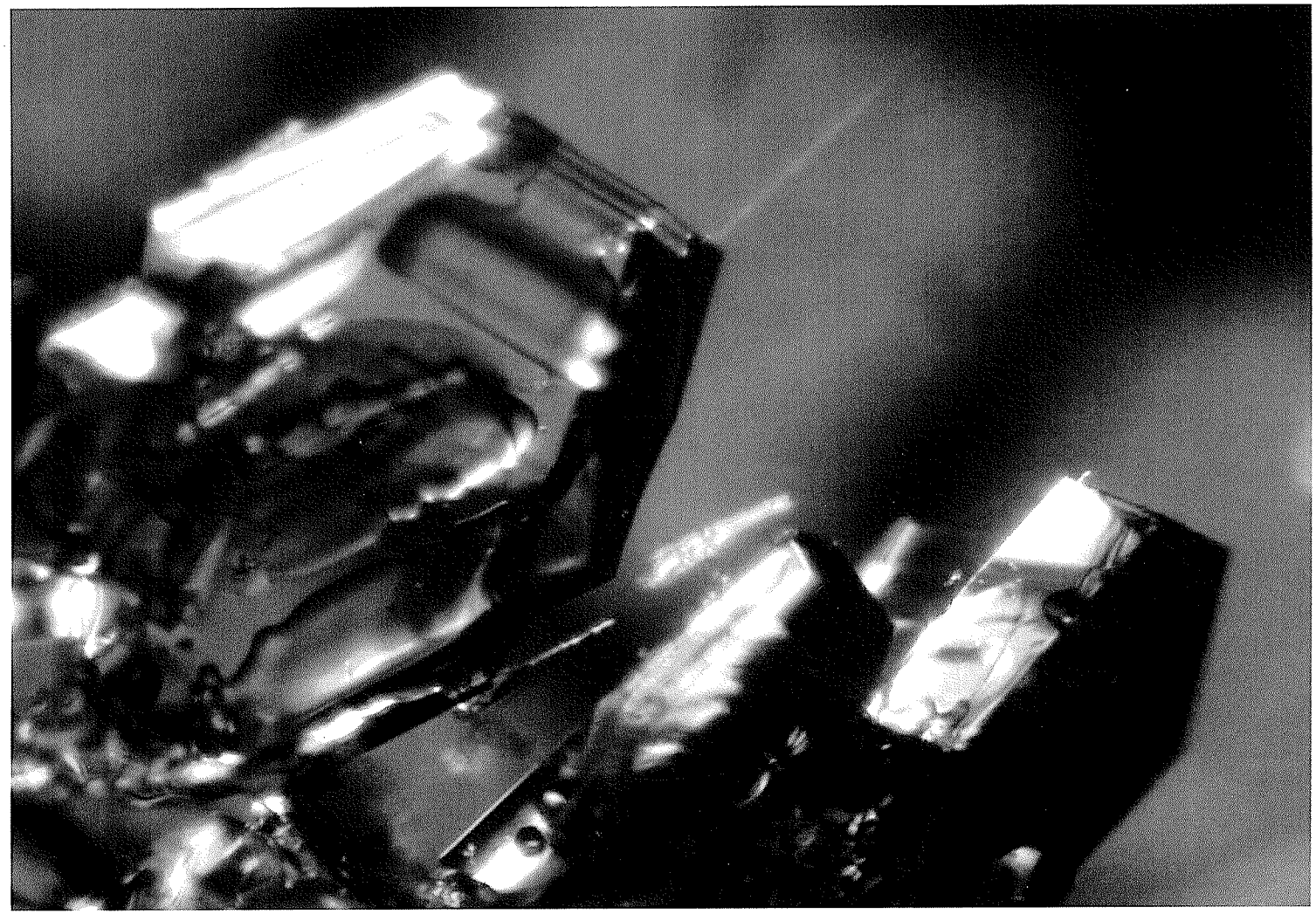

Figure 4.30: A few 1 mm near-surface faceted crystal harvested from the east-facing study site on 13 January 2004. These crystals are classified by Colbeck et al. (1990) as type 4a, solid faceted particles.

gradients also differed by slope aspect.

Temperature Gradient As shown in Figure 4.31 and Table 4.9, the south-facing aspect had a maximum daytime temperature gradient more than 12 times (123.7° C m^{-1}) the value considered necessary for faceting and a nighttime gradient almost 9 times (-86.9° C m^{-1}) the value considered necessary for faceting. The east-facing aspect, on which slightly less developed crystals were found, had a temperature gradient of 82.6° C m^{-1} and a nighttime gradient of -38.1° C m^{-1}. The north-facing aspect did not enter the positive realm during the day with the maximum temperature gradient reaching only -11.6° C m^{-1} but had a nighttime temperature gradient over 4 times (-44.2° C m^{-1}) the threshold level.

The south-facing aspect had the largest temperature gradient swing for the 24-hour period with a range of 210.6° C m^{-1}, followed by the east-facing aspect with a range of 128.4° C m^{-1}. The north-facing aspect never reached the 10° C m^{-1} positive threshold value for facet formation during the 24-hour period surrounding the near-surface faceting event and had a range of only 32.6° C m^{-1}.

Table 4.9: The median, minimum, maximum and the range of temperature gradients (° C m^{-1}) from -0.05 m to -0.10 m on north-, south-, and east-facing aspects from 0800 hours on 12 January 2004 to 0700 hours on 13 January 2004.

Aspect	N	Median	Minimum	Maximum	Range
East	24	-38.1° C m^{-1}	-45.8° C m^{-1}	82.6° C m^{-1}	128.4° C m^{-1}
South	24	-26.1° C m^{-1}	-86.9° C m^{-1}	123.7° C m^{-1}	210.6° C m^{-1}
North	24	-33.1° C m^{-1}	-44.2° C m^{-1}	-11.6° C m^{-1}	32.6° C m^{-1}

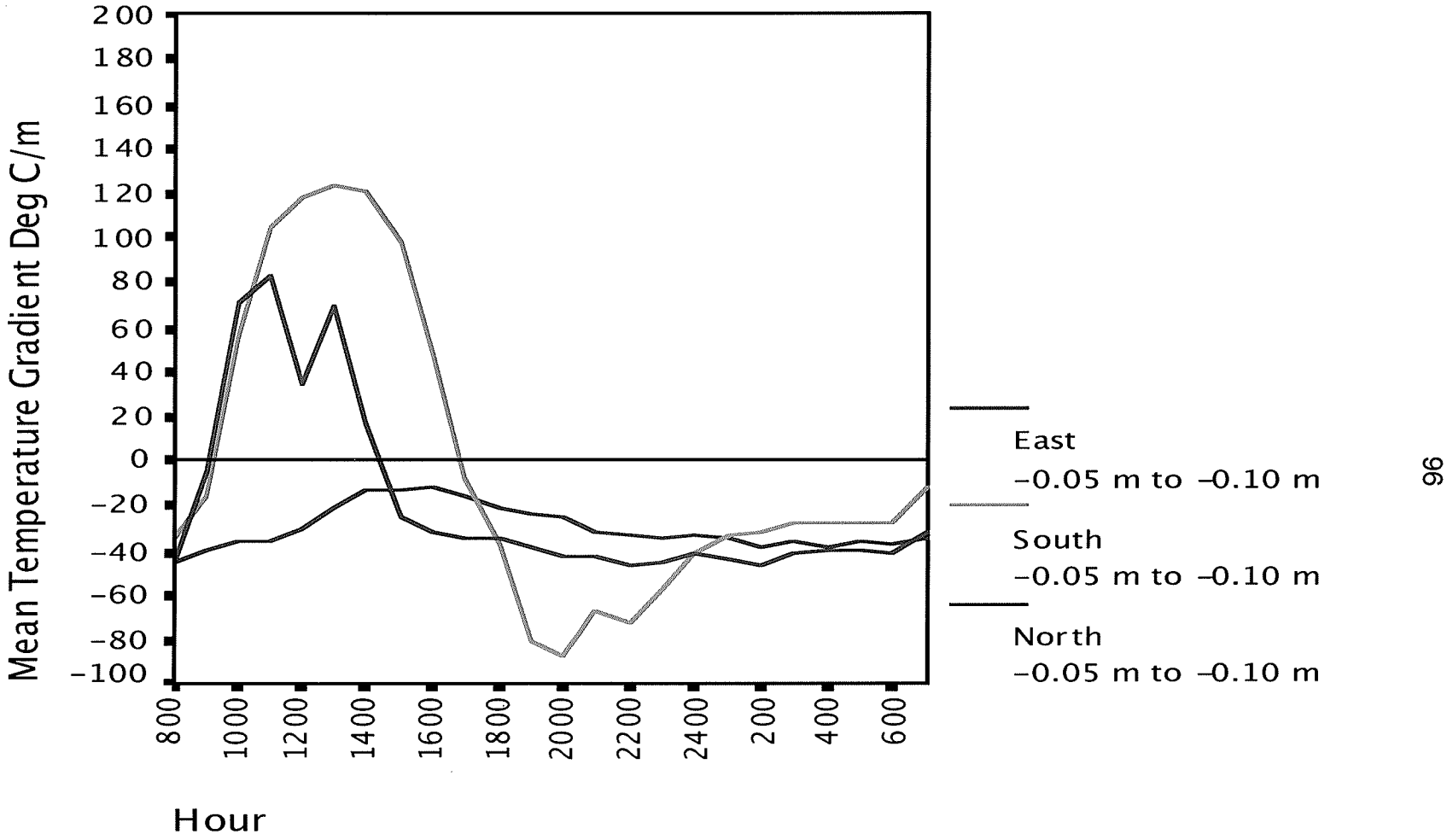

Figure 4.31: The mean temperature gradient by hour (° C m^{-1}) from 0800 hours on 12 January 2004 to 0700 hours on 13 January 2004 on the north-facing, south-facing, and east-facing aspects between -0.05 m to -0.10 m.

However, as stated previously, the range did not enter the positive realm. Since diurnal recrystallized near-surface facet formation requires a swing in temperature between night and day and, as stated by Birkeland 1998 and Birkeland et al. 1998, the greater the swing, with all other snow properties held constant, the larger and more developed the facets will be, the south-facing aspect should have the largest faceted crystals, followed by the east. Since the gradient was uni-directional on the north-facing aspect, true bi-directional near-surface faceted crystal formation was not possible on the north-facing aspect.

The Levene's Test for Homogeneity of Variance was conducted to test the hypothesis that the variance of the temperature gradients was the same on north-facing, south-facing, and east-facing aspects. The hypothesis of equality was rejected in all cases (Table 4.10), indicating that there is an aspect-dependent difference in near-surface facet formation based on slope aspect.

Vapor Pressure Gradient The south-facing aspect had the highest and lowest vapor pressure gradients and the greatest range, followed by the east-facing aspect. Again the north-facing aspect approached, but did not cross, the x-axis, thus the vapor pressure gradient was uni-directional and, therefore, the

Table 4.10: The Levene's f-statistic, the two tailed significance level, and the statistical decision between all aspects for the temperature gradients (Table 4.9) between -0.05 m and -0.10 m for 12-13 January 2004.

Aspect	f-statistic	p-value	Hypothesis
East/South	7.233	0.010	Reject
East/North	21.052	0.00	Reject
North/South	21.050	0.00	Reject

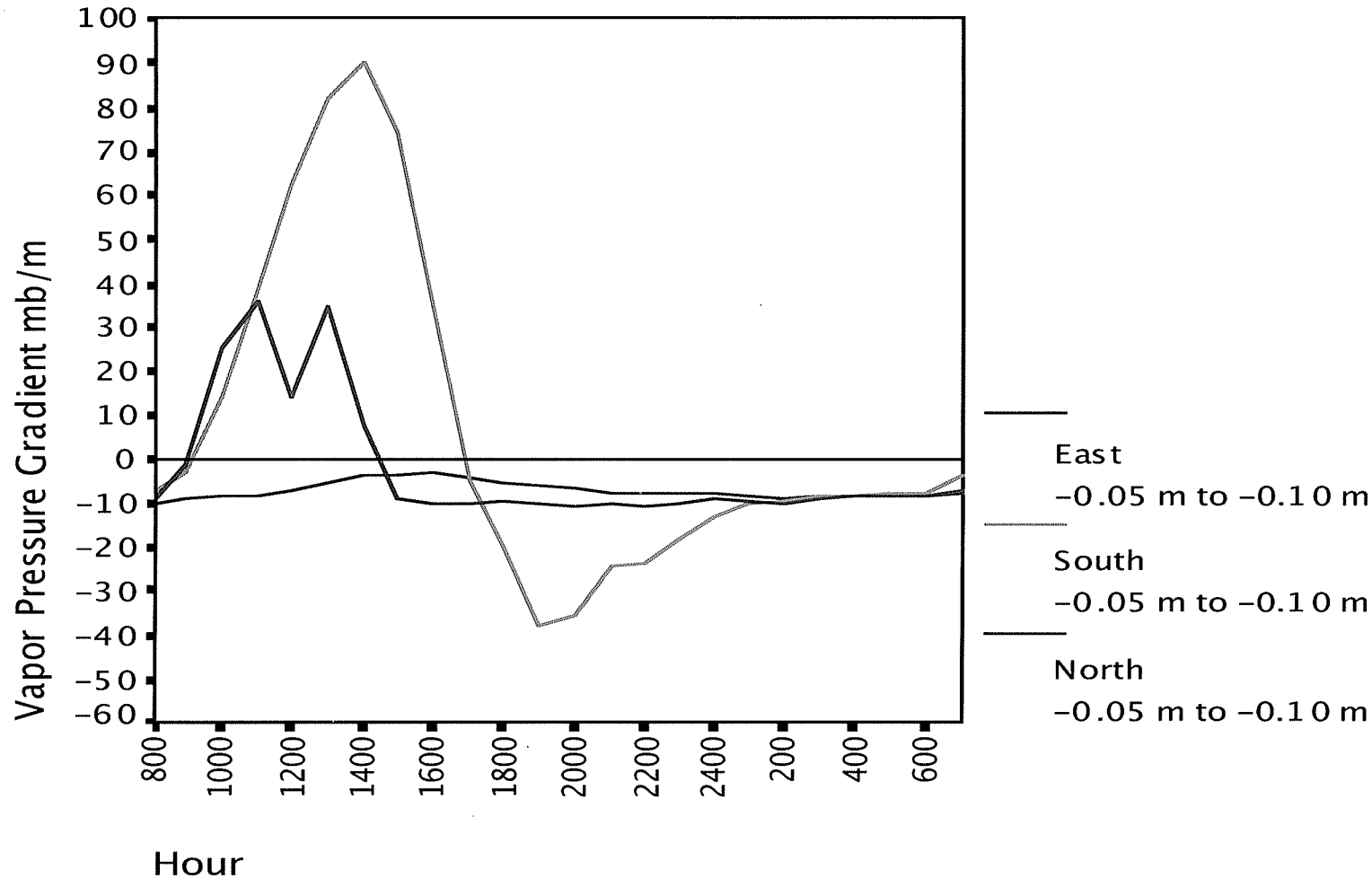

Figure 4.32: The vapor pressure gradient by hour from 0800 hours on 12 January to 0700 hours on 13 January on the north-facing, south-facing, and east-facing aspects from -0.05 m to -0.10 m in mb m^{-1}.

Table 4.11: The median, minimum, maximum and the range of vapor pressure gradients (mb m^{-1}) from -0.05 m to -0.10 m on north-, south-, and east-facing aspects from 0800 hours on 12 January 2004 to 0700 hours on 13 January 2004.

Aspect	N	Median	Minimum	Maximum	Range
East	24	-8.9 mb m^{-1}	-10.7 mb m^{-1}	36.1 mb m^{-1}	46.8 mb m^{-1}
South	24	-7.5 mb m^{-1}	-37.6 mb m^{-1}	89.9 mb m^{-1}	127.6 mb m^{-1}
North	24	-7.7 mb m^{-1}	-10.0 mb m^{-1}	-3.0 mb m^{-1}	6.9 mb m^{-1}

north-facing aspect should not be able to form true diurnal recrystallized near-surface faceted crystals (Figure 4.32 and Table 4.11).

Meteorological Variables To determine if aspect dependent differences in temperature and vapor pressure gradient were correlated with meteorological variables, the incoming shortwave radiation was compared between aspects. During the day, on the south-facing aspect, large inputs of solar radiation reaching a maximum of 800 W m^{-2} created large positive temperature gradients in excess of 120° C m^{-1} (Figure 4.33). The north-facing aspect, on the other hand, received at its maximum less than 100 W m^{-2} of solar radiation for that 24-hour period. Because of the lack of incoming solar radiation on the north-facing aspect, the top layers of the snow were never significantly warmed and the north-facing aspect never reached the required positive temperature gradient for near-surface faceting to occur.

The results of the incoming and outgoing radiation balance are evident in Figure 4.34, which shows the snow surface temperature (° C) and the snow

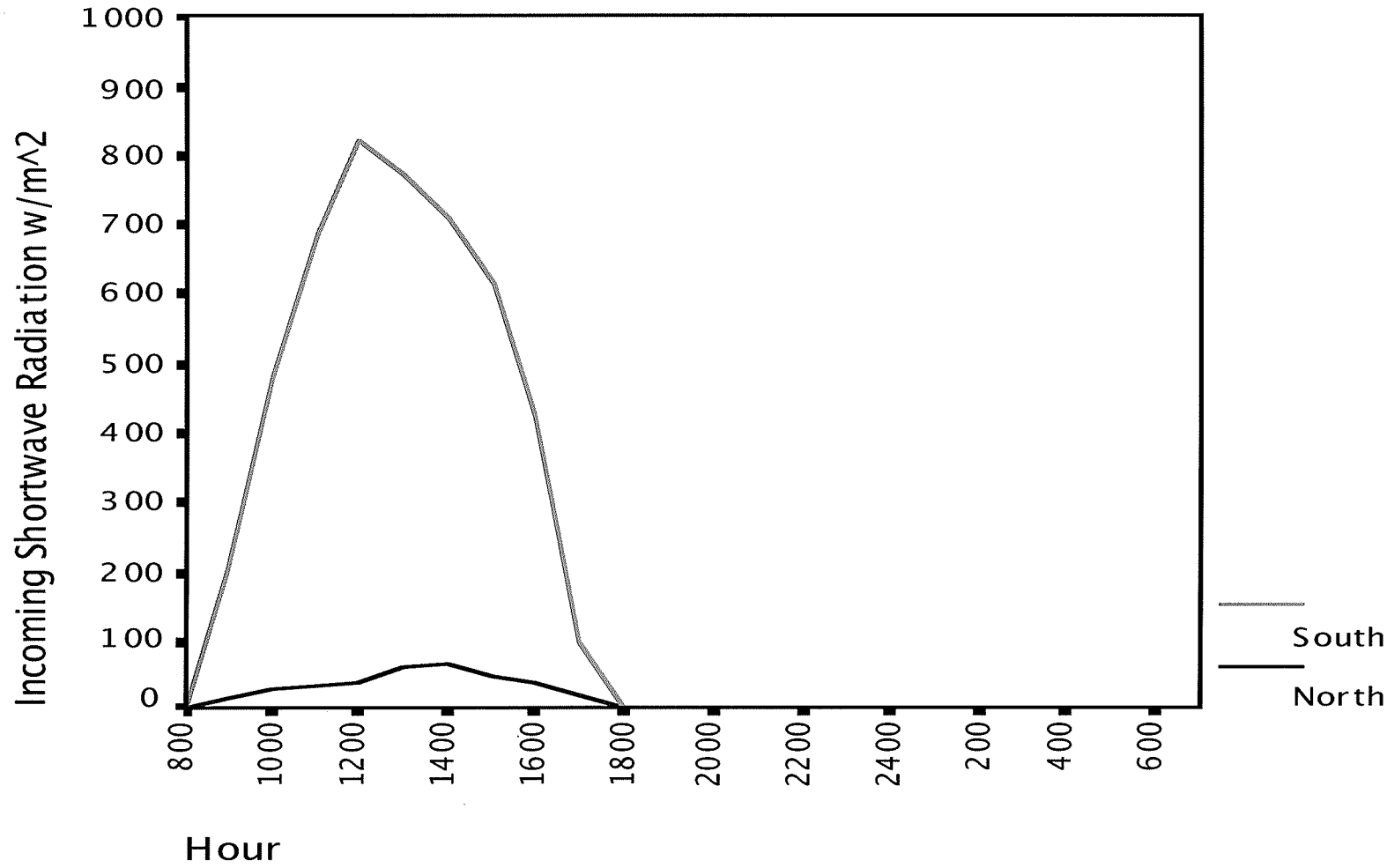

Figure 4.33: The mean incoming shortwave radiation (W m^{-2}) by hour from, 0800 hours on 12 January 2004 to 0700 hours on 13 January 2004 on north-facing and south-facing aspect.

temperature at -0.35 m (° C) by hour for the 24 hours surrounding the faceting event. The snow surface temperature on the south-facing aspect was about -13° C at 0800 hours on 12 January and very quickly increased and reached its maximum of -1° C by 1000 hours. It remained close to 0° C until about 1600 hours when it decreased rapidly until it reached its minimum of about -11° C at 2300 hours on the night of 12 January; however, the temperature at -0.35 m on the south did the opposite. The temperature at -0.35 m on the south was at its minimum and well below the temperature of the snow surface at about 0900 hours on 12 January when it began to warm and eventually became warmer than the snow surface temperature at about 1700 hours until it reached its maximum temperature of about -3° C at approximately 0300 hours on 13 January. This is what would be expected for near-surface facet formation.

The snow surface temperature on the north-facing aspect, on the other hand, began to increase at 0900 hours and reached its maximum of about -10° C at approximately 1600 hours when it began to decline again. The temperature at -0.35 m on the north remained fairly constant at about -4° C for the entire 24-hour period. Since the snow surface temperature on the north-facing aspect was always colder than the temperature at -0.35 m, true diurnal recrystallized near-surface faceting should not readily occur on the north-facing aspect but a net movement of water vapor from the warmer layers at -0.35 m toward the snow

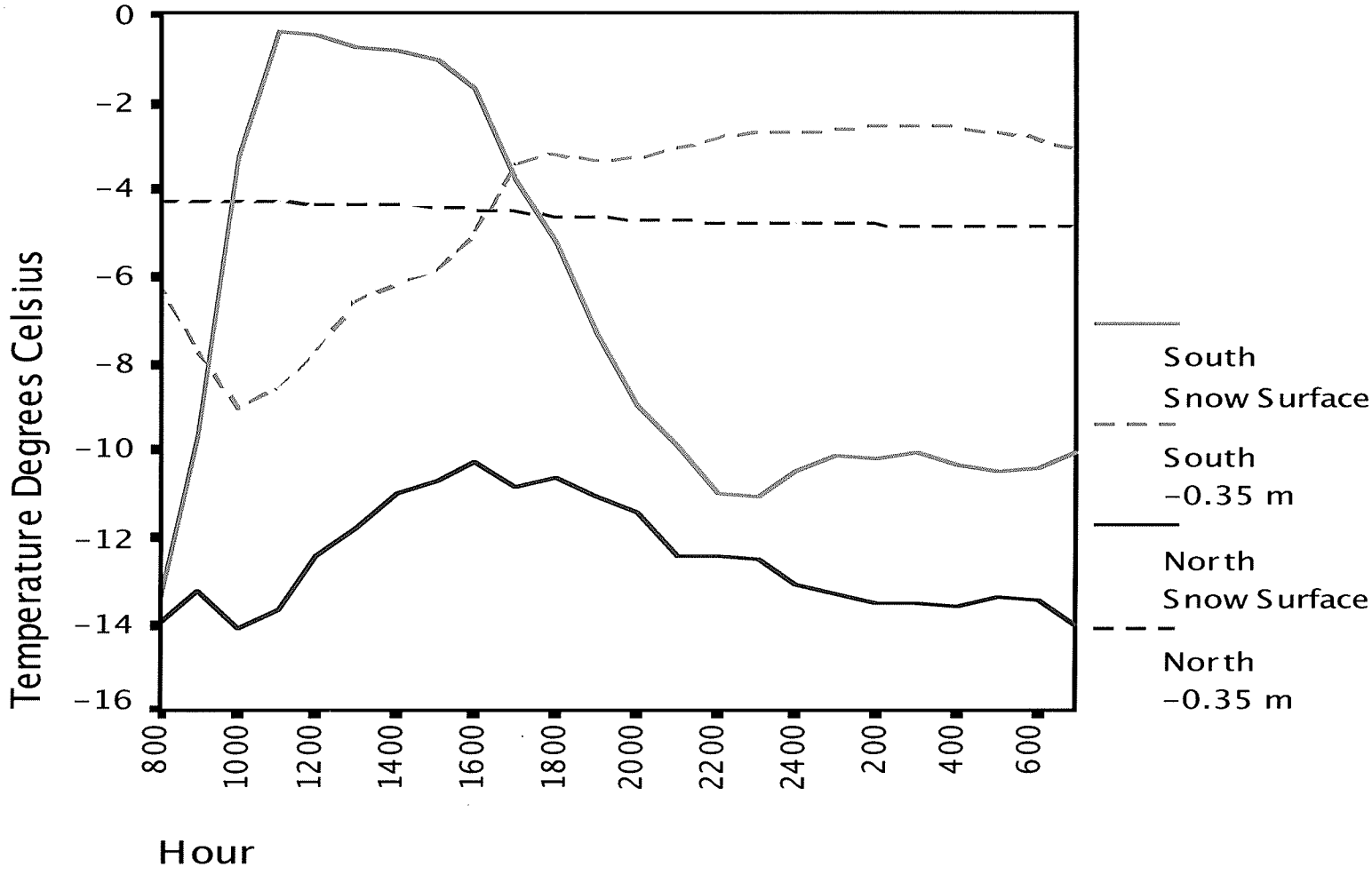

Figure 4.34: The snow surface temperature and the temperature at -0.35 m (° C) by hour from, 0800 hours on 12 January 2004 to 0700 hours on 13 January 2004 on north-facing and south-facing aspect.

surface would occur, creating faceting only on the bottoms of the crystals.

These figures and tables show that there was a significant difference in the formation of near-surface faceted crystals based on slope aspect. Near-surface faceting was more pronounced on the south-facing and east-facing aspects than on the north-facing aspect since the south- and east-facing aspects had the necessary switch in temperature and vapor pressure gradient to cause diurnal recrystallized near-surface facet crystal growth, and the gradients were large enough for near-surface faceting to occur. The north-facing aspect, however, did not have the necessary temperature and vapor pressure gradient switch and the gradients were less. The differences between the north-facing, south-facing and east-facing aspects appear to be caused by differences in the amount of incoming shortwave radiation.

Near-Surface Faceted Layer 22 January 2004

Crystal Characteristics Near-surface facets were noted on the south-facing aspect on the morning of 22 January. Crystals were collected from the south-facing study site at about 0815 hours on the morning of 22 January and were clearly identifiable as a mix of type 4a, solid faceted particles, and 5a, cup-shaped crystals (Figure 4.35). At about 0900 hours, the same procedure was used to sample the north-facing site, and this time the crystals were identified as types 1d, stellar dendrites, 1c, plates, and 1e, irregular crystals (Figure 4.36) that had not gone through any type of metamorphic processes once deposited. At

about 1030 hours, crystals were collected from the east-study site and were identified as type 4a, solid faceted particles (Figure 4.37), as classified by Colbeck et al. (1990). No cups or striations were noted on the east-facing site, but the crystals were obviously not precipitation particles like those on the north-facing aspect. Since there was again a disparity in the characteristics of the crystals that formed on 21-22 January based on slope aspect, the temperature gradients and the vapor pressure gradients between -0.05 m and -0.10 m from 0800 hours on 21 January to 0700 hours on 22 January were compared to determine if the gradients also differed by aspect.

Temperature Gradient As shown in Figure 4.38 and Table 4.12, the south-facing aspect had a maximum daytime and nighttime temperature gradient more than 22 times the value considered necessary for faceting (224.6° C m^{-1}) (-229.8° C m^{-1}), respectively. The east-facing aspect, on which slightly less developed crystals were found, had a temperature gradient almost 5 times (48.2° C m^{-1}) the threshold faceting value during the day and more than 8 times (-82.6° C m^{-1}) larger than the threshold value at night. The north-facing aspect never had a positive temperature gradient during the day with the maximum temperature gradient reaching only -14.4° C m^{-1}; consequently, no faceted crystals formed.

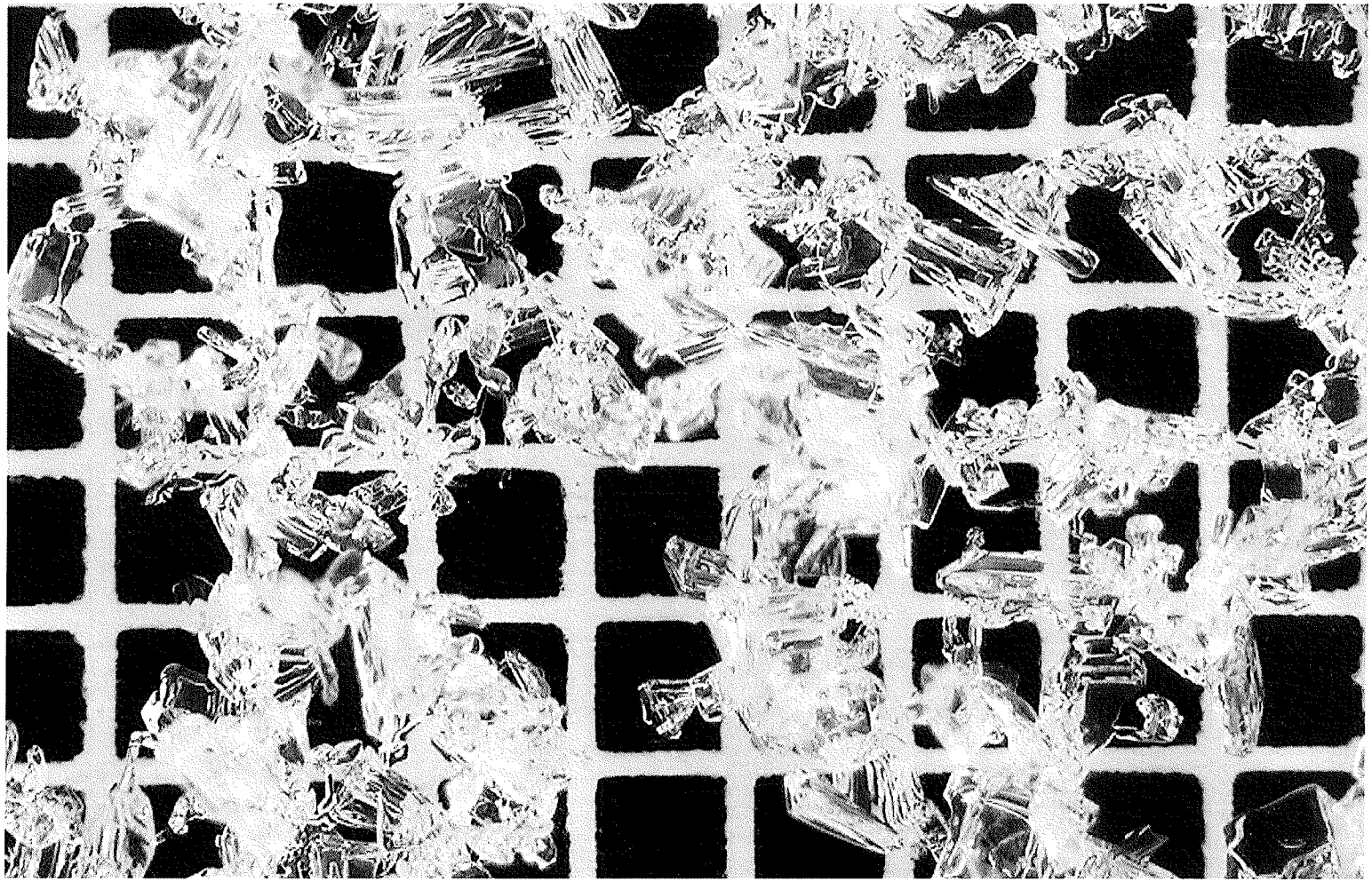

Figure 4.35: A to1.5 mm near-surface faceted crystal, type 4a, solid faceted particles and 5a, cup shaped crystal, as classified by Colbeck et al. (1990), harvested from the south-facing study site on 22 January 2004.

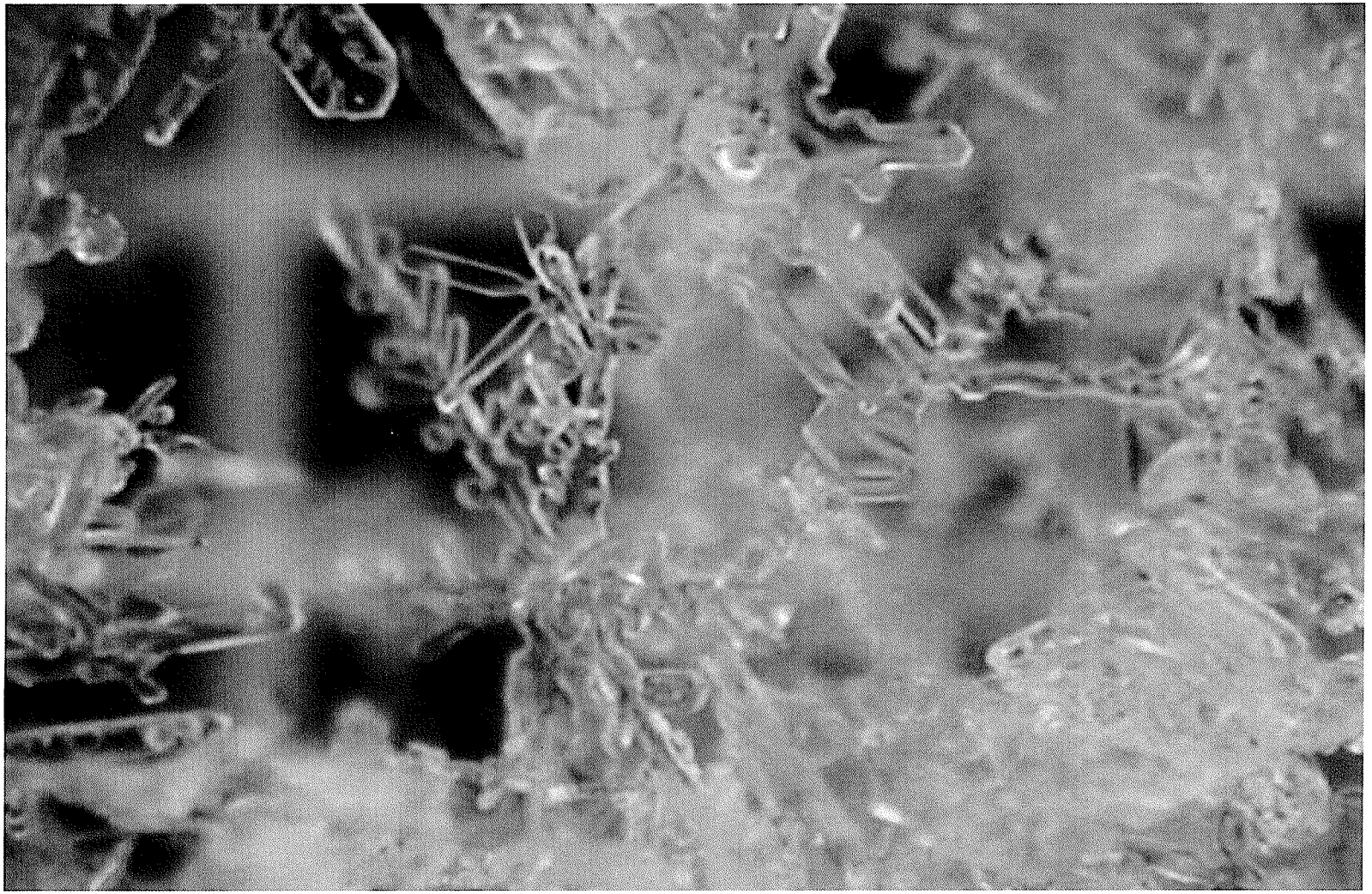

Figure 4.36: A 1-2 mm stellar crystal harvested from the north-facing study site on January 22, 2004 as classified by Colbeck et al. (1990) as type 1d, stellar dendrite.

Figure 4.37: A few 1 mm near-surface faceted crystal harvested from the east-facing study site on January 22, 2004. These crystals are classified by Colbeck et al. (1990) as type 4a, solid faceted particles.

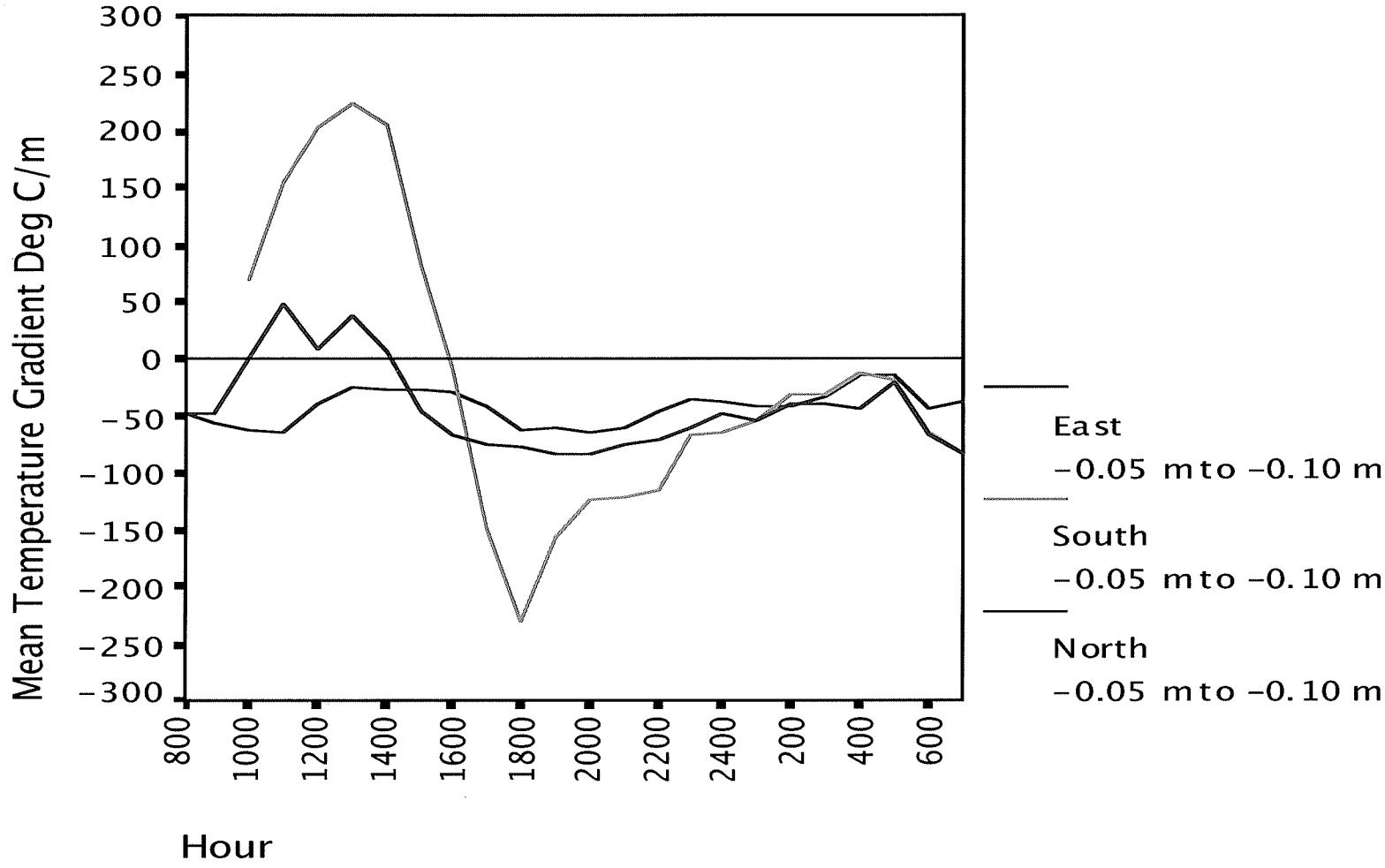

Figure 4.38: The mean temperature gradient by hour (° C m^{-1}) from 0800 hours on 21 January 2004, to 0700 hours on 22 January 2004 on the north-facing, south-facing, and east-facing aspects between -0.05 m to -0.10.

Table 4.12: The median, minimum, maximum and the range of temperature gradients (° C m^{-1}) from -0.05 m to -0.10 m on north-, south-, and east-facing aspects from 0800 hours on 21 January to 0700 hours on 22 January 2004.

Aspect	N	Median	Minimum	Maximum	Range
East	22	-48.5° C m^{-1}	-82.6° C m^{-1}	48.2° C m^{-1}	130.8° C m^{-1}
South	22	-43.6° C m^{-1}	-229.8° C m^{-1}	224.6° C m^{-1}	454.5° C m^{-1}
North	22	-42.3° C m^{-1}	-62.80° C m^{-1}	-14.4° C m^{-1}	48.4° C m^{-1}

The south-facing aspect had the largest temperature gradient swing for the 24-hour period with a range of 454.5° C m^{-1}, followed by the east-facing aspect with a range of 130.8° C m^{-1}. The north-facing aspect never reached the 10° C m^{-1} positive threshold value during the 24-hour period surrounding the near-surface faceting event. Since diurnal recrystallized near-surface facet formation typically requires a swing in temperature gradient between night and day and the greater the swing, with all other snow properties held constant, the larger and more developed the facets will be (Birkeland 1998 and Birkeland et al. 1998), the south-facing aspect had the largest faceted crystals, followed by the east. Because the gradient was uni-directional on the north-facing aspect, true near-surface faceted crystal formation was not possible.

Table 4.13: The Levene's f-statistic, the two tailed significance level, and the statistical decision between all aspects for the temperature gradients (Table 4.12) between -0.05 m and -0.10 m for 21-22 January 2004.

Aspect	f-statistic	p-value	Hypothesis
East/South	16.945	0.00	Reject
East/North	8.831	0.005	Reject
North/South	26.505	0.00	Reject

The Levene's Test for Homogeneity of Variance showed that there is an aspect-dependent difference in temperature gradient based on slope aspect (Table 4.13).

Vapor Pressure Gradient As shown in Figure 4.39, the mean vapor pressure gradient from 0800 hours on 21 January to 0700 hours on 22 January on all three aspects was similar to the temperature gradient. The south-facing aspect had the highest and lowest vapor pressure gradients and the greatest range, followed by the east-facing aspect. Again the north-facing aspect approached, but did not cross, the x-axis and, therefore, should not form true, diurnal recrystallized near-surface faceted crystals.

Meteorological Variables To determine if aspect dependent differences in temperature and vapor pressure gradient were correlated with meteorological variables, the incoming shortwave radiation was compared on the north- and south-facing aspects. During the day, on the south-facing aspect, large inputs of solar radiation reaching a maximum of almost 900 W m^{-2} created large positive temperature gradients in excess of 200° C m^{-1} (Figure 4.40). The north-facing aspect, on the other hand, received at its maximum less than 50 W m^{-2} of solar radiation for that 24-hour period. Because of the lack of incoming solar radiation on the north-facing aspect, the top layers of the snow were never significantly warmed and the north-facing aspect never reached a positive temperature gradient which is necessary for near-surface faceting to occur.

Figure 4.39: The vapor pressure gradient by hour from 0800 hours on 21 January 2004 to 0700 hours on 22 January 2004 on the north-facing, south-facing, and east-facing aspects from -0.05 m to -0.10 m in mb m^{-1}.

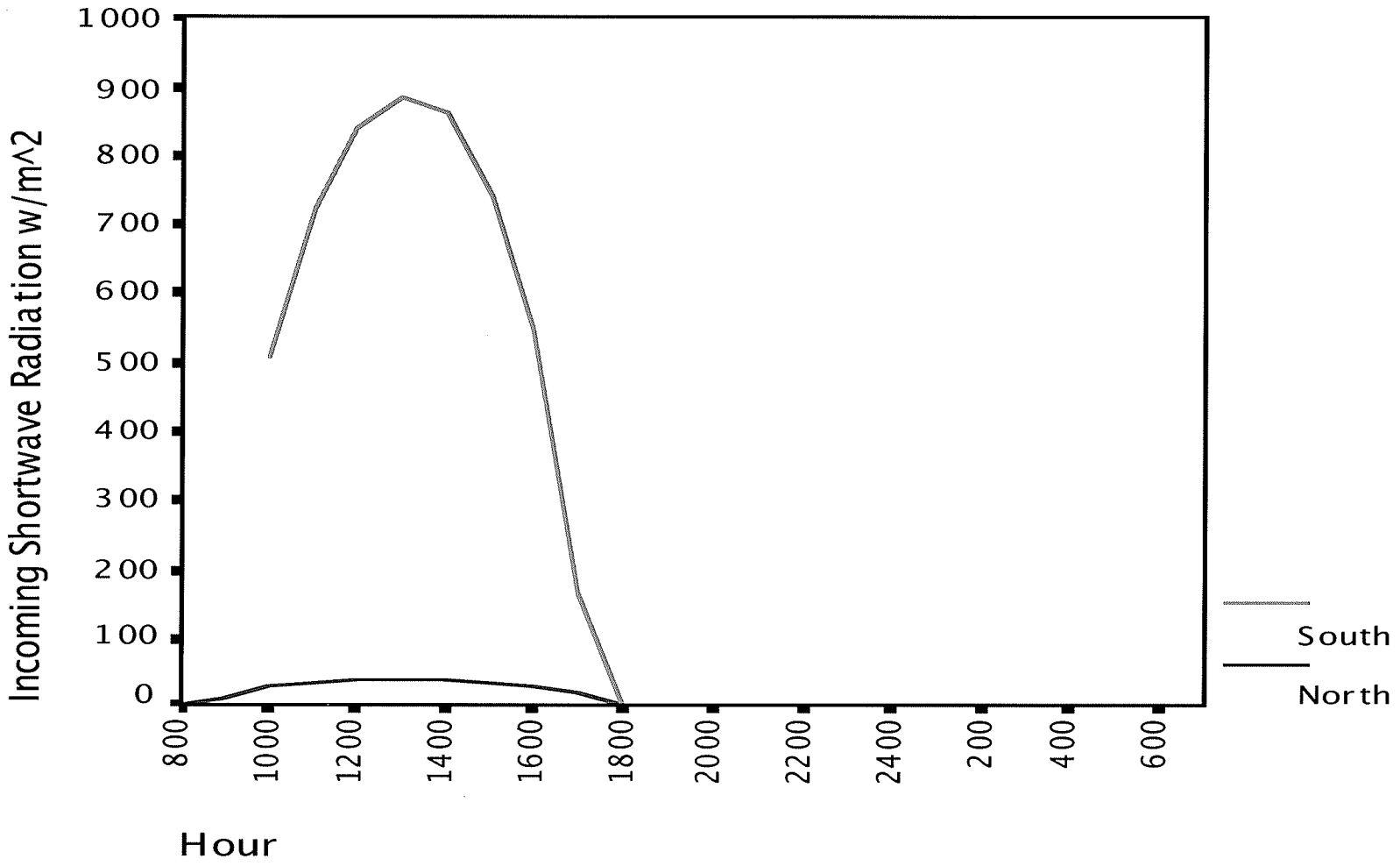

Figure 4.40: The mean incoming shortwave radiation (W m^{-2}) by hour from 0800 hours on 21 January 2004 to 0700 hours on 22 January 2004 on north-facing and south-facing aspect.

The results of the incoming and outgoing radiation balance are evident in Figure 4.41, which shows the snow surface temperature (° C) and the snow temperature at -0.35 m (° C) by hour for the 24 hours surrounding the faceting event. The snow surface temperature on the south-facing aspect very quickly increased and reached its maximum of -4° C at 1400 hours. It remained close to -4° C until about 1600 hours when it decreased rapidly until it reached its minimum of about -17° C at 2200 hours on the night of 21 January 2004; however, the temperature at -0.35 m on the south did the opposite.

The snow surface temperature on the north-facing aspect, on the other hand, began to increase at 1000 hours and reached its maximum of about -14° C at approximately 1300 hours when it began to decline again. The temperature at -0.35 m on the north remained fairly constant at about -4° C for the entire 24-hour period. Since the snow surface temperature on the north-facing aspect was always colder than the temperature at -0.35 m, true diurnal-recrystallized near surface faceting could not readily occur on the north-facing aspect.

These results again show that there was a difference in the formation of near-surface faceted crystals based on slope aspect. Near-surface faceting was more pronounced on the south- and east-facing aspects than on the north-facing aspect since the south- and east- facing aspects had the necessary switch in temperature and vapor pressure gradient to cause diurnal recrystallized near-surface facet crystal growth, and the gradients were large enough for near-

Figure 4.41: The snow surface temperature and the temperature at -0.35 m (° C) by hour from, 0800 hours on 21 January 2004 to 0700 hours on 22 January 2004 on north-facing and south-facing aspect.

surface faceting to occur. The north-facing aspect, however, did not have the necessary temperature and vapor pressure gradient switch and the gradients were not sufficient for faceting. The difference between the aspects again appears to be caused by differences in incoming shortwave radiation.

Near-Surface Faceted Layer 13 March 2004

Crystal Characteristics Near-surface facets were noted on all three aspects on the morning of 13 March. Crystals were collected from the north-facing study site at about 0845 hours on the morning of 13 March. The crystals were clearly identifiable as type 4a, solid faceted particles (Figure 4.42). At about 0925 hours, the same procedure was used to sample the south-facing site and crystals were collected. The crystals were also clearly identifiable as type 4a, solid faceted particles (Figure 4.43). At about 1040 hours, crystals were collected from the east-facing study site. These crystals were identified as type 4a, solid faceted particles (Figure 4.44), as classified by Colbeck et al. (1990). No cups were noted on any aspect. The temperature and vapor pressure gradients were graphed to see why there was no discernable difference in the crystals that formed on 12-13 March based on slope aspect.

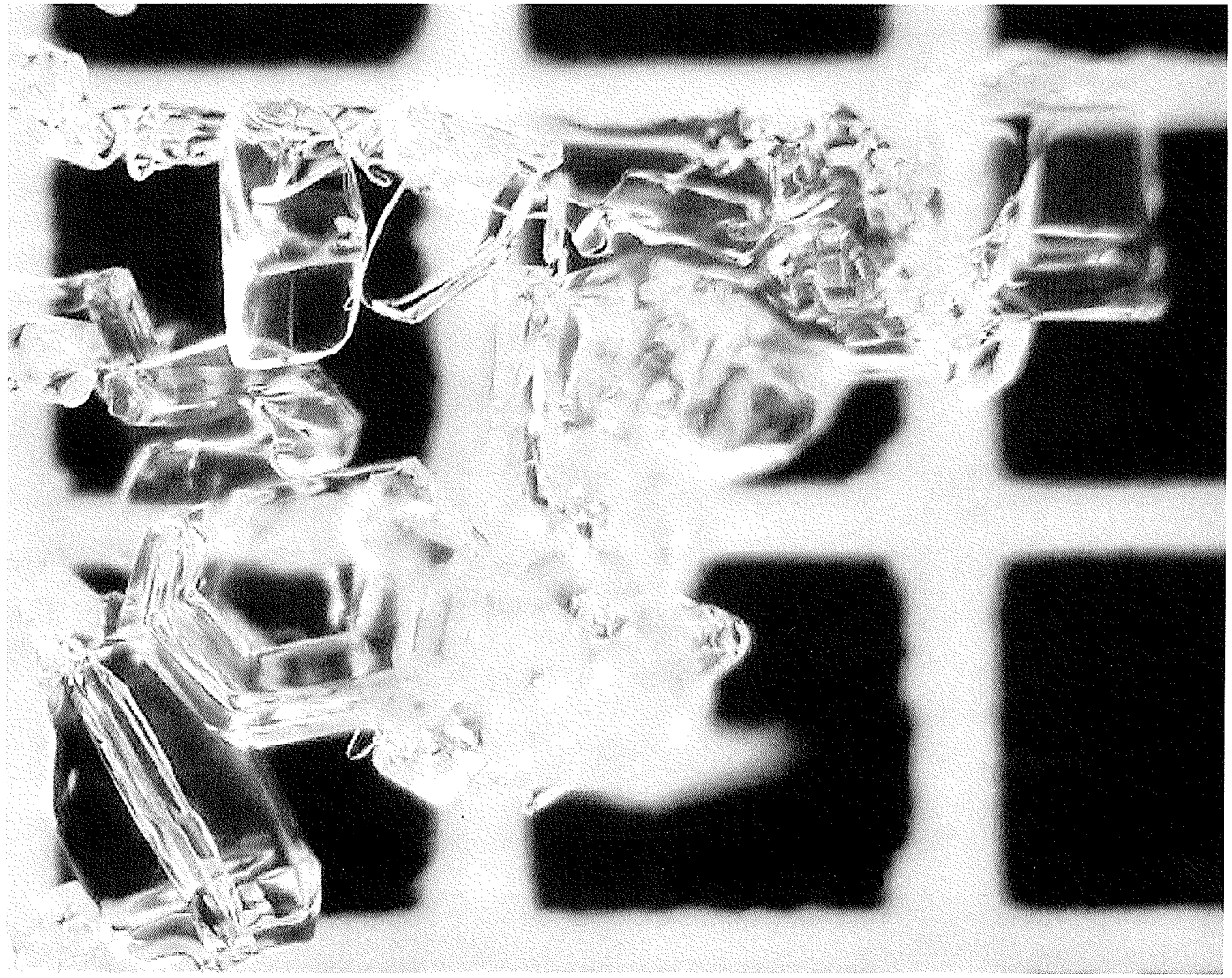

Figure 4.42: One mm faceted crystals harvested from the north-facing study site on 13 March 2004. These crystal would be classified by Colbeck et al. (1990) as type 4a, solid faceted particles.

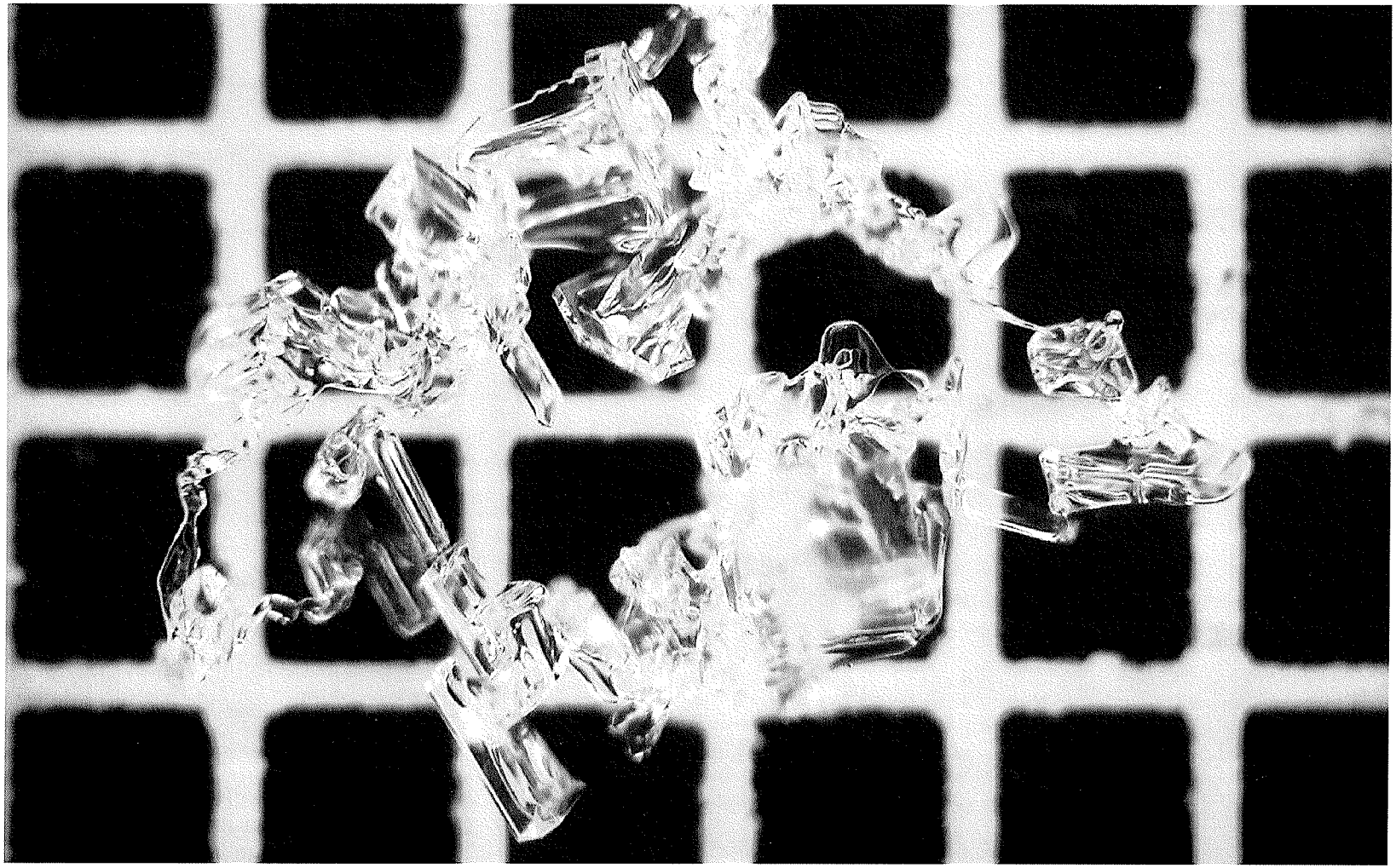

Figure 4.43: One mm near-surface faceted crystals harvested from the south-facing study site on 13 March 2004. These crystals would be classified by Colbeck et al. (1990) as type 4a, solid faceted particles.

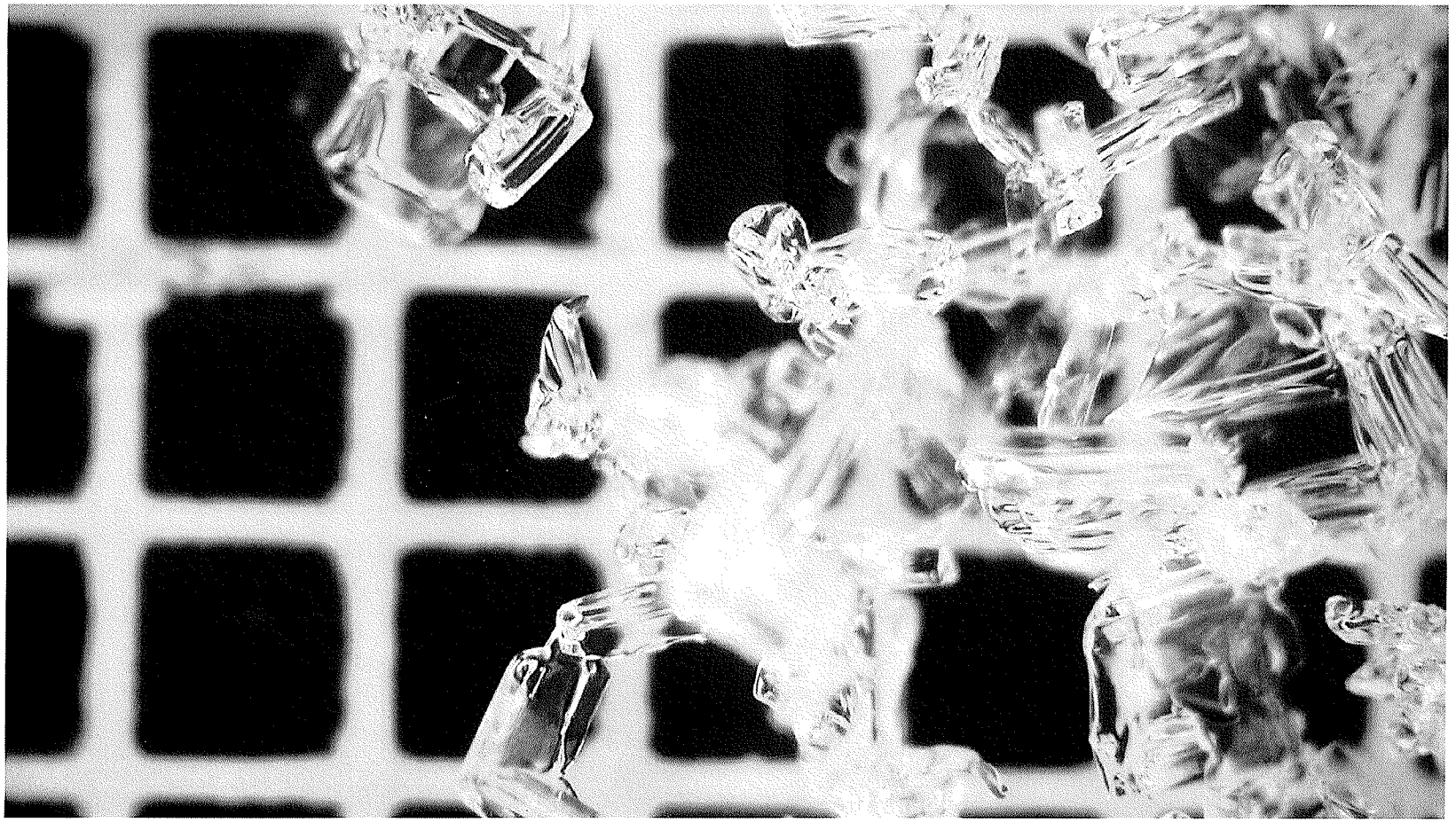

Figure 4.44: One mm near-surface faceted crystals harvested from the east-facing study site on 13 March 2004. These crystals would be classified by Colbeck et al. (1990) as type 4a, solid faceted particles.

Temperature Gradient The south-facing aspect had a maximum daytime temperature gradient of 93.7° C m^{-1} and a nighttime temperature gradient of -84.6° C m^{-1} well in excess of the value considered necessary for faceting (Figure 4.45 and Table 4.14). The temperature gradient at the east-facing site ranged from 121.2° C m^{-1} during the day to -79.9° C m^{-1} at night while the north-facing aspect varied from 43.2° C m^{-1} during the day to -58.6° C m^{-1} at night. The east-facing aspect had the largest temperature gradient swing for the 24-hour period with a range of 201.1° C m^{-1}, followed by the south-facing aspect with a range of 177.8° C m^{-1}, and then by the north-facing aspect with a temperature gradient range of 101.8° C m^{-1}. Since diurnal recrystallized near-surface facet formation requires a swing in temperature between night and day, the east- and south-facing aspects should have the most developed faceted crystals, followed by the north-facing aspect.

The Levene's Test for Homogeneity of Variance was conducted to test the hypothesis that the variance of the temperature gradients were the same on north-facing, south-facing, and east-facing aspects. The hypothesis of equality was only rejected in the North/South case (Table 4.15), indicating that there was

Table 4.14: The median, minimum, maximum and the range of temperature gradients (° C m^{-1}) from -0.05 m to -0.10 m on north-, south-, and east-facing aspects from 0800 hours on 12 March 2004 to 0800 hours on 13 March 2004.

Aspect	N	Median	Minimum	Maximum	Range
East	21	-47.9° C m^{-1}	-79.9° C m^{-1}	121.2° C m^{-1}	201.1° C m^{-1}
South	21	-44.2° C m^{-1}	-84.6° C m^{-1}	93.7° C m^{-1}	177.8° C m^{-1}
North	21	-30.7° C m^{-1}	-58.6° C m^{-1}	43.2° C m^{-1}	101.8° C m^{-1}

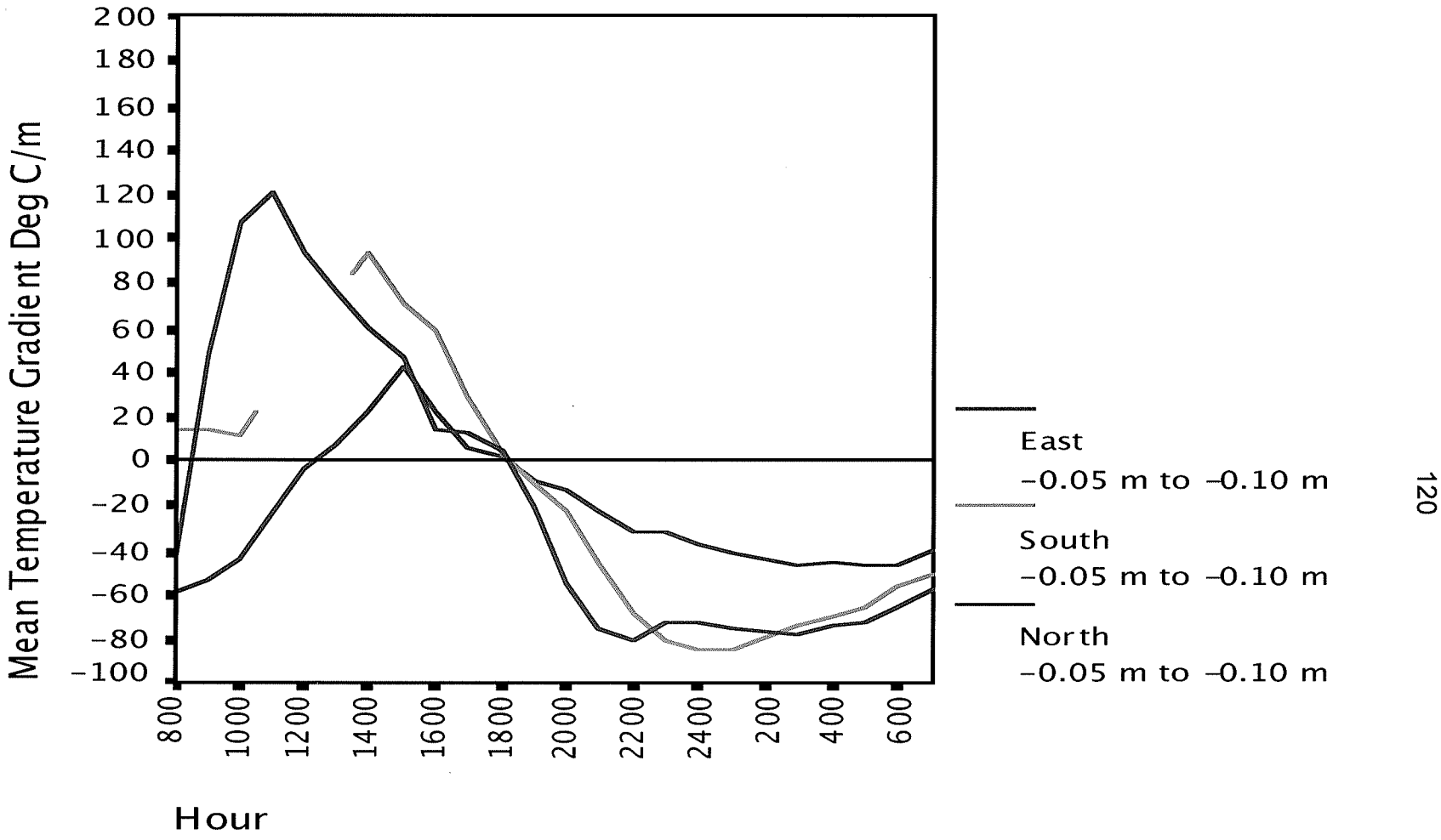

Figure 4.45: The mean temperature gradient by hour (° C m^{-1}) from 0800 hours on 12 March 2004 to 0700 hours on 13 March 2004 on the north-facing, south-facing, and east-facing aspects between -0.05 m to -0.10.

an aspect-dependent difference in near-surface facet formation between the north and south aspects but not between the north and east aspects nor between the south and east aspects on 12-13 March.

Vapor Pressure Gradient The vapor pressure gradients on the north-facing, south-facing, and east-facing aspects were also studied. As shown in Figure 4.46, the mean vapor pressure gradients from 0800 hours on 12 March 2004 to 0700 hours on 13 March for all three aspects was similar to the temperature gradient. The east- and south-facing aspects had the highest and lowest vapor pressure gradients and the greatest range, followed by the north-facing aspect.

Meteorological Variables To determine if aspect dependent similarities and differences in temperature and vapor pressure gradients were correlated with meteorological variables, the incoming shortwave radiation was compared between aspects. During the day, on the south-facing aspect, large inputs of solar radiation reached a maximum of over 950 W m^{-2} and created large positive temperature gradients in excess of 90° C m^{-1} (Figure 4.47). The north-facing

Table 4.15: The Levene's f-statistic, the two tailed significance level, and the statistical decision between all aspects for the temperature gradients (Table 4.14) between -0.05 m and -0.10 m for 12-13 March 2004.

Aspect	f-statistic	p-value	Hypothesis
East/South	3.61	0.062	Fail to Reject
East/North	1.493	0.228	Fail to Reject
North/South	14.82	0.00	Reject

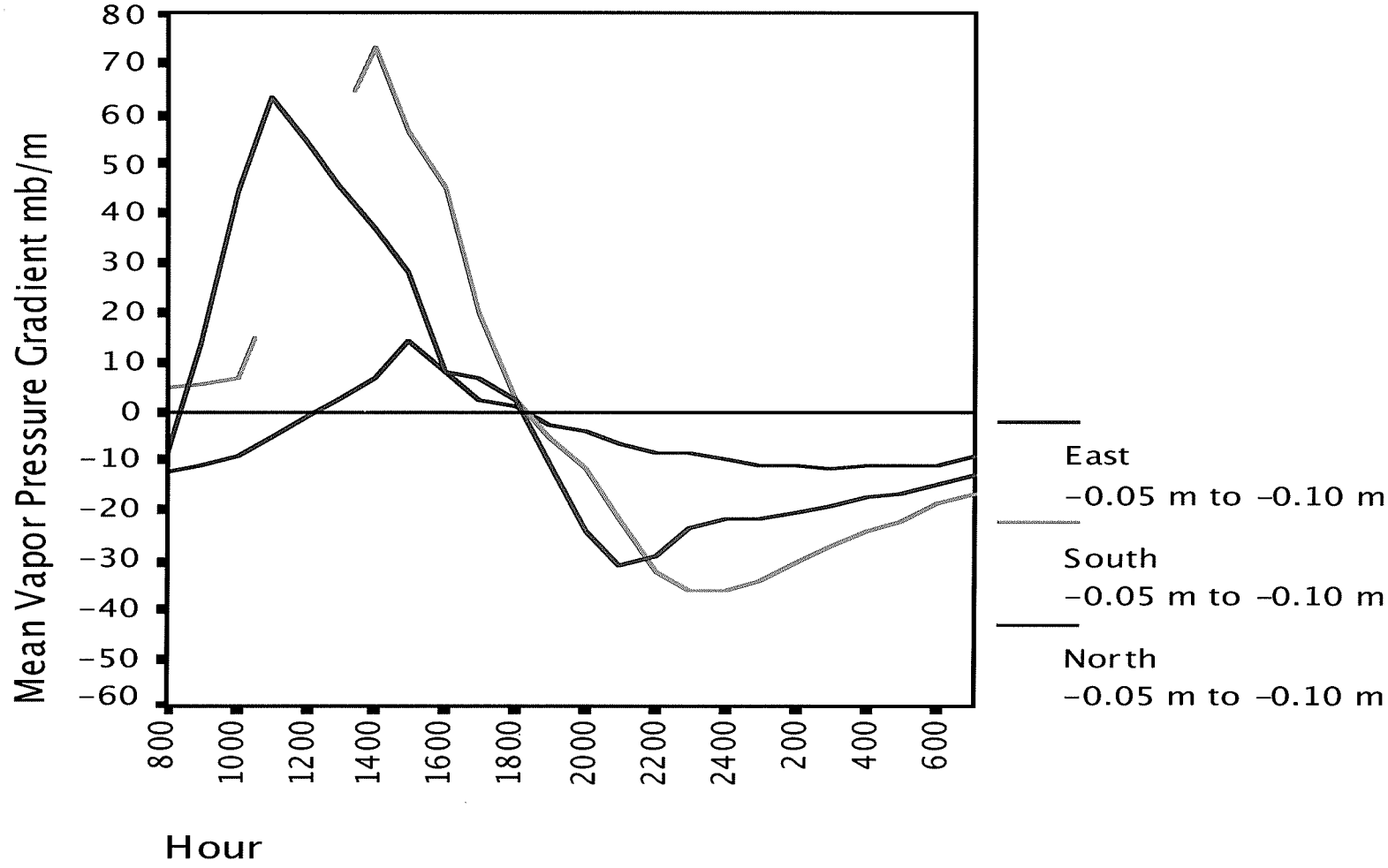

Figure 4.46: The vapor pressure gradient by hour from 0800 hours on 12 March 2004 to 0700 hours on 13 March 2004 on the north-facing, south-facing, and east-facing aspects from -0.05 m to -0.10 m in mb m^{-1}.

aspect received a maximum of 250 W m^{-2} of solar radiation for that 24-hour period. This was the largest amount of incoming and absorbed shortwave radiation that the north-facing aspect received during any of the faceting days and may be the reason facets were noted on the north-facing aspect on 13 March.

These results show that there was a difference in the meteorological variables based on slope aspect. However, they also show that the difference was not as significant as it was on previous days. This helps to explain the similarity in the observed near-surface faceted crystals. These tables and figures also show that diurnally recrystalized near-surface faceting was possible on north-facing aspect and it appears that the probability for diurnal recrystallized near-surface faceted crystal formation on north-facing aspects increased as the spring months approached. The increase in faceting on the north-facing aspect is probably caused by an increase in incoming shortwave radiation as spring approaches.

Aspect Comparison During Overcast Conditions 9 February 2004

Temperature and vapor pressure gradients were also studied on a day when near-surface faceted crystal growth did not occur to see if the temperature and vapor pressure gradients differed by slope aspect. 9 February was a randomly picked day from the pool of all of the overcast days. No near-surface facets were noted on the north-facing, south-facing, or east-facing aspects on the morning of 9 February.

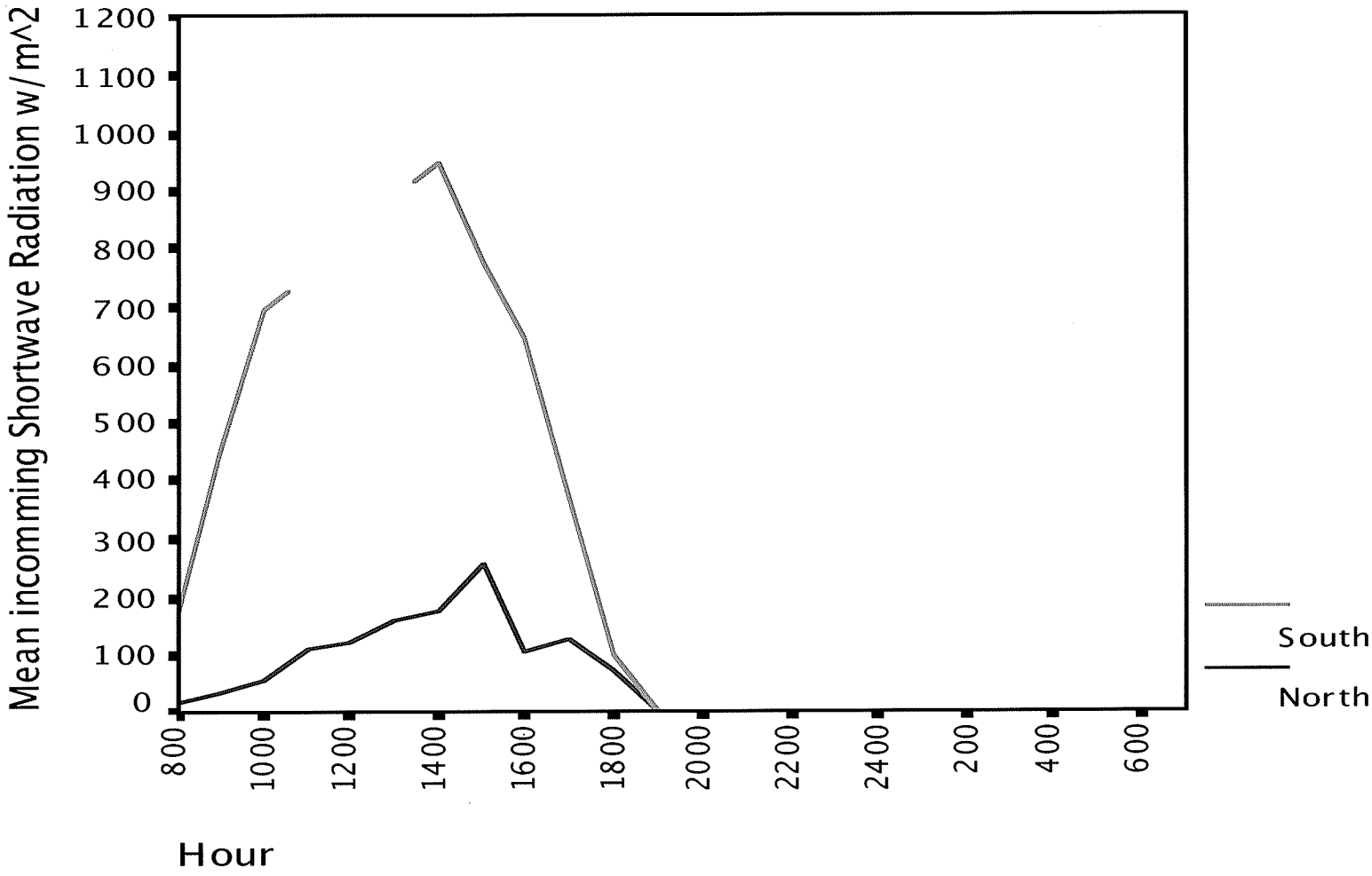

Figure 4.47: The mean incoming shortwave radiation (W m $^{-2}$) by hour from, 0800 hours on 12 March 2004 to 0700 hours on 13 March 2004 on north-facing and south-facing aspect.

Crystal Characteristics Crystals were collected from the south-facing study site at about 0800 hours on the morning of 9 February. The crystals were clearly identifiable as type 1d, stellar dendrites, and type 2a, partly decomposed precipitation particles, (Figure 4.48) (Colbeck et al. 1990). At about 0925 hours the same procedure was used to sample the north-facing site and crystals were collected. The crystals were also identified as types 1d and 2a (Figure 4.49). At about 1050 hours, crystals were collected from the east-study site. These crystals were the same as those on the other aspects (Figure 4.50). No signs of faceting, square formations on the arms, cups, or striations were noted on any of the aspects.

Temperature Gradient The temperature gradient between -0.05 m and -0.10 m from 0800 hours on 8 February to 0700 hours on 9 February is shown in Figure 4.51 and Table 4.16 for the north-facing, south-facing, and east-facing aspects. The north-facing aspect had a maximum daytime temperature gradient of 16.3° C m^{-1}, only 6° C over the threshold value considered necessary for faceting and a nighttime temperature gradient that just barely reached the threshold level (-9.8° C m^{-1}), and the east-facing site had a maximum daytime temperature gradient of 1.4° C m^{-1}, well below the threshold value for daytime faceting and a maximum nighttime temperature gradient of only -13.8° C m^{-1}, just over the threshold value for nighttime faceting. The north-facing aspect had a maximum daytime temperature gradient reaching only 6.2° C m^{-1}, and a

Figure 4.48: One to two mm stellar and broken particle crystals harvested from the south-facing study site on 9 February 2004. The crystals are classified by Colbeck et al. (1990) as type 1d, stellar dendrite, and 2a, broken.

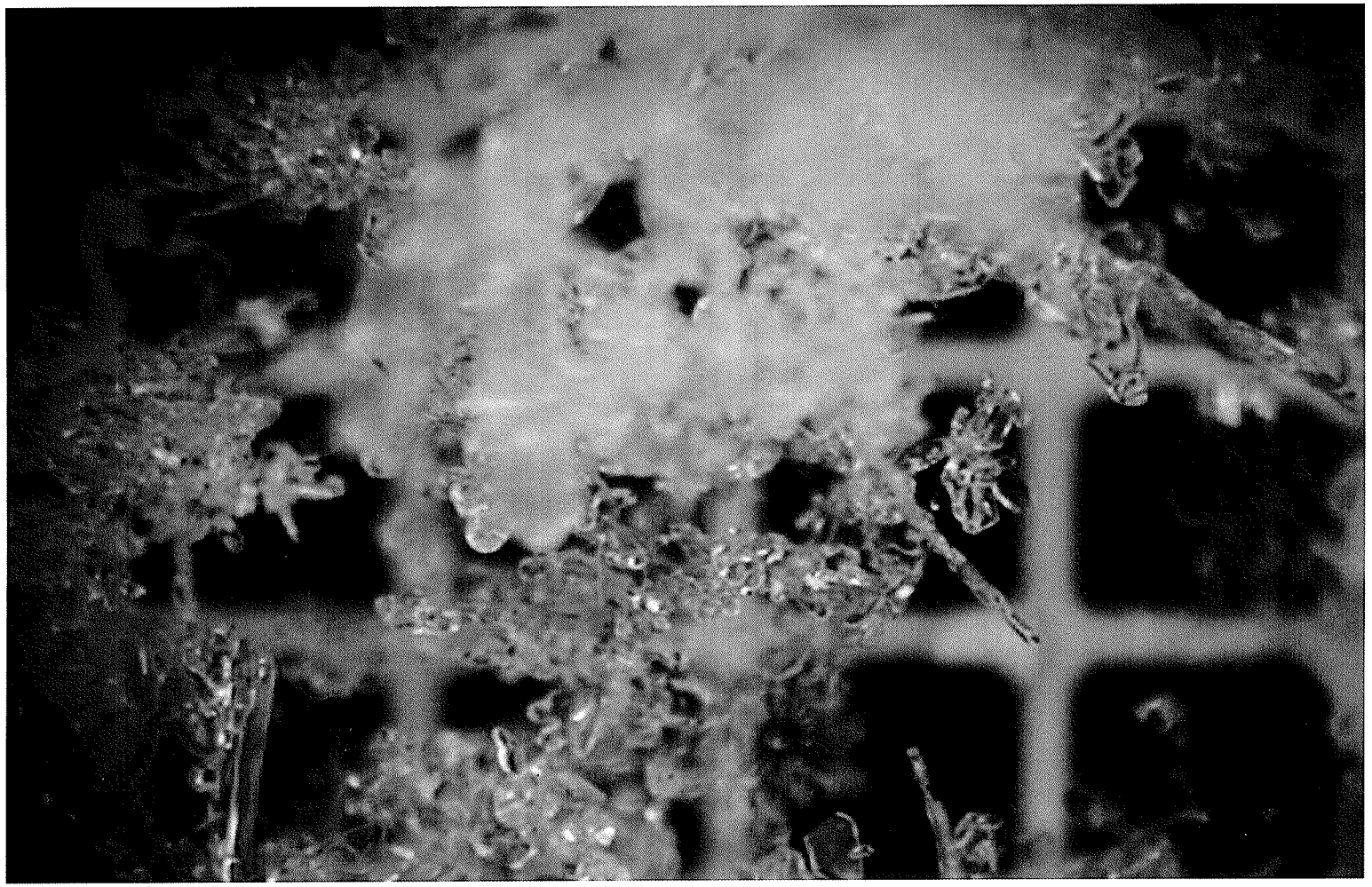

Figure 4.49: One to two mm stellar and broken particle crystals harvested from the north-facing study site on 9 February 2004. The crystals are classified by Colbeck et al. (1990) as type 1d, stellar dendrite, and 2a, broken.

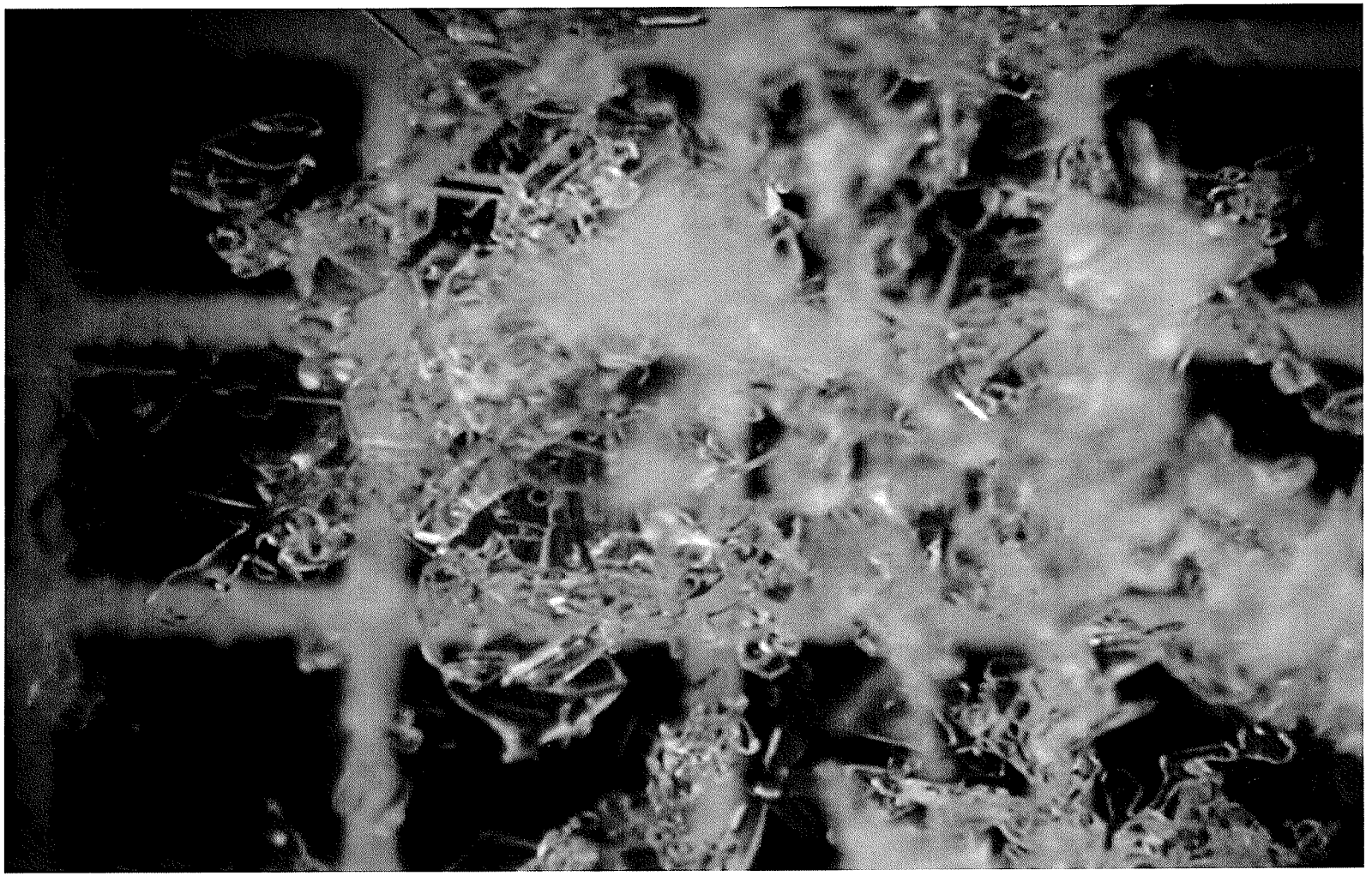

Figure 4.50: One to two mm stellar and broken particle crystals harvested from the east-facing study site on 9 February 2004. The crystals are classified by Colbeck et al. (1990) as type 1d, stellar dendrite, and 2a, broken.

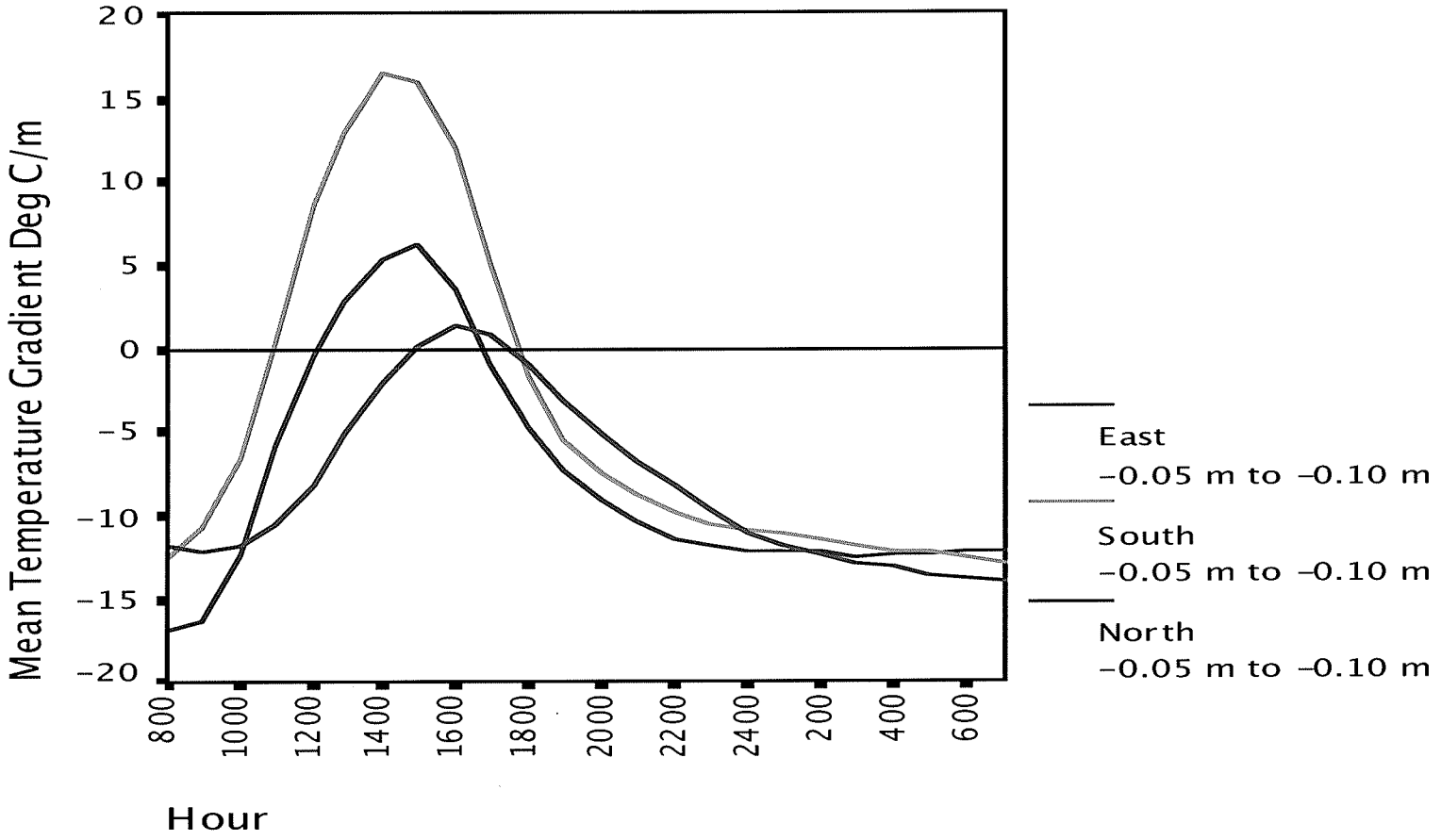

Figure 4.51: The mean temperature gradient by hour (° C m^{-1}) from 0800 hours on 8 February 2004 to 0700 hours on 9 February 2004 on the north-facing, south-facing, and east-facing aspects between -0.05 m to -0.10.

Table 4.16: The median, minimum, maximum and the range of temperature gradients (° C m^{-1}) from -0.05 m to -0.10 m on north-, south-, and east-facing aspects from 0800 hours on 8 February 2004 to 0700 hours on 9 February 2004.

Aspect	N	Median	Minimum	Maximum	Range
East	24	-10.1° C m^{-1}	-13.8° C m^{-1}	1.4° C m^{-1}	15.2° C m^{-1}
South	24	-9.3° C m^{-1}	-12.8° C m^{-1}	16.3° C m^{-1}	29.1° C m^{-1}
North	24	-11.5° C m^{-1}	-16.8° C m^{-1}	6.2° C m^{-1}	23.0° C m^{-1}

maximum nighttime temperature gradient of -16.8° C m^{-1}.

The south-facing aspect had the largest temperature gradient swing for the 24-hour period with a range of -29.1° C m^{-1}, followed by the north-facing aspect with a range of 23.0° C m^{-1}, followed by the east-facing aspect with a range of only 15.2° C m^{-1}. Since diurnal recrystallized near-surface facet formation requires a swing in temperature between night and day, and as stated in Birkeland 1998 and Birkeland et al. 1998, the greater the swing, with all other snow properties held constant, the larger and more developed the facets will be, no facets were formed on 9 February. There was, however, a swing in the temperature gradients between night and day on the south-facing and east-facing aspects on 9 February which was similar in direction but smaller in quantity to the other two days, previously described, on which faceted crystals formed. The north-facing aspect behaved more like the south- and east-facing aspects on 8-9 February. This was probably due to the overcast skies which began on 7 February and continued through the entire period.

The Levene's Test for Homogeneity of Variance showed that there is an aspect-dependent difference in temperature gradient based on slope aspect

Table 4.17: The Levene's f-statistic, the two tailed significance level, and the statistical decision between all aspects for the temperature gradients (Table 4.16) between -0.05 m and -0.10 m for 8-9 February 2004.

Aspect	f-statistic	p-value	Hypothesis
East/South	12.346	0.001	Reject
East/North	2.311	0.135	Fail to Reject
North/South	4.551	0.038	Reject

between the east- and south- and between the north- and south-facing aspects, but no difference between the north- and east-facing aspects (Table 4.17).

Vapor Pressure Gradient The vapor pressure gradients on the north-facing, south-facing, and east-facing aspects were also studied. Figure 4.52 shows the mean vapor pressure gradient from 0800 hours on 8 February to 0700 hours on 9 February. The results were similar to the results for the temperature gradient. The north-facing, south-facing, and east-facing aspects did not have sufficient vapor pressure gradients nor sufficient swings in vapor pressure gradient to initiate near-surface faceted crystal development.

Meteorological Variables During the day, the solar radiation on the south-facing aspect reached a maximum of almost 400 W m^{-2} and the north-facing aspect received at its maximum about 170 W m^{-2} (Figure 4.53). Because small amounts of incoming solar radiation were being absorbed on the north-facing and south-facing aspect, the top layers of the snow were never significantly warmed and neither aspect reached a significant positive temperature gradient necessary for near-surface faceting to occur. The amount of incoming shortwave radiation

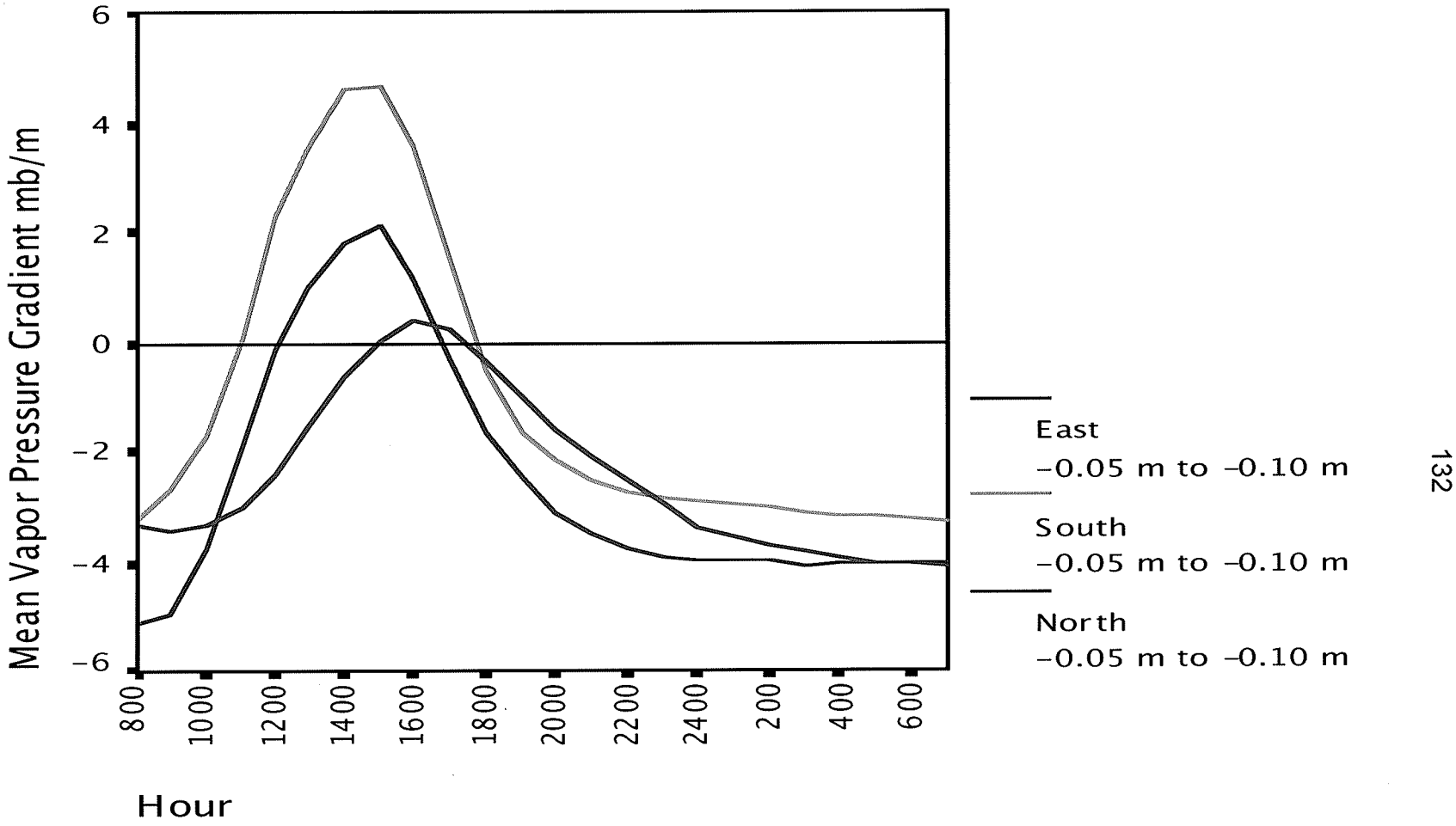

Figure 4.52: The vapor pressure gradient by hour from 0800 hours on 8 February to 0700 hours on 9 February on the north-facing, south-facing, and east-facing aspects from -0.05 m to -0.10 m in mb m^{-1}.

was also evenly distributed between the two aspects which is quite different from the two days previously discussed where the south-facing aspect received and absorbed larger amounts of shortwave radiation. The results of the incoming and outgoing radiation balance are evident in Figure 4.54, which shows the snow surface temperature (° C) and the snow temperature at -0.35 m (° C) by hour for the 24 hours on 8-9 February. The snow surface temperature on both the north-facing and south-facing aspects was always colder than the snow at -0.35 m. There was no temperature swing between these two levels in the snowpack like there was on the two faceting days previously described. Consequently, the snow surface stayed cold enough to preserve the stellar crystals and no near-surface faceting occurred.

These results show that, on cloudy days, although there are significant differences between the temperature and vapor pressure gradients between north and south and between south and east aspects, there is less aspect dependent variability and near-surface faceting may be precluded on all aspects if there is not enough incoming shortwave radiation and enough outgoing longwave radiation losses at the snow surface to set up large enough gradients.

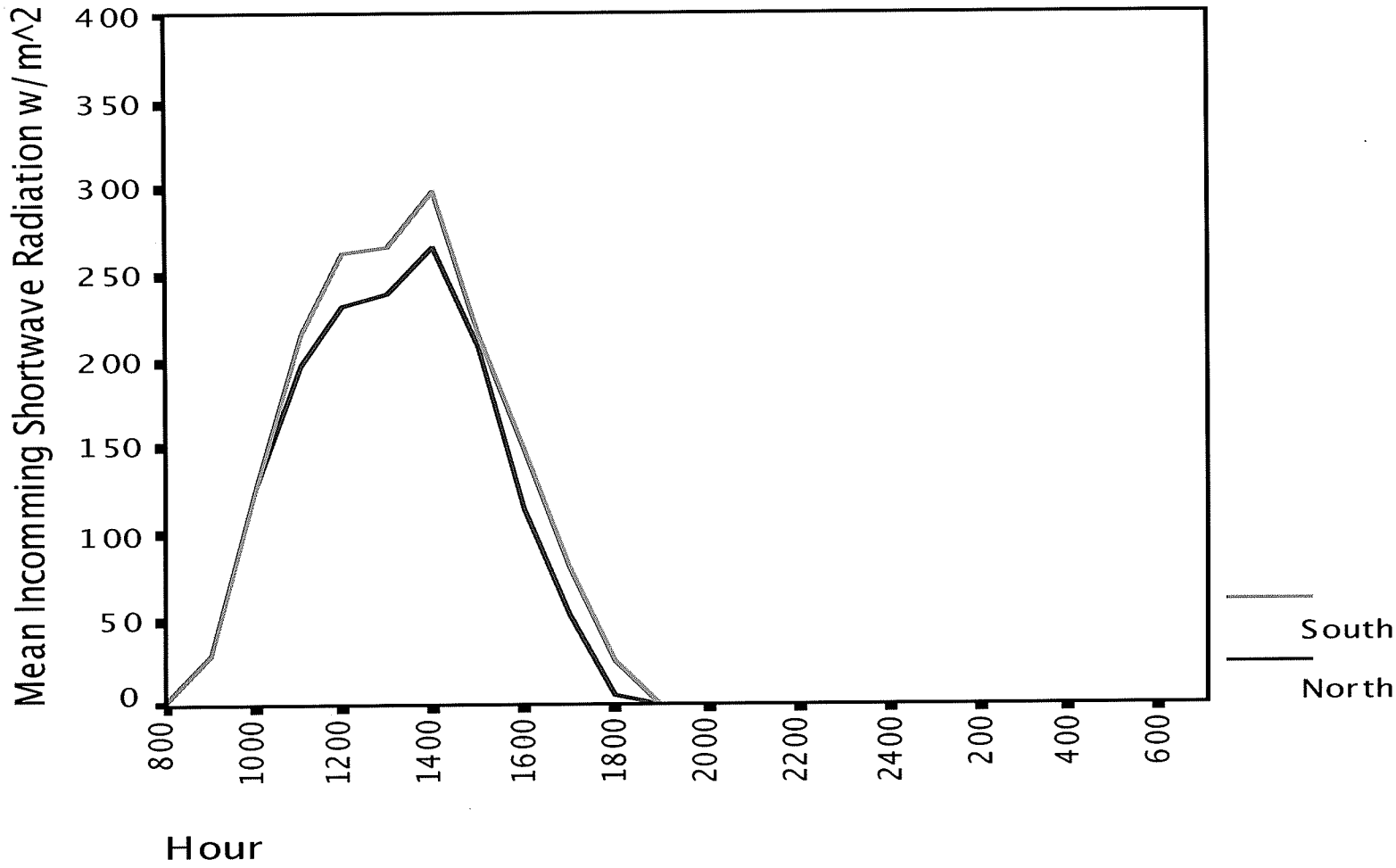

Figure 4.53: The mean incoming shortwave radiation (W m^{-2}) by hour from, 0800 hours on 8 February to 0700 hours on 9 February on north-facing and south-facing aspect.

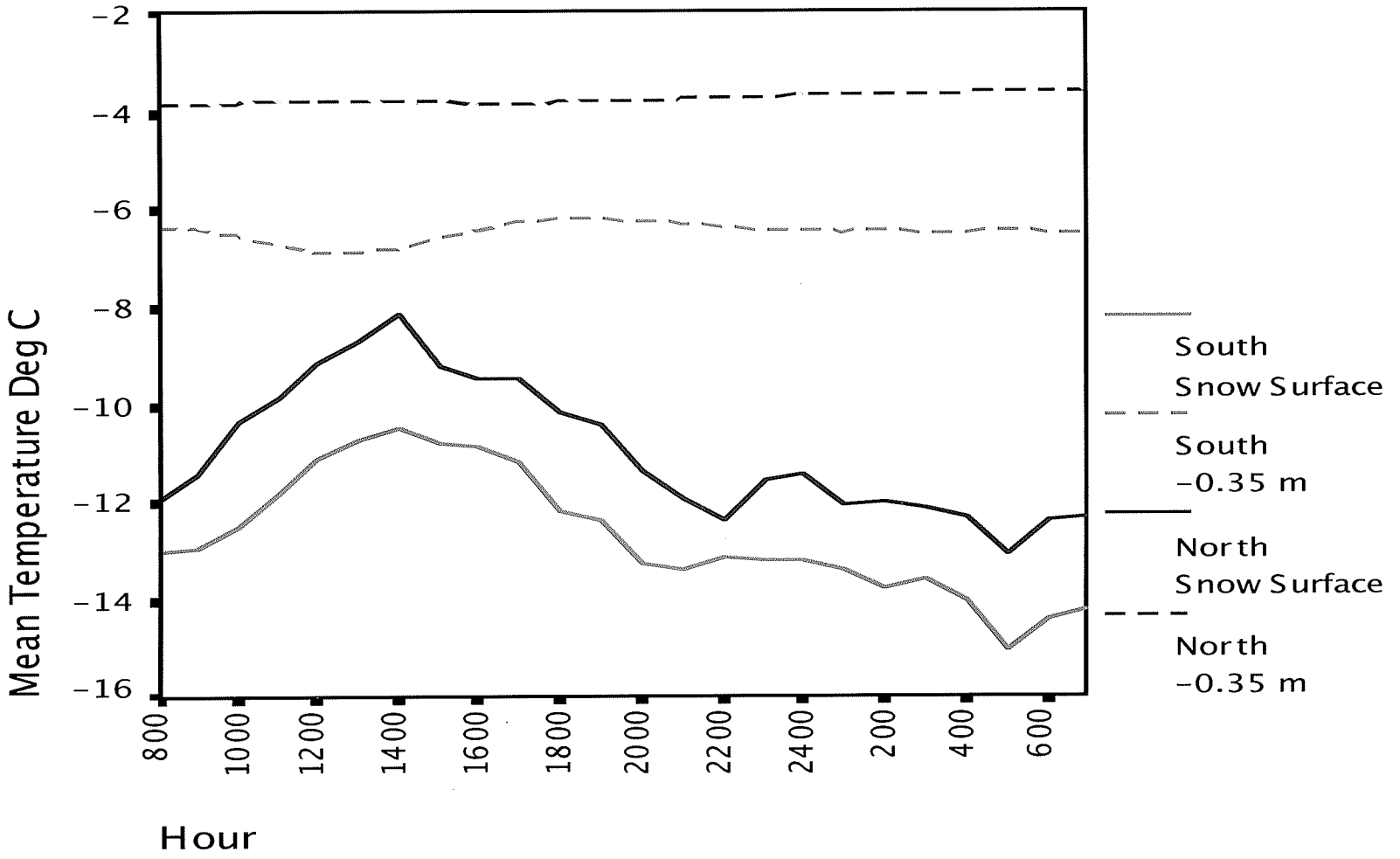

Figure 4.54: The snow surface temperature and the temperature at -0.35 m (° C) by hour from, 0800 hours on February 8, 2004, to 0800 hours on February 9, 2004 on north-facing and south-facing aspect.

CHAPTER 5
CONCLUSIONS

Prior to this research, several studies investigated the conditions necessary for forming surface hoar (Lang et al. 1984; Hachikubo and Akitaya 1997 a,b; Colbeck 1988) and near-surface faceted crystals (Birkeland 1998; Birkeland et al. 1998; McElwaine 2000; Hood 2005). A few studies had even taken a cursory look at the spatial distribution of surface hoar layers (Höller 1998; Feick et al. 2007; Schweizer and Kronholm 2004). However, none of that research rigorously documented the difference in crystal size and shape on different slope aspects.

This research demonstrates that there is a statistically significant difference in the size, shape, and physical characteristics of both surface hoar and diurnally recrystallized near-surface faceted crystals based solely on slope aspect. The differences in crystal size, shape, and structure are related to statistically significant differences in the temperature gradient and the resultant vapor pressure gradient on different slope aspects and qualitative relationships can be be drawn between the size and direction of the gradients and the size and shape of the surface hoar and near-surface faceted crystals based on slope aspect. The differences in the temperature and vapor pressure gradients on different slope aspects can be attributed to differences in incoming shortwave and outgoing longwave radiation. Such differences are critically important for understanding spatial variations in avalanche formation at the mountain range

scale. These aspect-dependent differences may have far reaching implications for avalanche forecasting, avalanche hazard rating, and avalanche hazard mitigation. This study demonstrates the importance of carefully documenting the formation of different weak layers on different aspects for reliable prediction of patterns of avalanche activity.

Surface Hoar

Surface hoar forming events can sometimes cover hundreds of square kilometers (Hageli and McClung 2002). Despite this my research demonstrates that such events are unlikely to deposit absolutely uniform layers since distinct differences in the size and shape of the crystals can be found on different aspects. Qualitative and quantitative analyses of the size and extent of surface hoar crystal formation, temperature gradients, and vapor pressure gradients demonstrate clear differences in the geographic distribution of surface hoar based solely on aspect. In this study, surface hoar crystals grew larger (sometimes up to 4 times larger) and were more advanced on the north-facing aspect than on the east- and south-facing aspects, respectively.

Statistically significant differences in the temperature and vapor pressure gradients existed. The nighttime temperature and vapor pressure gradients were the largest on the north-facing aspect with nighttime temperature gradients in excess of 160° C m^{-1} and nighttime vapor pressure gradients of 60 mb m^{-1}

recorded during the winter. The daytime and nighttime temperature and vapor pressure gradients at the snow/air interface on the north-facing aspect during every day studied were positive. These data indicate that surface hoar formation can begin earlier and last longer on north-facing aspects, consequently forming larger crystals than on the south- and east-facing aspects. Temperature and vapor pressure gradient data also indicate that surface hoar can persist during daylight hours on the north-facing aspect since the snow surface is usually colder than the air above. The extent and duration of the positive gradients on the north-facing aspect show that, if conditions are right and there is enough relative humidity in the air, surface hoar may have the ability to grow during the day on north-facing aspects in Montana. This has been observed in Alaska (Fesler and Fredston 2007) but was not observed in this study.

The south-facing aspect had positive temperature and vapor pressure gradients at night. However, they were not as strong as those on the east- and north-facing aspects. The south-facing aspect, however, had negative temperature and vapor pressure gradients during the day, something that did not occur on the north- and east-facing aspects. Due to the large negative daytime gradients on the south-facing aspect, surface hoar persistence may have been impeded.

The east-facing aspect tended to be similar to the north-facing aspect at night and the south-facing aspect during the day. The east-facing aspect had positive temperature and vapor pressure gradients at night. Though not as

strong as those on the north-facing aspect, surface hoar crystals in excess of 7 mm formed during the winter. The east-facing aspect sustained its positive temperature and vapor pressure gradients during the day, unlike the south-facing aspect, but the temperature gradients and the vapor pressure gradients usually decreased to less than 10° C m^{-1} and 5 mb m^{-1}, respectively. Consequently, surface hoar crystals were able to form at night, but were not be able to grow larger during daytime hours and may be eroded as the snow crystals are warmed by incoming shortwave radiation, especially in the morning. The crystals on the east-facing aspect may be able to persist longer than the surface hoar crystals on the south-facing aspects since the temperature and vapor pressure gradients decreased but did not change direction.

Because of these differences in temperature and vapor pressure gradients during days when surface hoar crystals formed, surface hoar tended to grow larger on the north-facing aspects followed by the east- and south-facing aspects respectively. This discrepancy in crystal formation was noted on two separate occasions during the 2003-2004 winter season.

These qualitative and quantitative differences in the temperature and vapor pressure gradients and the direction of the temperature and vapor pressure gradients, which have a major effect on the size and extent of surface hoar crystal formation on the north-, south-, and east-facing aspects, appear to be caused by unequal inputs of incoming shortwave radiation and by differing

radiation balances on these aspects (Bakermans 2006; Bakermans and Jamieson 2006).

The sky cover plays a major role in the formation of large positive temperature and vapor pressure gradients and, consequently, in the amount of faceting. On overcast days the temperature and vapor pressure gradients tended to be similar on all three aspects. All of the surface hoar layers studied here occurred on days with clear or mostly clear sky covers, which agrees well with previous research (Lang et al. 1984; Hachikubo and Akitaya 1997 a,b).

This research demonstrates that there is a significant difference in the size and shape of surface hoar crystals based on slope aspect. Surface hoar crystals formed larger on the north-facing aspect followed by the east- and south-facing aspects respectively. The unequal distribution of incoming shortwave radiation on the north-, south-, and east-facing aspects appears to cause differences in the temperature and vapor pressure gradients on north-facing, south-facing and east-facing aspects and ultimately difference in surface hoar formation. More data to support these findings can be found in Appendix A (Figures A11-A12).

Near-Surface Faceted Crystals

Qualitative and quantitative analyses of the size and extent of near-surface faceted crystal formation, temperature gradients, and vapor pressure gradients between -0.05 m and -0.10 m demonstrate clear differences in the geographic distribution of near-surface faceted crystals based solely on slope

aspect. In this study, near-surface faceted crystals formed more often and the crystals were more advanced, with cupping and striations, which are indicative of advanced development, on the south-facing aspect than on the east- and north-facing aspects respectively.

The crystals grew largest on the south-facing aspect where the diurnal temperature and vapor pressure swings were the largest. There were again statistically significant differences in the temperature and vapor pressure gradient between -0.05 m and -0.10 m based on slope aspect. The south-facing aspect recorded 24-hour temperature gradient swings in excess of 400° C m^{-1} and 24-hour vapor pressure gradient swings larger than 240 mb m^{-1} which is in the range recorded by Birkeland et al. 1998.

The north-facing aspect had large negative temperature and vapor pressure gradients, but the temperature and vapor pressure gradients rarely swung back into the positive realm. The largest temperature and vapor pressure swings on the north-facing aspect tended to be after the month of February, while the south-and east-facing aspects experienced large temperature and vapor pressure gradient swings during all months of the winter. The east-facing aspect was intermediate between the large temperature and vapor pressure gradient swings on the south-facing aspect and the negative gradients on the north-facing aspect.

As with the surface hoar, the sky cover plays a major role in the range of the temperature and vapor pressure gradients and, consequently, in the amount

of faceting. On overcast days the temperature and vapor pressure gradients tended to be similar on all three aspects and tended to be lower than the threshold level for facet formation.

These qualitative and quantitative differences in the temperature and vapor pressure gradients, the direction of the temperature and vapor pressure gradients, the range and amount of swing of the temperature and vapor pressure gradients, the time of day and the time of year of the maximum temperature and vapor pressure gradients, and, consequently, the size and extent of near-surface faceted crystal formation on the north-, south-, and east-facing aspects appear to be caused by unequal inputs of incoming shortwave radiation and by differing radiation balances on these aspects (Bakermans 2006; Bakermans and Jamieson 2006).

On clear days, the south-facing aspect receives very large inputs of shortwave radiation, often in excess of 900 w m^{-2}. A net warming of the snow surface to temperatures well above the temperature of the snow at -0.35 m occurs creating large (in excess of 200° C m^{-1}) positive temperature and vapor pressure gradients (120 mb m^{-1}). The north-facing aspect, on the other hand, receives an average of only 100 w m^{-2} of incoming shortwave radiation during the day resulting in less warming of the snow surface. Since the snow surface is never significantly warmed above the temperature at -0.35 the daytime temperature and vapor pressure gradients remain negative. Since a positive gradient seldom occurs on north-facing aspects near-surface faceted crystal

formation does not often occur. When night arrives, and the incoming shortwave radiation is removed from the slopes, the longwave radiation losses overcome the shortwave radiation gains and all three aspects tend to have negative temperature and vapor pressure gradients.

This research demonstrates that there is a significant difference in the formation of near-surface faceted crystals based on slope aspect. The difference in formation is the result of the unequal distribution of incoming shortwave radiation on the north-, south-, and east-facing aspects resulting in statistically significant difference between the temperature and vapor pressure gradients and larger more developed near-surface faceted crystals on the south-facing aspect than on the north- and east-facing aspects. More data to support these findings can be found in Appendix A (Figures A13-A19).

This research documents the variability in the formation of weak layers on different aspects. Surface hoar and near-surface faceted crystal size and shape can significantly differ by aspect during the same weak layer forming event. Since differing crystal sizes and shapes will respond differently to added snow loads and will stabilize at different rates once they are buried, these results emphasize the complexities involved in forecasting snow avalanches, and the challenges facing ski area, highway, helicopter ski, and backcountry avalanche forecasters.

LITERATURE CITED

Akitaya, E. 1974. Studies on depth hoar. *Contributions from the Institute of Low Temperature Science, Series A*, No. 26,1-67.

Armstrong, R. L. 1985. Metamorphism in a subfreezing, seasonal snow cover: The role of thermal and vapor pressure conditions. Ph.D. dissertation, University of Colorado at Boulder.

Avalanche.org. 2007. Accident Reports. http://www.avalanche.org/accidnt1 (last accessed April 2007).

Bain, L. J., and M. Engelhardt. 1992. *Introduction to probability and mathematical statistics*. Boston: PWS-Kent.

Bakermans, L. 2006. Near-Surface Snow Temperature Changes Over Terrain, M.Sc. thesis, Department of Civil Engineering, University of Calgary, Calgary, Alberta..

Bakermans, L. and Jamieson,B . 2006. Measuring Near-Surface Snow Temperature Changes Over Terrain. *Proceedings of the 2006 International Snow Science Workshop*, Telluride, CO, pp. 377-86.

Birkeland, K. W. 1998. Terminology and predominant processes associated with the formation of weak layers of near-surface faceted crystals in the mountain snowpack. *Arctic and Alpine Research* 30:193-99.

Birkeland, K. W., R. F. Johnson, and D. S. Schmidt. 1998. Near-surface faceted crystals formed by diurnal recrystallization: A case study of weak layer formation in the mountain snowpack and its contribution to snow avalanches. *Arctic and Alpine Research* 30:200-04.

Birkeland, K. W., K. Kronholm, M. Schneebeli, and C. Pielmeier. 2004. Changes in the shear strength and micro-penetration hardness of a buried surface-hoar layer. *Annals of Glaciology*. 38:223-28.

Bradley, C. C. 1970. The location and timing of deep slab avalanches. *Journal of Glaciology* 9:253-61.

Bradley, C. C., R. L. Brown, and T. Williams. 1977. On depth hoar and the strength of snow. *Journal of Glaciology* 18:145-47.

Canadian Avalanche Association. 2005. http://www.avalanche.ca/default.aspx?DN=433,582,558,3,Documents (last accessed June 2006).

Colbeck, S. C. 1980. Thermodynamics of snow metamorphism due to variations in curvature. *Journal of Glaciology* 26:291-301.

———. 1982. *Growth of faceted crystals in a snow cover*, CRREL Report 82-29. Hanover, NH: U.S. Army Cold Regions Research Engineering Lab.

———. 1988. On the micrometeorology of surface hoar growth on snow in mountainous area. *Boundary-Layer Meteorology* 44:1-12.

———. 1989. Snow-crystal growth with varying surface temperatures and radiation penetration. *Journal of Glaciology* 35:23-29.

Colbeck, S. C., E. Akitaya, R. Armstrong, H. Gubler, J. Lafeuille, K. Lied, D. McClung, and E. Morris. 1990. *The International Classification for Seasonal Snow on the Ground*. International Commission on Snow and Ice of the International Association of Scientific Hydrology and International Glaciology Society. http://www.crrel.usace.army.mil/techpub/CRREL_Reports/reports/Seasonal_Snow.pdf (last accessed 15 April 2008).

Cooperstein, M. S., Birkeland, K. W., and Hansen, K. J. 2004. The Effects of Slope Aspect on the Formation of Surface Hoar and Diurnally Recrystalized Near-Surface Faceted Crystals; Implications for Avalanche Forecasting. *Proceedings of the 2004 International Snow Science Workshop*, Jackson, WY, pp. 83-93.

Davis, R. E., B. Jamieson, J. Hughes, and C.Johnston. 1996. Observations on buried surface hoar – Persistent failure planes for slab avalanches in British Columbia, Canada. *Proceedings of the 1996 International Snow Science Workshop*, Banff, Canada, pp. 81-85. http://www.avalanche.org/~issw/96/art_16_.html (last accessed 15 April 2008).

Davis, R. E., B. Jamieson, and C. Johnston. 1998. Observations on buried surface hoar in British Columbia, Canada: Section analyses of layer evolution and associated strength measurements. *Proceedings of the 1998 International Snow Science Workshop*, Sunriver, OR, pp. 86-92.

Deems, J. S. 2003. Topographic effects on the spatial and temporal patterns of snow temperature gradients in a mountain snowpack, M.Sc. thesis, Department of Earth Sciences, Montana State University, Bozeman, MT.

Feick, S., K. Kronholm, and J. Schweizer. 2007. Field observations on spatial variability of surface hoar at the basin scale. *Journal of Geophysical Research-Earth Surface* 112:(F02002).

———. 1992. Characteristics of weak snow layers or interfaces. *Proceedings of the 1992 International Snow Science Workshop*, Breckenridge, CO, pp. 160-70.

Fukuzawa, T., and E. Akitaya. 1993. Depth-hoar crystal growth in the surface layer under high temperature gradient. *Annals of Glaciology* 18:39-45.

Giddings, J. C., and E. R. LaChapelle. April 1961. *The formation rate of depth hoar.* Alta Avalanche Study Center, Project C, Progress Report No 2. http://www.avalanche.org/~moonstone/snowpack/the%20formation%20rate%20of%20depth%20hoar.htm (last accessed 15 April 2008).

Giddings, J. C., and E. R. LaChapelle. 1962. The formation rate of depth hoar. *Journal of Geophysical Research. 67:* 2377-82.

Google. 2006. Google Earth: by Digital Globe, Europa Technologies, TeraMetrics.

Greene, E., K. Birkeland, K. Elder, G. Johnson, C. Landry, I. McCammon, M. Moore, D. Sharaf, C. Sterbenz, B. Tremper, and K. Williams. 2004. *Snow, Weather, and Avalanches: Observational Guidelines for Avalanche Programs in the United States*. Pagosa Springs, CO: American Avalanche Association. http://www.avalanche.org/~research/guidelines (last accessed 15 April 2008).

Hachikubo, A. 2001. Numerical modelling of sublimation on snow and comparison with field measurements. *Annals of Glaciology* 32:27-32.

Hachikubo, A., and E. Akitaya. 1997a. Observation and numerical experiment concerning the wind effect on surface hoar condensation. *International Conference for Avalanche Related Subjects,* Kirovsk, Russia, pp. 72-76.

Hachikubo, A., and E. Akitaya. 1997b. Effect of wind on surface hoar growth on snow. *Journal of Geophysical Research-Atmospheres* 102:4367-73.

Hageli, P., and McClung, D. 2002. Analysis of Weak Layer Avalanche Activity in the Columbia Mountains, British Columbia, Canada. *Proceedings of the 2002 International Snow Science Workshop*, Penticton, BC.

Hardy, D., M. W. Williams, and C. Escobar. 2001. Near-surface faceted crystals, avalanches and climate in high-elevation, tropical mountains of Bolivia. *Cold Regions Science and Technology* 33:291-302.

Höller, P. 1998. Tentative investigations on surface hoar in mountain forests. *Annals of Glaciology* 26:31-34.

Hood, E., K. Scheler, and P. Carter. 2005. Near-surface faceted crystal formation and snow stability in a high-latitude maritime snow climate, Juneau, Alaska. *Arctic, Antarctic, and Alpine Research* 37:316-22.

Jamieson, J. B., and A. van Herwijnen. 2002. Preliminary results from controlled experiments on the growth of faceted crystals above a wet snow layer. *Proceedings of the 2002 International Snow Science Workshop*, Penticton, British Columbia, pp. 337-42.

Jamieson, J. B., and C. D. Johnston. 1992. Snowpack characteristics associated with avalanche accidents. *Canadian Geotechnical Journal* 29:862-66.

Jamieson, J. B., and C. D. Johnston. 1997. The faceted layer of November 1996 in Western Canada. *Canadian Avalanche Association Avalanche News*, 52: 10-15 http://www.schulich.ucalgary.ca/Civil/Avalanche/Papers/Nov_Facets.pdf (last accessed 15 April 2008).

Jamieson, J. B., and C. D. Johnston. 1999. Snowpack factors associated with strength changes of buried surface hear layers. *Cold Regions Science and Technology* 30:19-34.

Jamieson, J. B., and J. Schweizer. 2000. Texture and strength changes of buried surface-hoar layers with implications for dry snow-slab avalanche release. *Journal of Glaciology* 46:151-160.

LaChapelle, E. R. 1970. Principles of avalanche forecasting. *Ice Engineering and Avalanche Forecasting and Control: Proceedings of a Conference Held at the University of Calgary, 23-24 October 1969.* Technical Memorandum 98. Ottawa: National Research Council of Canada, pp. 106-13.

LaChapelle, E. R., and R. L. Armstrong. 1977. Temperature patterns in an alpine snow cover and their influence on snow metamorphism. U.S. Army Research Office, Institute of Arctic and Alpine Research Technical Report. University of Colorado at Boulder.

Lang, R. M., B. R. Leo, and R. L. Brown. 1984. Observations on the growth processes and strength characteristics of surface hoar. *Proceedings of the 1984 International Snow Science Workshop*, Aspen, CO, pp188-95.

List, R. J. 1949. *Smithsonian Meteorological Tables*. Washington, D.C.: Smithsonian Institute, pp. 350-64.

Logan, S. 2005. Temporal changes in the spatial patterns of weak layer shear strength and stability on uniform slopes. M.Sc. thesis, Department of Earth Sciences, Montana State University, Bozeman, MT.

Logan, S., K. Birkeland, K. Kronholm, and K. Hansen. 2007. Temporal changes in the slope-scale spatial variability of the shear strength of buried surface hoar layers. *Cold Regions Science and Technology* 47:148-58.

Marbouty, D. 1980. An experimental-study of temperature-gradient metamorphism. *Journal of Glaciology* 26:303-12.

McCammon, I., and J. Schweizer. 2002. A field method for identifying structural weaknesses in the snowpack. *Proceedings of the 2002 International Snow Science Workshop*. Penticton, British Columbia pp. 477-81. http://www.snowpit.com/articles/lemons%20reprint%20copy.pdf (last accessed 15 April 2008).

McClung, D., and P. Schaerer. 1992. *The Avalanche Handbook*. Seattle: Mountaineers.

McElwaine, J., A. Hachikubo, M. Nemoto, T. Kaihara, T. Yamada, and K. Nishimura. 2000. Observations and simulations of the formation of the faceted snow crystals in the weak-layer of the 1998 Niseko Haru no Taki avalanche. *Cold Regions Science and Technology* 31:235-47.

Mock, C. J., and K. W. Birkeland. 2000. Snow avalanche climatology of the western United States mountain ranges. *Bulletin of the American Meteorological Society* 81:2367-92. http://ams.allenpress.com/archive/1520-0477/81/10/pdf/i1520-0477-81-10-2367.pdf (last accessed 15 April 2008).

Morstad, B. W. 2004. Analytical and experimental study of radiation-recrystallized near-surface facets in snow, M.Sc. thesis, Department of Mechanical Engineering, Montana State University, Bozeman, MT.

Morstad, B. W., E. E. Adams, and L. R. McKittrick. 2007. Experimental and analytical study of radiation-recrystallized near-surface facets in snow. *Cold Regions Science and Technology* 47:90-101.

Perla, R., and M. Martinelli. 1978. *Avalanche Handbook*. Fort Collins, CO: U.S. Department of Agriculture, Forest Service.

Radbruch-Hall, D. H., R. B. Colton, W. E. Davies, I. Lucchitta, B. A. Skipp, and D. J. Varnes. 1982. *Landslide Overview Map of the Conterminous United States.* Geological Survey Professional Paper 1183. Washington, D.C.: U.S. G.P.O. http://pubs.usga.gov/pp/p1183/pp1183.html (last accessed 24 April 2008).

Schweizer, J. 1999. Review of dry snow slab avalanche release. *Cold Regions Science and Technology* 30:43-57.

Schweizer, J., and K. Kronholm. 2004. Multi-scale spatial variability of a layer of buried surface hoar. *Proceedings of the 2004 International Snow Science Workshop*, Jackson Hole, WY. pp. 335-42. http://www.slf.ch/schneep/pdf/Schweizer_Kronholm_ISSW2004.pdf (last accessed Oct 2006).

———. 2007. Snow cover spatial variability at multiple scales: Characteristics of a layer of buried surface hoar. *Cold Regions Science and Technology* 47:207-23.

Stratton, J. 1977. "Development of upper level temperature gradient crystals" and "Upper level temperature gradient avalanche cycle - February 1 -2, 1977." Short unpublished papers that were circulated around Utah avalanche community in the early 1980's by John Stratton. Snowbird, UT: Snow Safety Department.

Stull, R. B. 1988. An introduction to boundary layer meterology. London: Kluwer Academic Publishers.

Sturm, M., and Bennson, C. 1997. Vapor transport, grain growth and depth-hoar development in the subarctic snow. *Journal of Glaciology* 43:143-60.

Tremper, B. 2001. Staying alive in avalanche terrain. Seattle: Mountaineers.

Voight, B., B. R. Armstrong, R. L. Armstrong, D. Bowles, R. L. Brown, S. A. Ferguson, J. A. Fredston, J. Kiusalaas, R. C. McFarlane, and R. Penniman. 1990. *Snow avalanche hazards and mitigation.* Washington, D.C.: National Academy Press. http://books.nap.edu/openbook.php?record_id=1571&page=R1 (last accessed 25 April 2008).

APPENDIX A

WEATHER AND YEAR LONG GRADIENT DATA

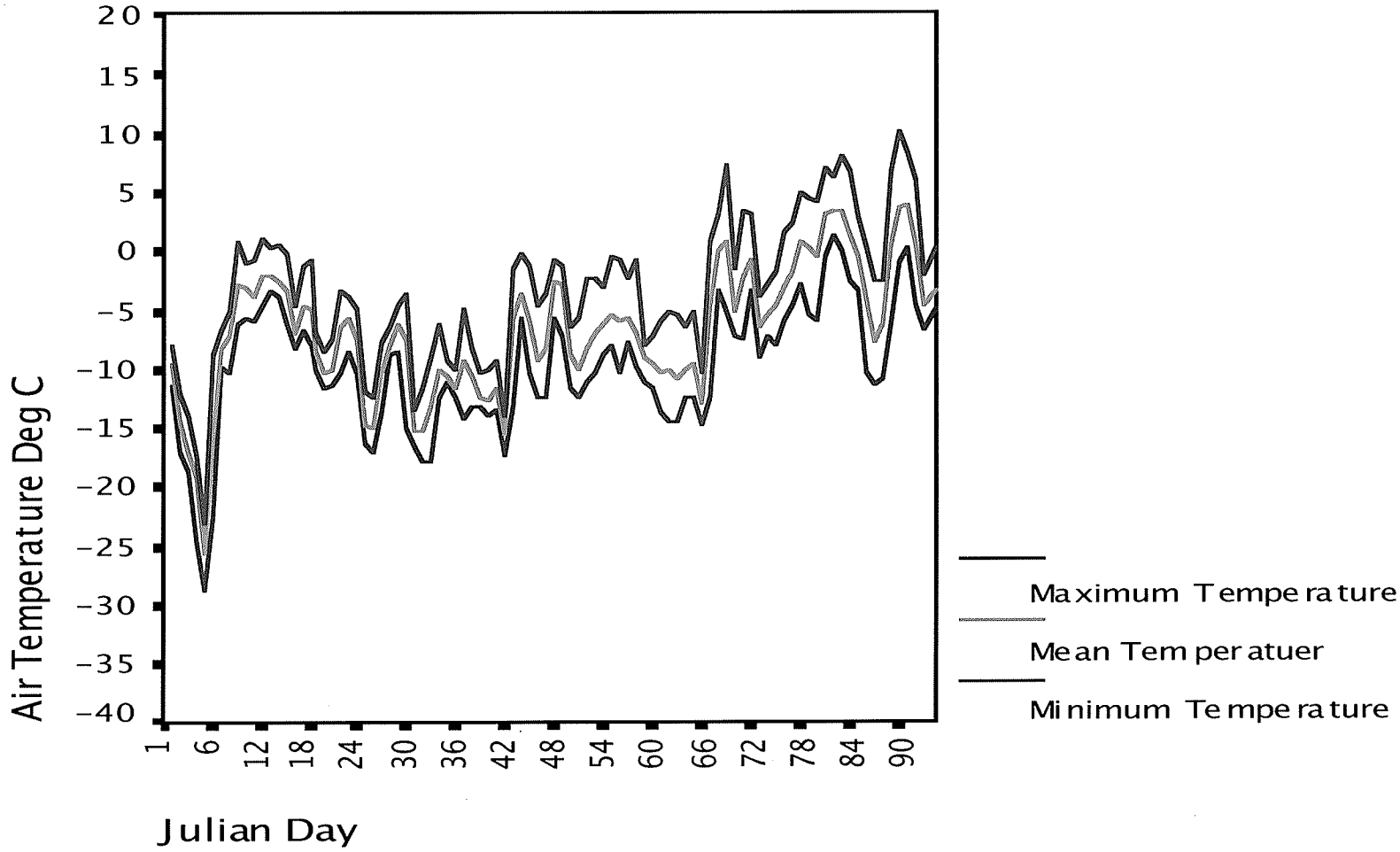

Figure A1: The minimum, maximum, and mean temperature in degrees Celsius at the Timberline Study Site by Julian Day for the winter 2003–2004

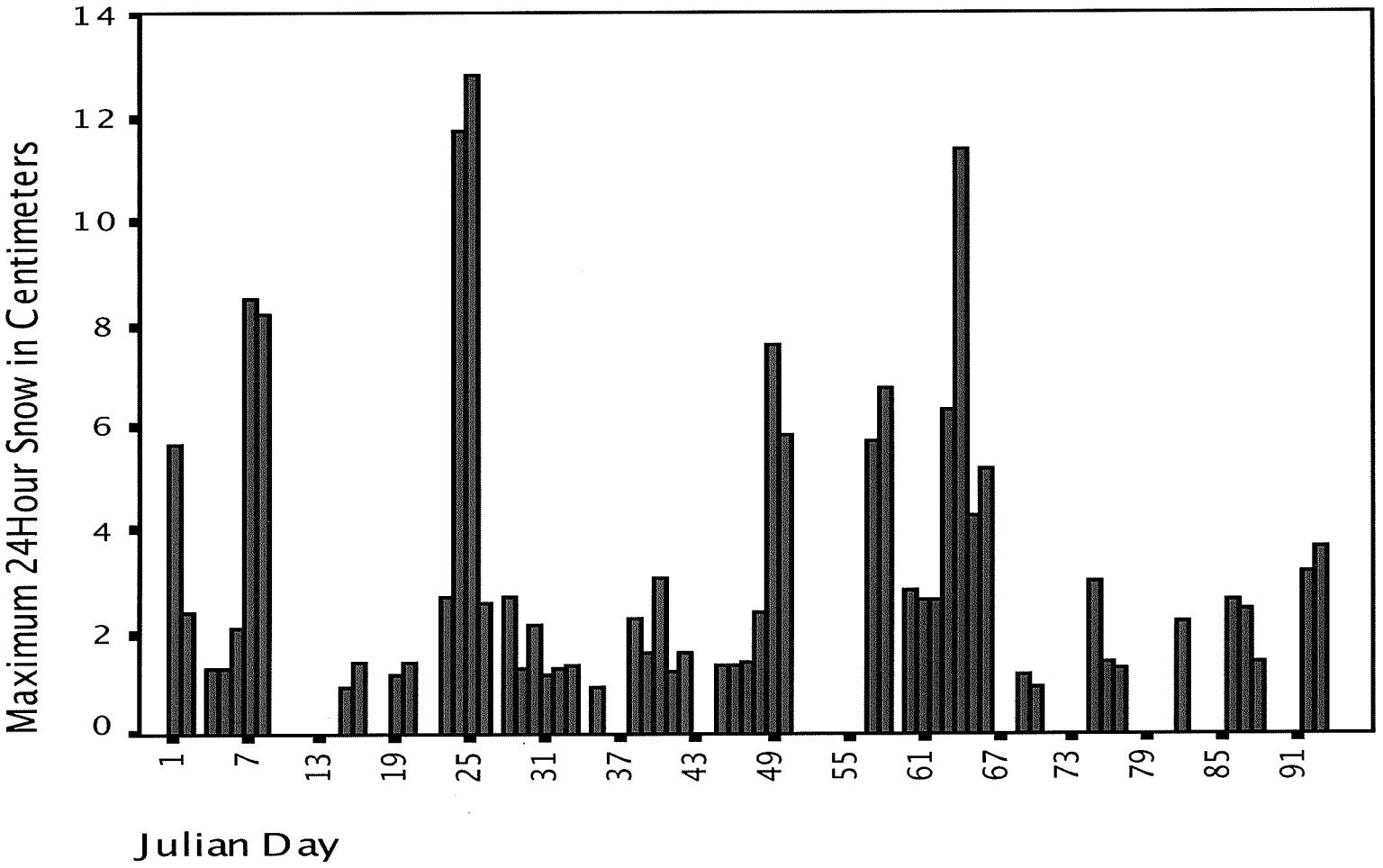

Figure A2: The maximum 24-hour snowfall in centimeters at the Timberline Snow Study Site by Julian Day for the winter 2003-2004.

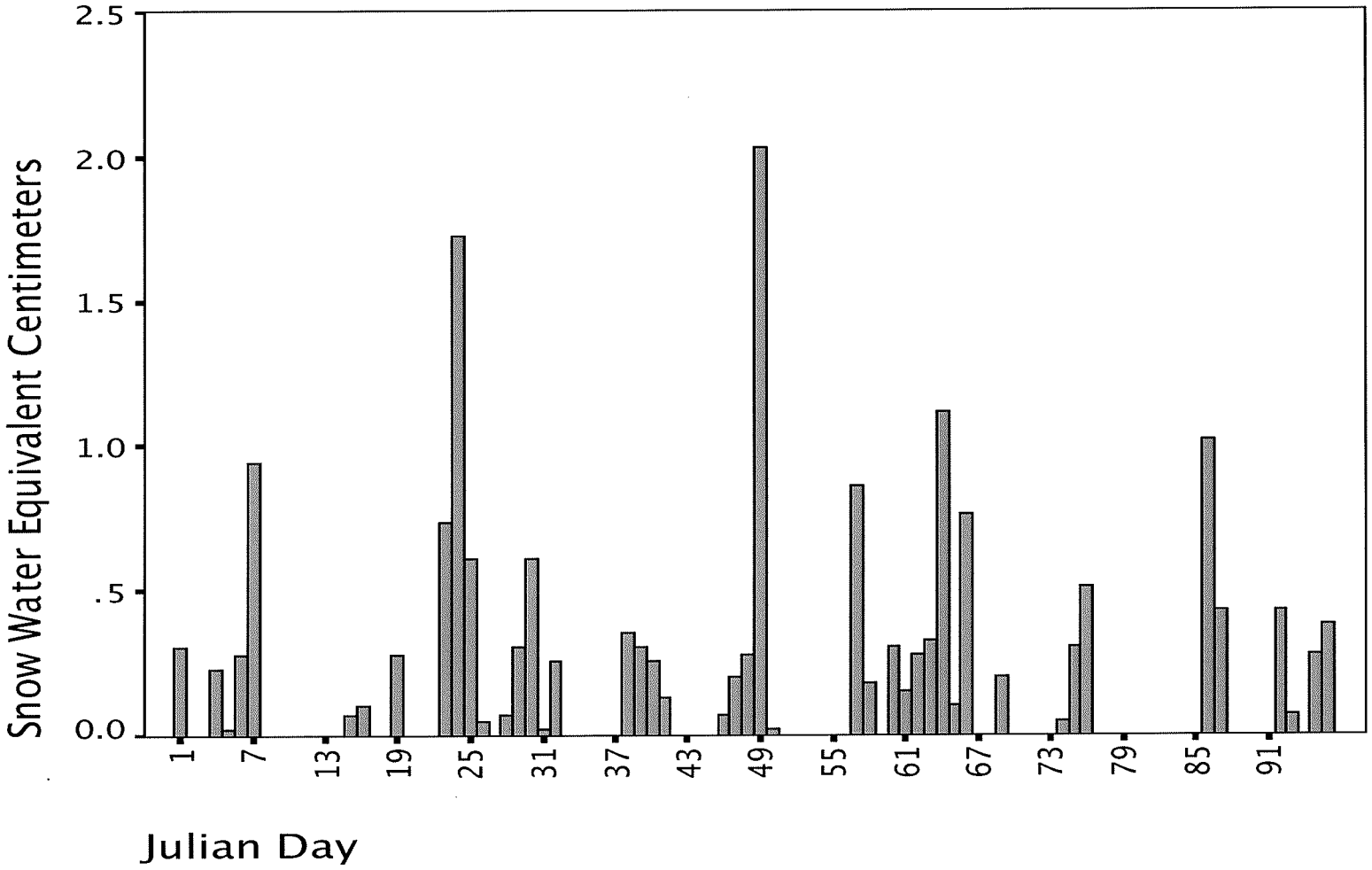

Figure A3: The snow water equivalent in Centimeters at the Timberline Snow Study Site by Julian Day for the winter 2003-2004.

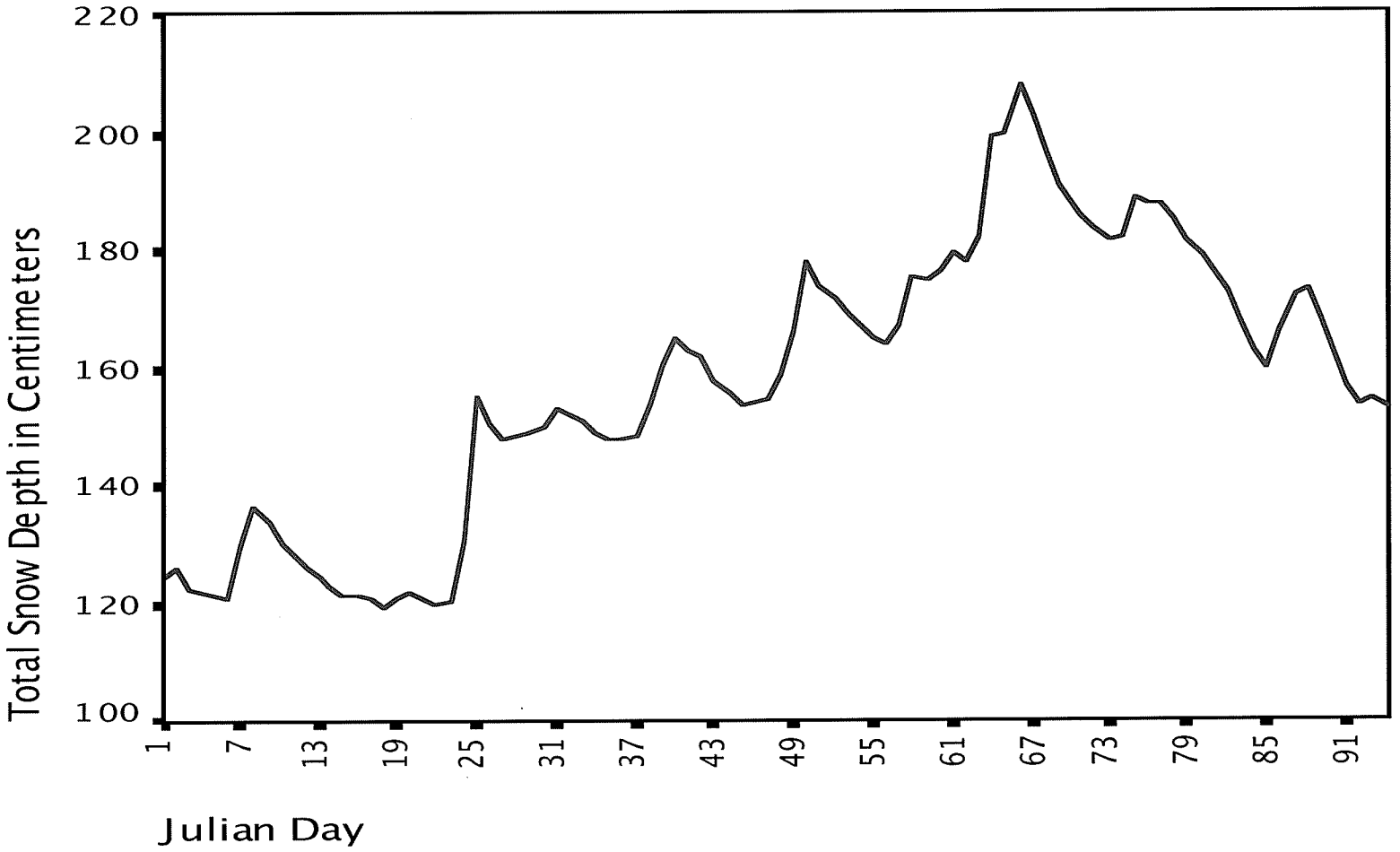

Figure A4: The total snow depth in centimeters at the Timberline Snow Study Site by Julian Day for the winter 2003-2004.

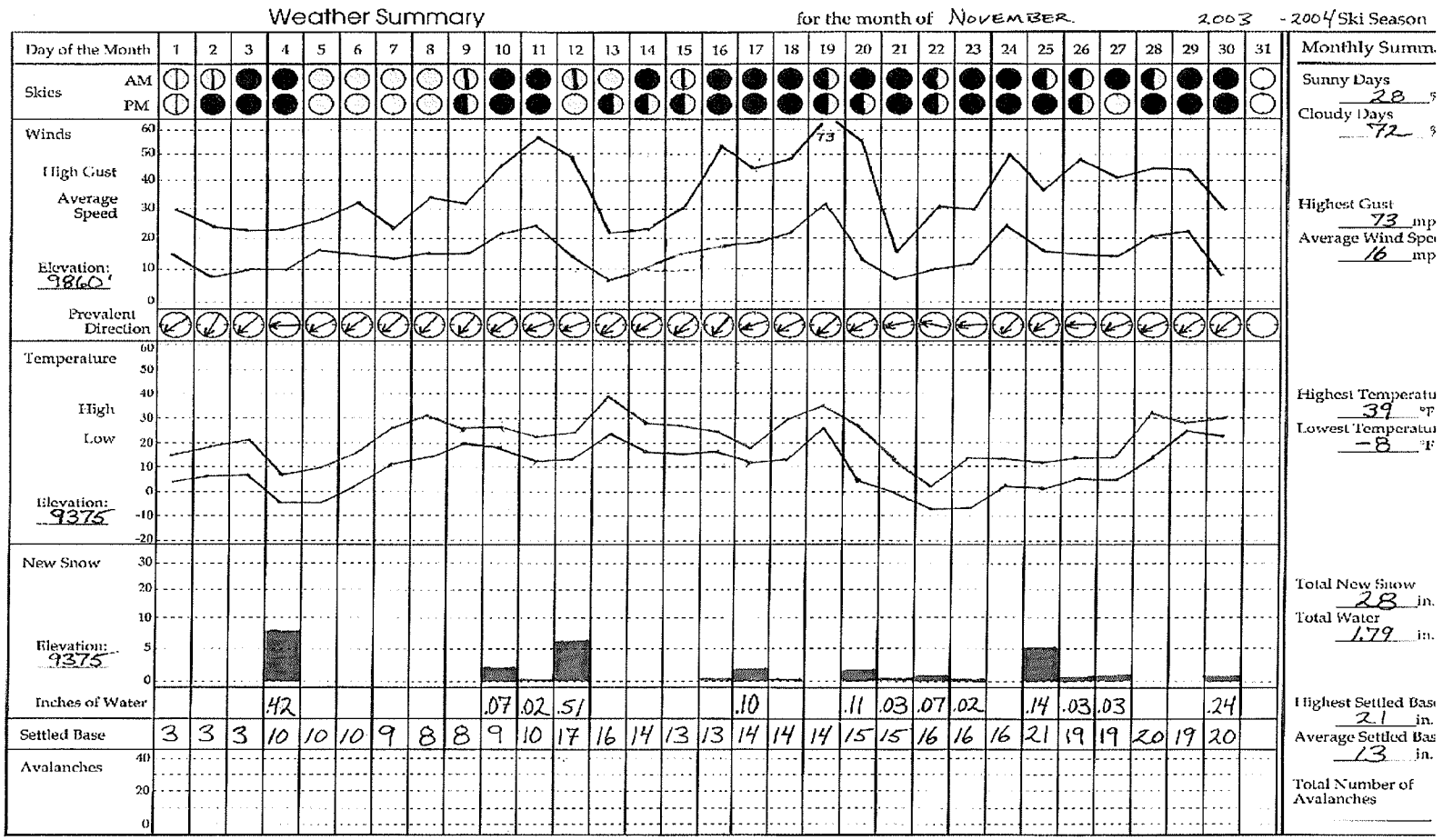

Figure A5: The sky cover, maximum wind gust (mph), average wind speed (mph), wind direction (°), maximum and minimum temperature (° F), new snow (inches), snow water equivalent (inches), snow base (inches), and number of avalanches recorded by the Yellowstone Club for November 2003.

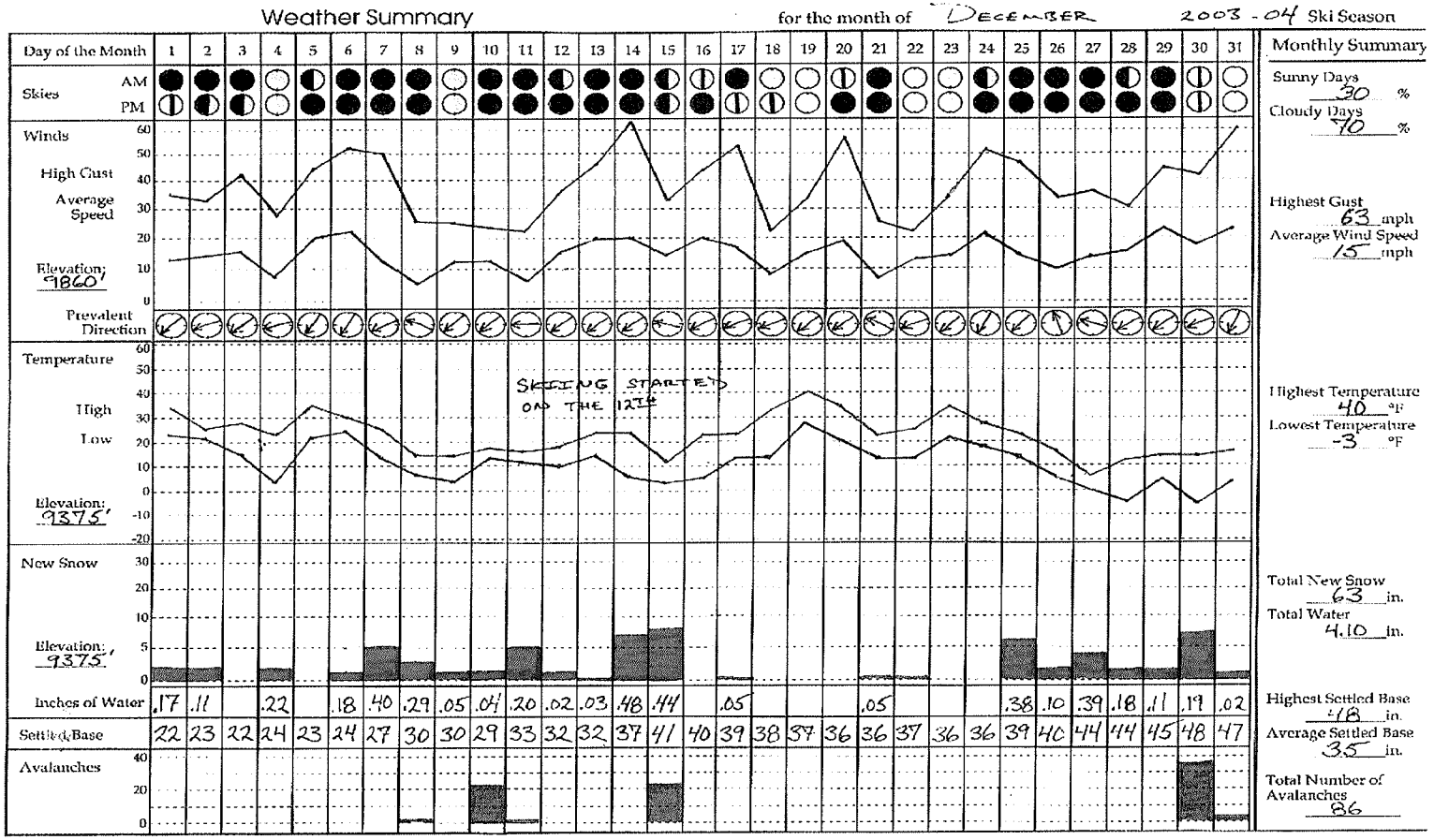

Figure A6: The sky cover, maximum wind gust (mph), average wind speed (mph), wind direction (°), maximum and minimum temperature (° F), new snow (inches), snow water equivalent (inches), snow base (inches), and number of avalanches recorded by the Yellowstone Club for December 2003.

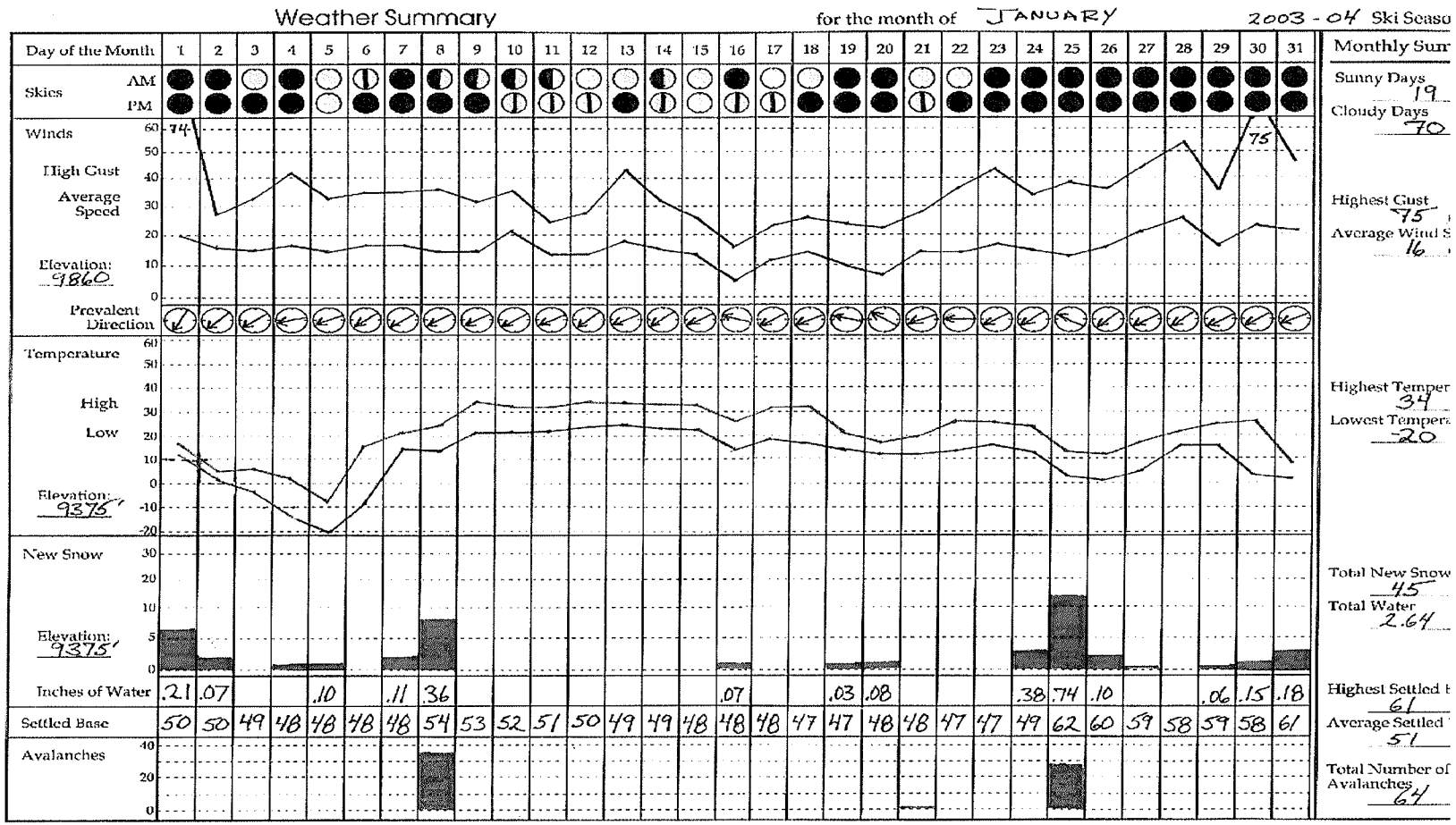

Figure A7: The sky cover, maximum wind gust (mph), average wind speed (mph), wind direction (°), maximum and minimum temperature (° F), new snow (inches), snow water equivalent (inches), snow base (inches), and number of avalanches recorded by the Yellowstone Club for January 2004.

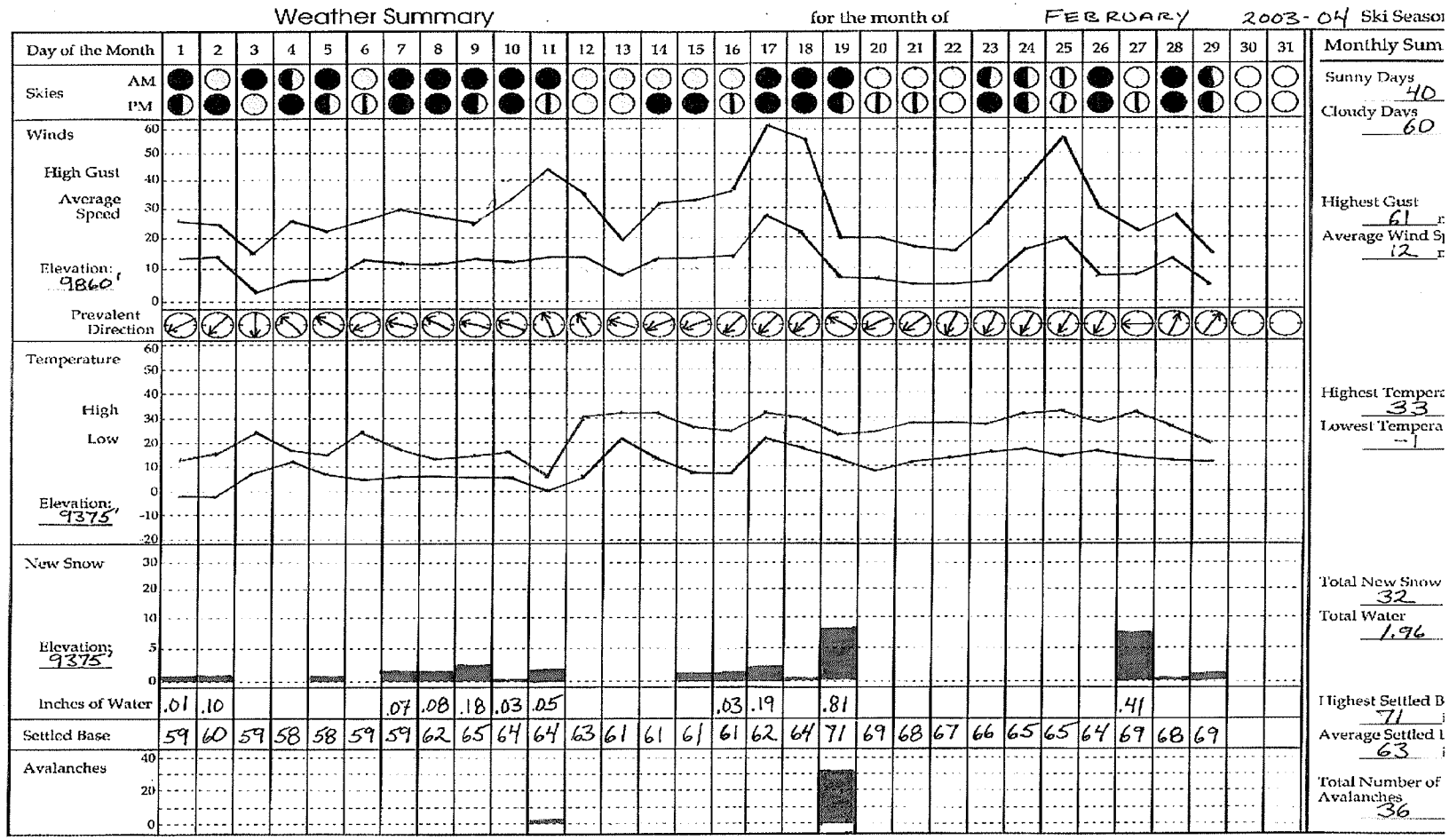

Figure A8: The sky cover, maximum wind gust (mph), average wind speed (mph), wind direction (º), maximum and minimum temperature (º F), new snow (inches), snow water equivalent (inches), snow base (inches), and number of avalanches recorded by the Yellowstone Club for February 2004.

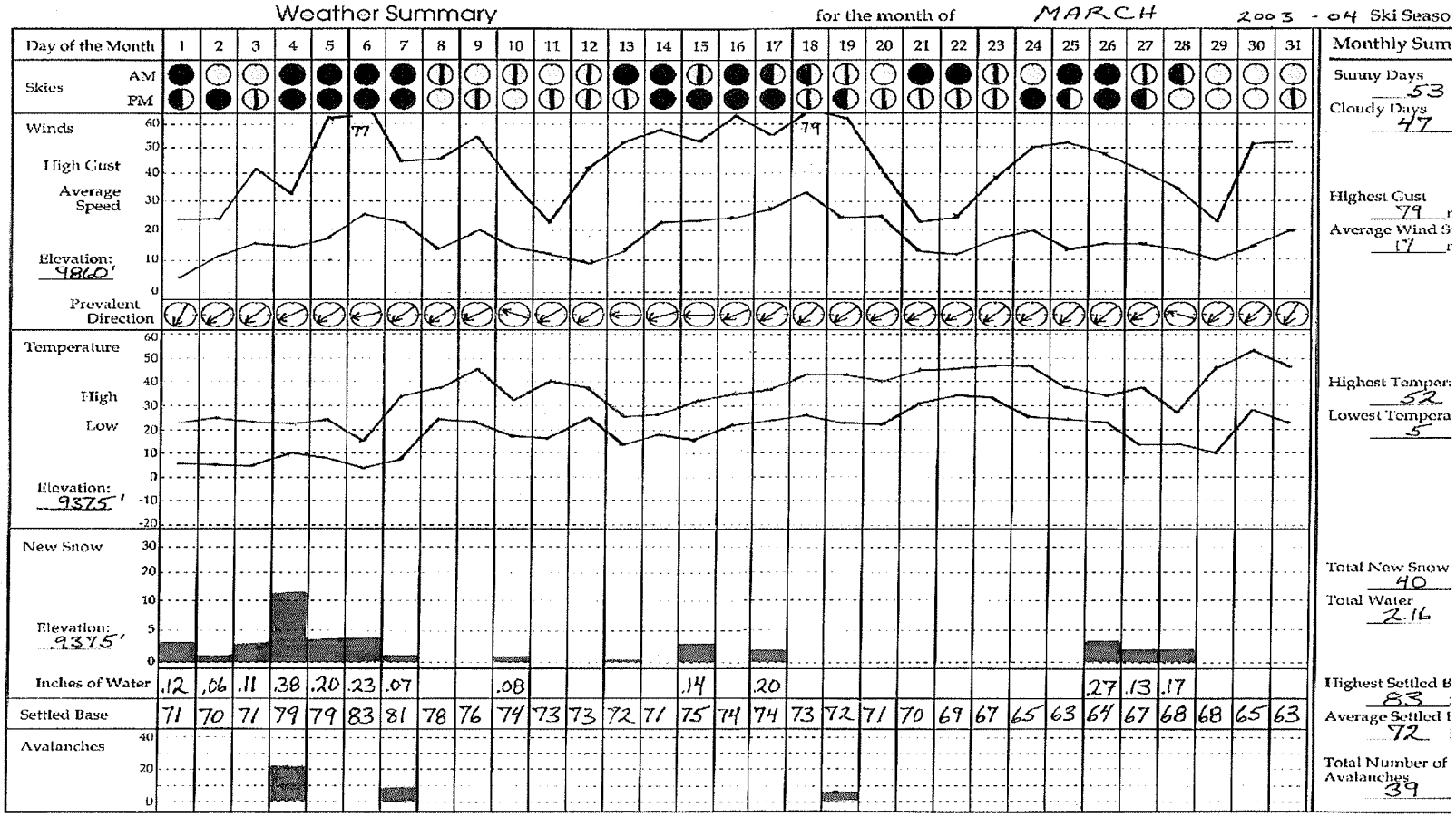

Figure A9: The sky cover, maximum wind gust (mph), average wind speed (mph), wind direction (º), maximum and minimum temperature (º F), new snow (inches), snow water equivalent (inches), snow base (inches), and number of avalanches recorded by the Yellowstone Club for March 2004.

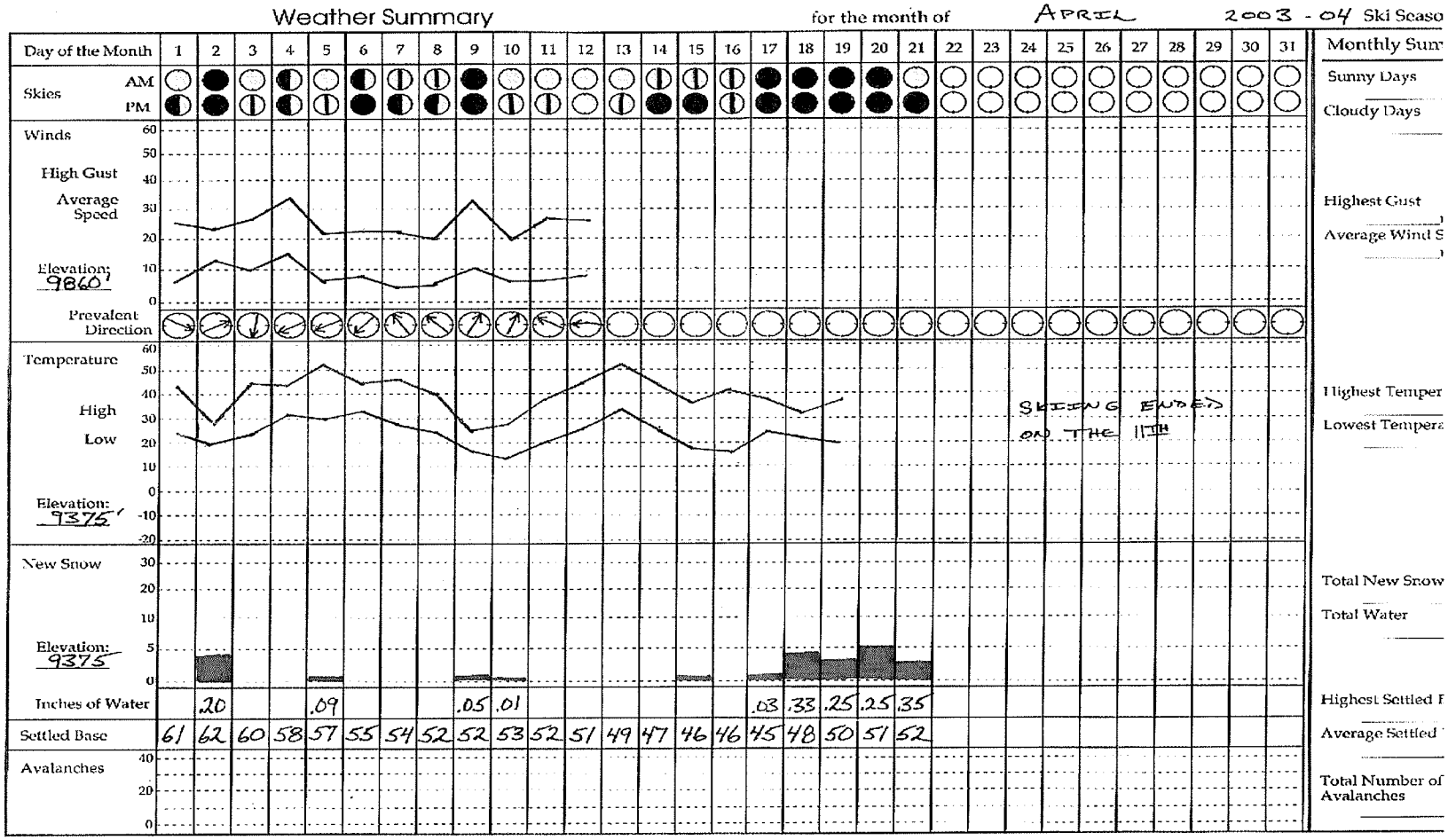

Figure A10: The sky cover, maximum wind gust (mph), average wind speed (mph), wind direction (º), maximum and minimum temperature (º F), new snow (inches), snow water equivalent (inches), snow base (inches), and number of avalanches recorded by the Yellowstone Club for April 2004.

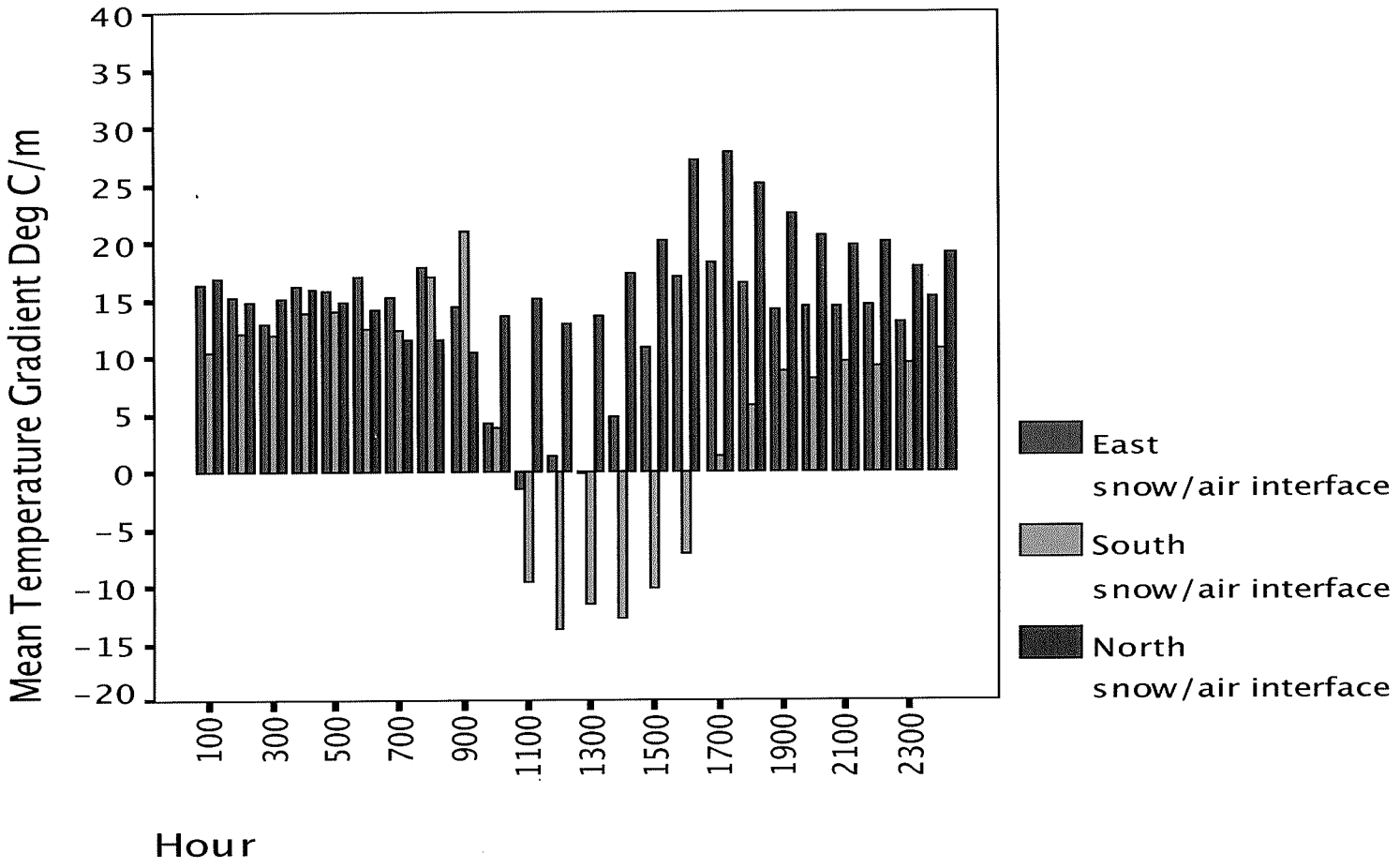

Figure A11: The mean temperature gradient at the snow air interface (°C m^{-1}) by hour on the north, south, and east aspects by hour for the entire winter season 2003–2004.

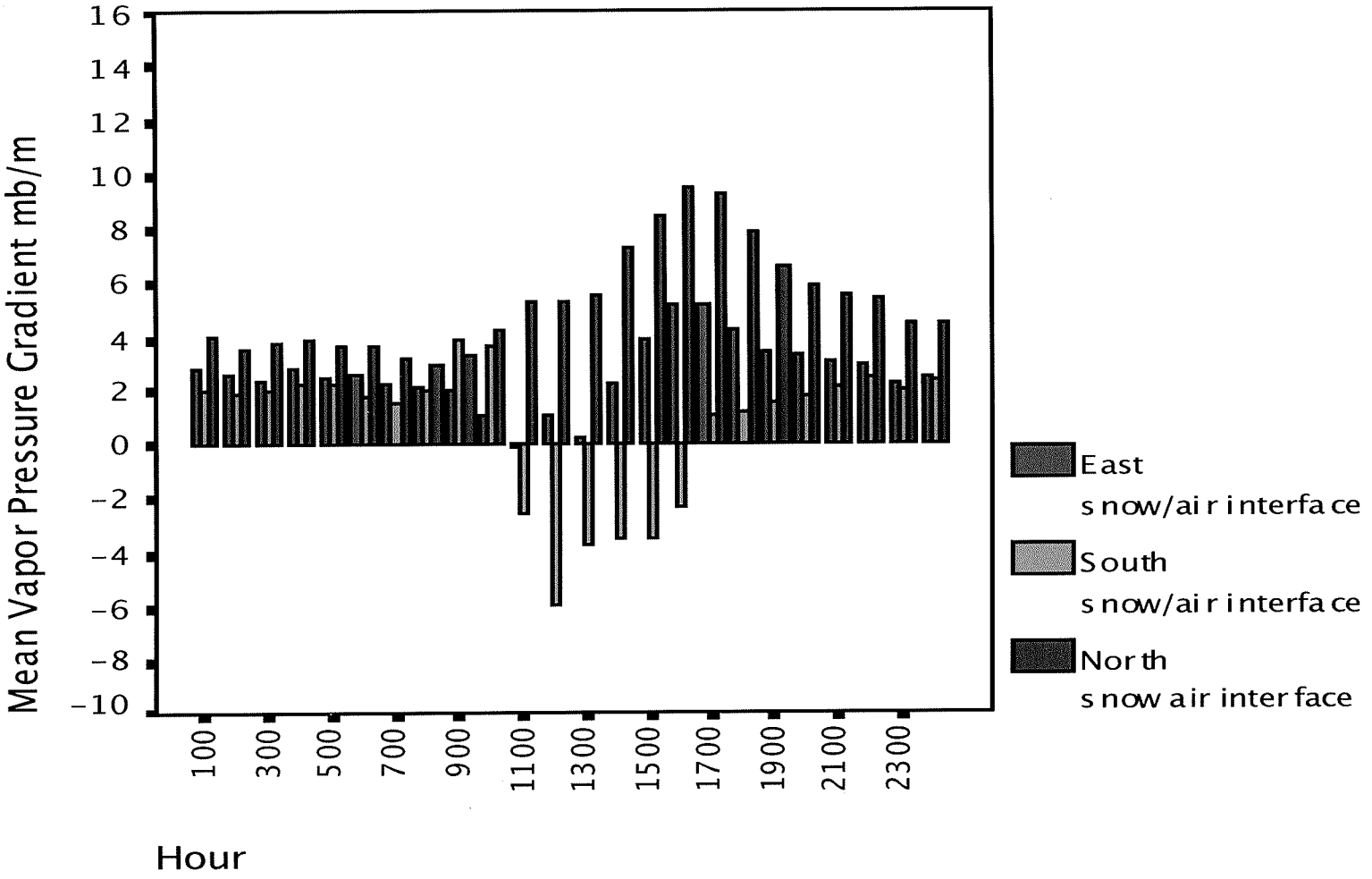

Figure A12: The mean vapor pressure gradient at the snow/air interface (mb m^{-1}) on the north, south, and east aspects by hour for the entire winter season 2003–2004.

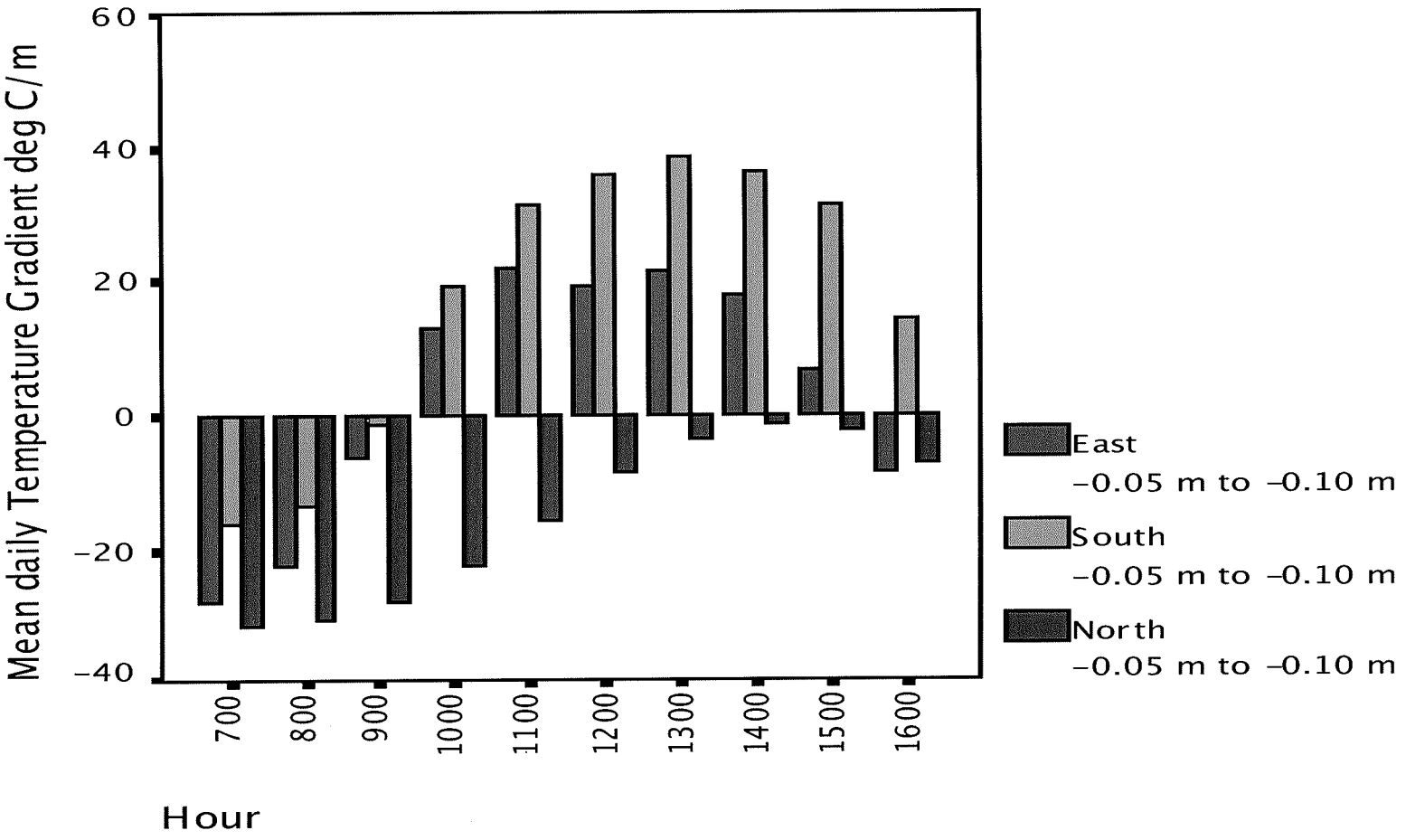

Figure A13: The mean daily temperature gradient (°C m $^{-1}$) between -0.05 m and -0.10 m by hour on the north, south, and east aspects for the entire winter season 2003–2004.

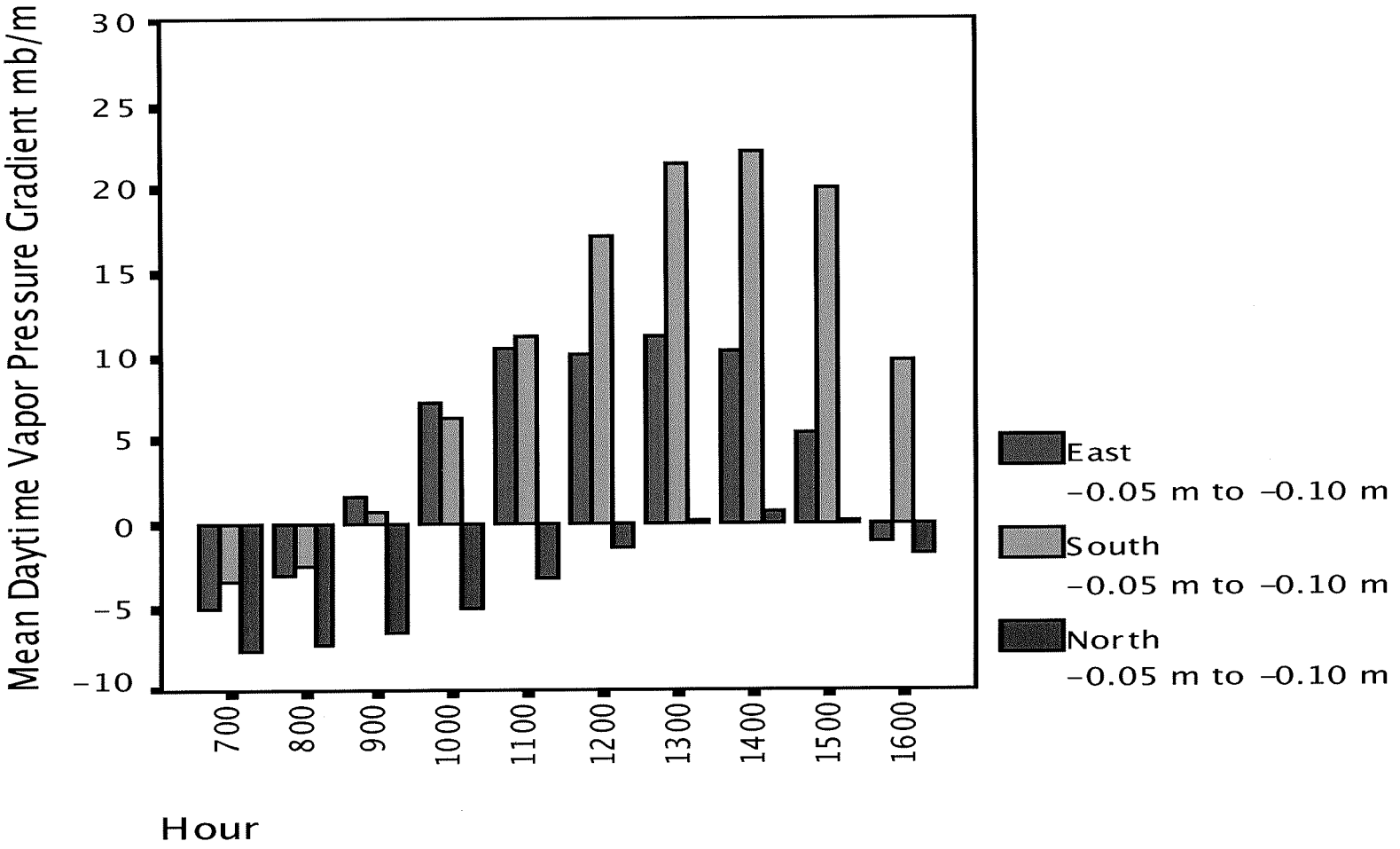

Figure A14: The mean daily vapor pressure gradient (mb m^{-1}) between -0.05 m and -0.10 m by hour on the north, south, and east aspects for the entire winter season 2003–2004.

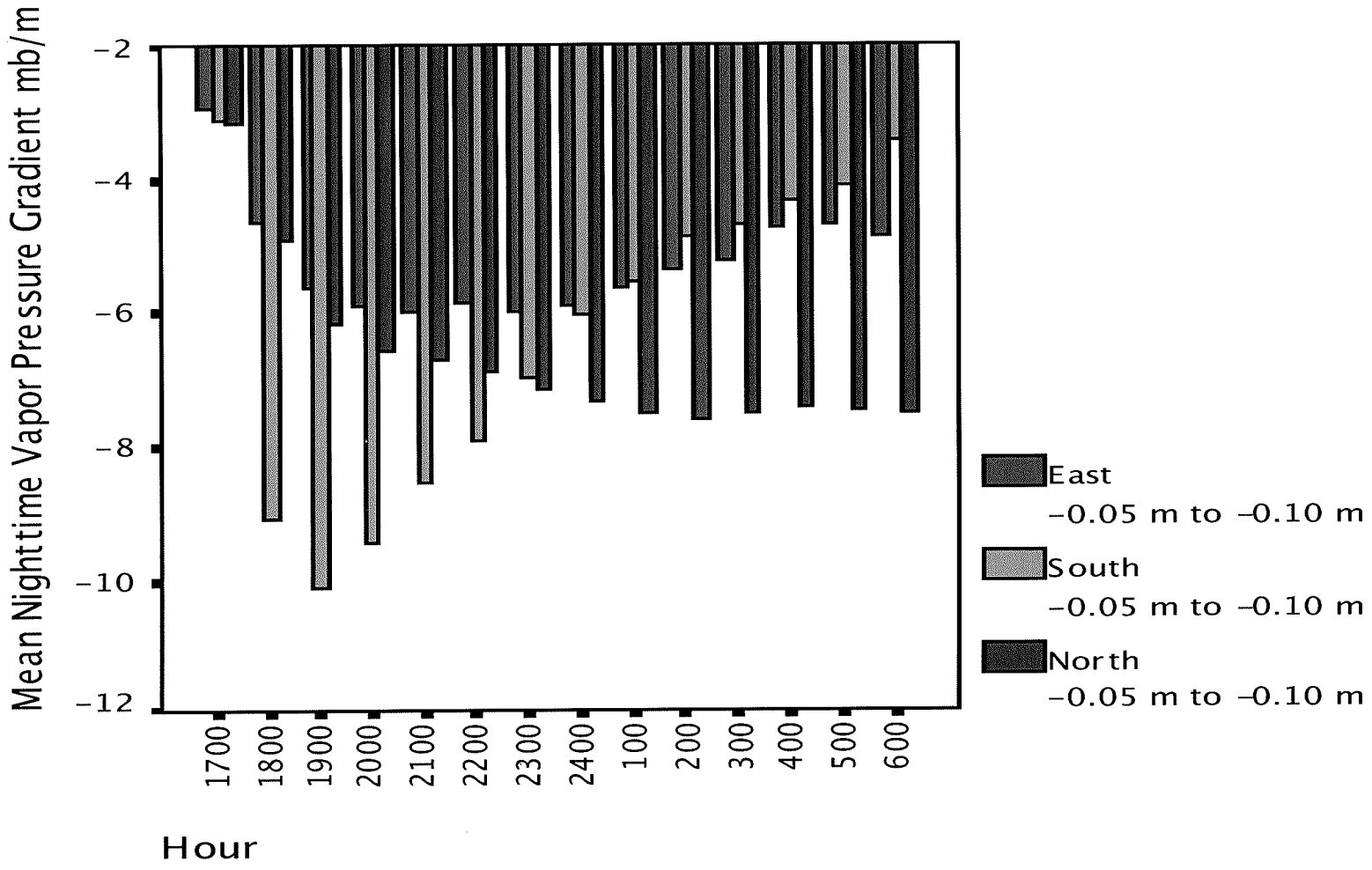

Figure A15: The mean nightly vapor pressure gradient (mb m^{-1}) between -0.05 m and -0.10 m by hour on the north, south, and east aspects for the entire winter season 2003–2004.

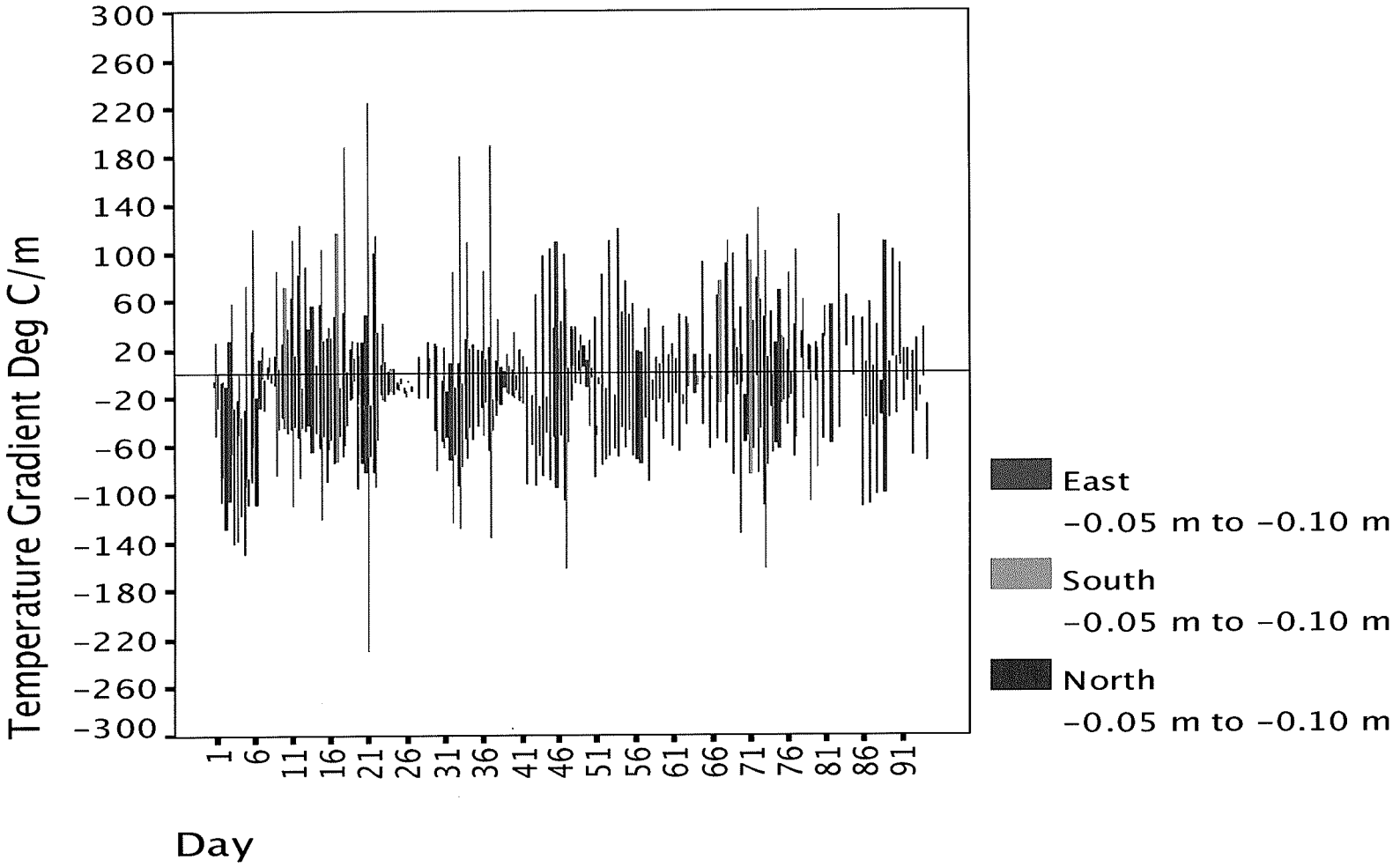

Figure A16: The fluctuation between the minimum and maximum temperature gradient (° C m^{-1}) by Julian Day for the winter season 2003-2004 on the north-, south-, and east-facing aspects between -0.05 m and -0.10 m.

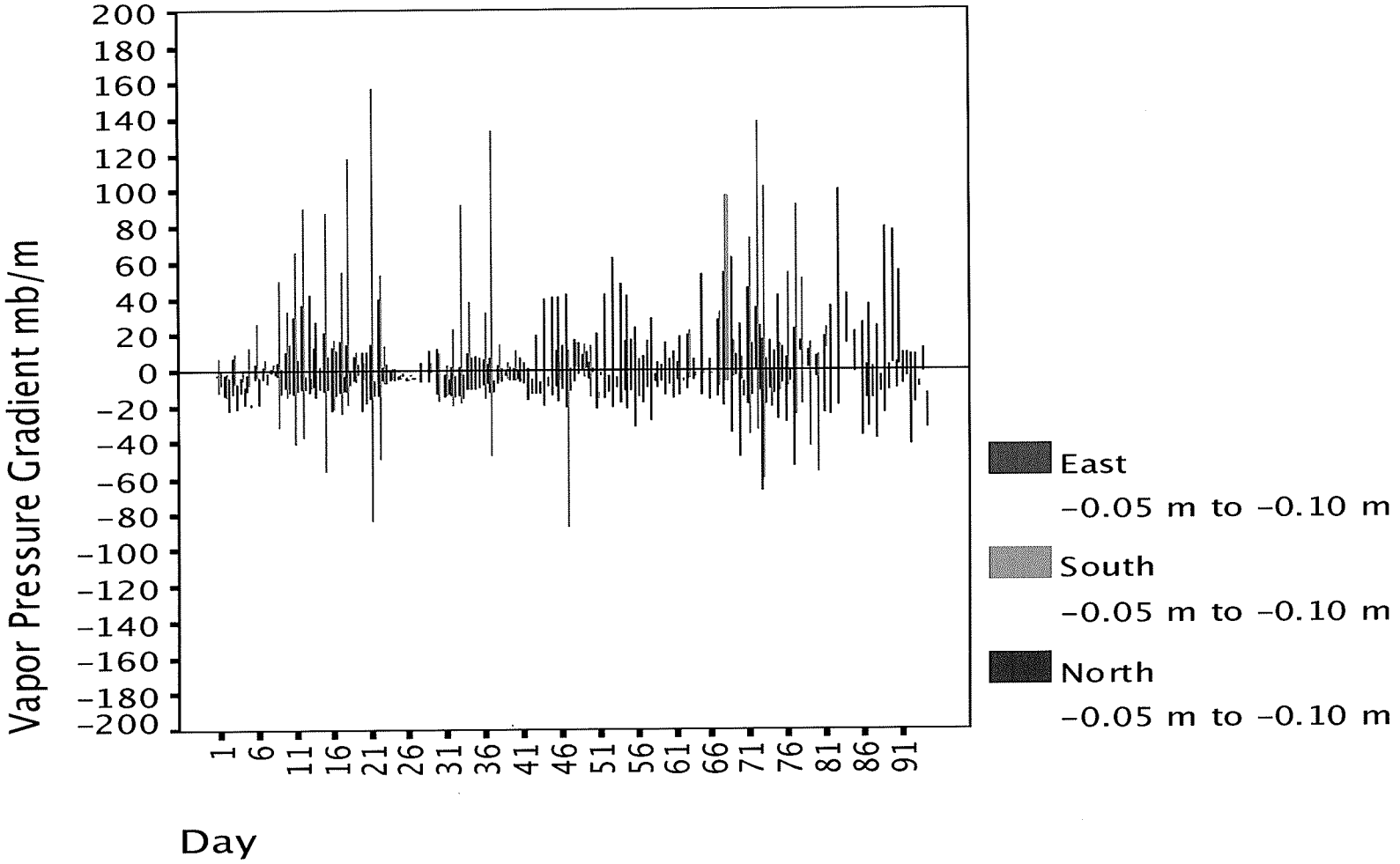

Figure A17: The fluctuation between the minimum and maximum vapor pressure gradient (mb m^{-1}) by Julian Day for the winter season 2003-2004 on the north-, south-, and east-facing aspects between -0.05 m and -0.10 m.

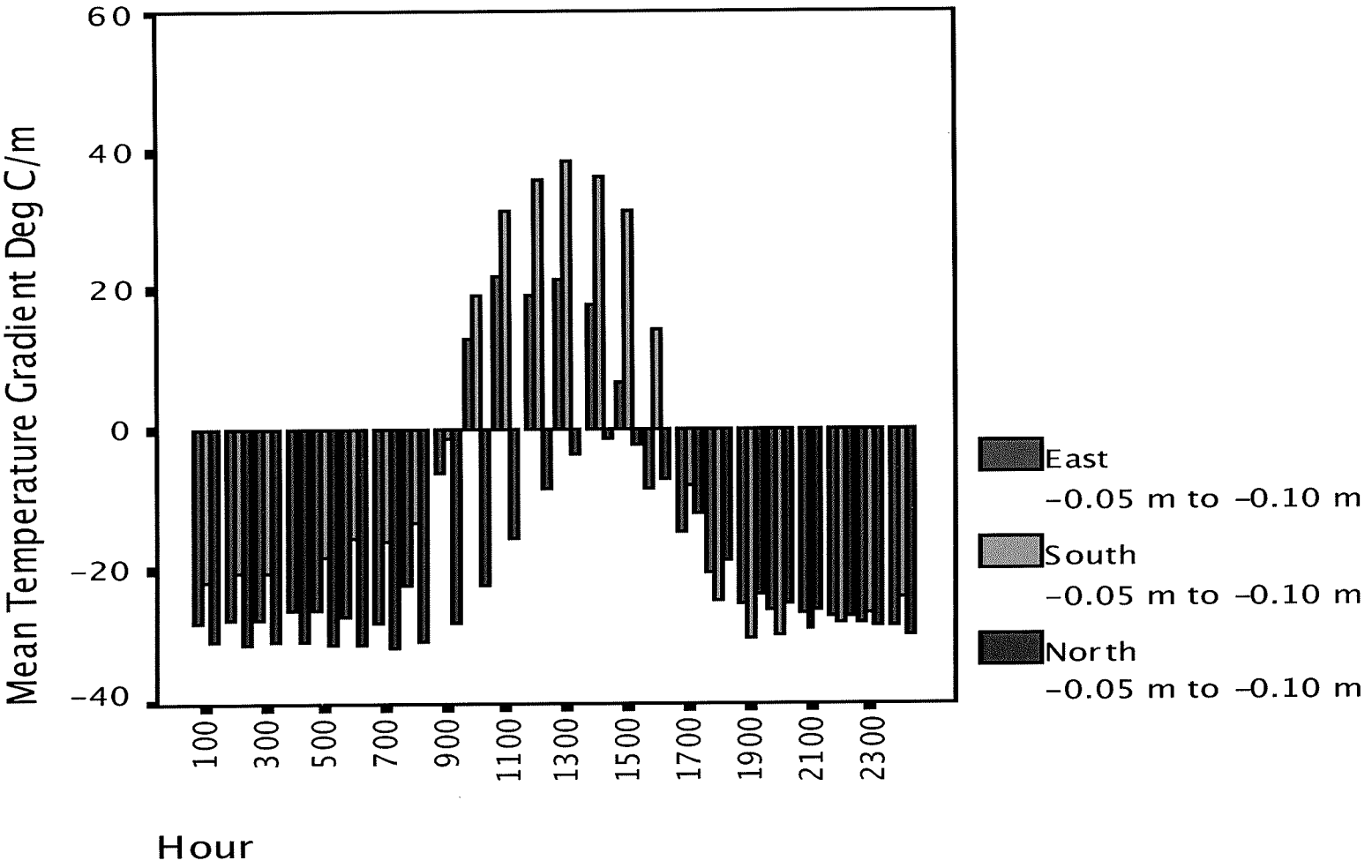

Figure A18: The mean temperature gradient (° C m^{-1}) by Hour for the winter season 2003-2004 on the north-, south-, and east-facing aspects between -0.05 m and -0.10 m.

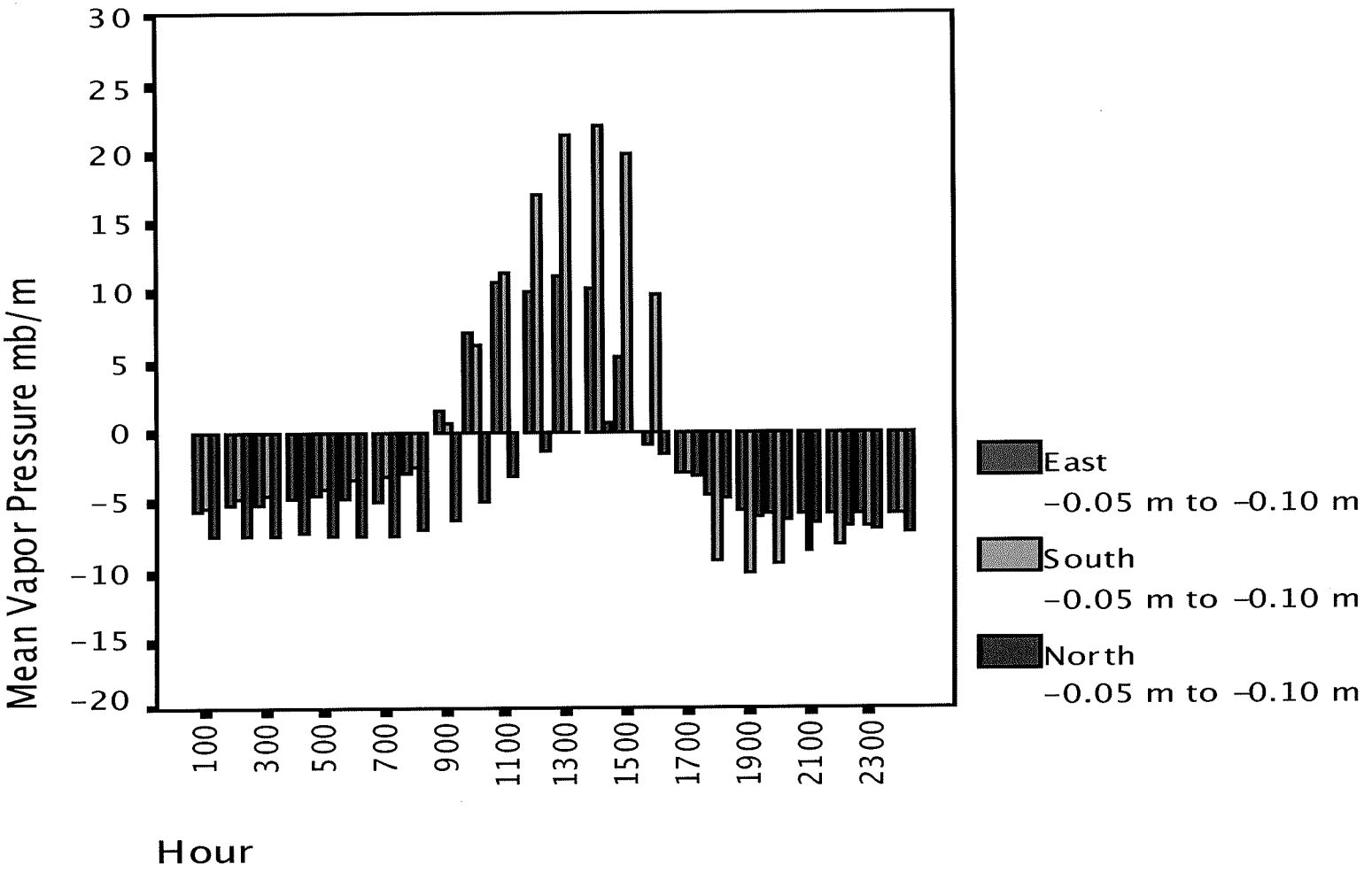

Figure A19: The average vapor pressure gradient (mb m^{-1}) by Hour for the winter season 2003-2004 on the north-, south-, and east-facing aspects between -0.05 m and -0.10 m.